2003

Wavelet-based multi-carrier code division multiple access systems

Muayyadi, Ali

WAVELET-BASED MULTI-CARRIER CODE DIVISION MULTIPLE ACCESS SYSTEMS

by

ALI MUAYYADI

A Thesis submitted to the University of Plymouth

in partial fulfilment for the Degree of

DOCTOR OF PHILOSOPHY

Mobile Communication Networks Research Group

Department of Communication & Electronic Engineering

Faculty of Technology

December 2003

COPYRIGHT STATEMENT

ABSTRACT

Wavelet-Based Multi-Carrier Code Division Multiple Access Systems

by Ali Muayyadi

This thesis proposes a wavelet-based multicarrier CDMA system that uses wavelet basis instead of DFT basis to deal with the problem of inter-channel interference (ICI) and spectral bandwidth efficiency. The theoretical analysis shows that the proposed system has lower side lobe components and higher bandwidth efficiency. The simulation further shows that the wavelet-based multi-carrier CDMA system gives lower ICI and better BER performance than that using DFT basis under multipath fading channel. Moreover the proposed system is more robust against narrow band interference signal.

This thesis exploits the wavelet correlation properties to perform timing synchronisation in multicarrier CDMA systems. This synchronisation is required to maintain the signal orthogonality. This timing synchronisation consists of maximum likelihood acquisition for coarse time synchronisation and early late sample tracking for fine time synchronisation. The performance of ML acquisition and ELS tracking under AWGN channel have been obtained analytically and through simulation and compared with the Cramer-Rao Bound. The designed acquisition circuit performs close to the Cramer-Rao Bound. The characteristic of the tracking circuit has also been discussed and shown the unambiguous locking capability.

The thesis also proposes a blind frequency error estimation based on the variation of the signal phase. The performance of the frequency error estimator has been obtained and shown that the error variance is inversely proportional to Eb/No value.

This thesis considers a new approach where the detection to get the original data symbol from the multicarrier CDMA system signal is performed using minimum mean-square error (MMSE) algorithm in both levels of orthogonality (subband and user axis). The joined MMSE combining (MMSEC) and MMSE multiuser detection (MMSE-MUD) shows better BER performance under Rayleigh fading channel compared with decorrelator, MMSEC alone and MMSE-MUD alone. The proposed MUD gets BER improvement at the cost of higher computation complexity but still retains the near-far resistance. The adaptive MMSE multiuser detection has shown further improvement of BER performance and lower computation complexity but requires a training sequence.

CONTENTS

3. Analysis Filters
4. Code Spreading
5. Code Despreading
6. FB-MC-CDMA Transmitter
7. FB-MC-CDMA Receiver
8. WB-MC-CDMA Transmitter
9. WB-MC-CDMA Receiver
10. BER Calculation
11. Frequency Error Estimator
12. Phase Offset Estimator
13. M-band Wavelet Display

Appendix B. Papers

1. A. Muayyadi and MNA Abu-Rgheff : 'Wavelet-based MC-CDMA cellular systems', IEEE Sixth International Symposium on Spread Spectrum Techniques & Applications, Sept 2000, New Jersey, USA. pp.145-149.

2. A. Muayyadi and MNA Abu-Rgheff: 'Wavelet-based multicarrier CDMA systems and its corresponding multiuser detection', *Proceeding IEE – Communications* (accepted to appear on Vol. 150, Issue 07, Dec 2003).

3. A. Muayyadi and MNA Abu-Rgheff: 'Wavelet-based Synchronisation in MC-CDMA systems' , PREP 2003 Conference, Exeter, April 2003, pp. 1-2.

4. A. Muayyadi and MNA Abu-Rgheff : 'Wavelet-based multicarrier CDMA systems and its time synchronisation', *Int'l journal on Wireless Communications and Mobile Computing* (submitted).

LIST OF ILLUSTRATIONS

LIST OF TABLES

GLOSSARY

3GPP Third Generation Partnership Project

Additive White Gaussian Noise

Statistically random radio noise characterised by a wide frequency range with regards to a signal in a communications channel

Advanced Mobile Phone System

The original standard specification for analog systems. Operates in the frequency range of 800 MHz, with a bandwidth of 30kHz. Used primarily in North America, Latin America, Australia and parts of Russia and Asia

aliasing

The process where a signal changes from one frequency to another as a result of sampling or other nonlinear action which usually results in a loss of the signal's information

AMPS Advanced Mobile Phone System

analysis filter

A filter for decomposing a signal into a number of subband signals

autocorrelation

The complex inner product of a sequence with a shifted version of its self. It is a measure of how closely a signal matches a delayed version of itself shifted n units in time

AWGN Additive White Gaussian Noise

Base Station Controller

A device and software associated with a base station that permits it to register mobile phones in the cell, assign control and traffic channels, perform handoff and process call set up and termination

basis function

The set of functions that a decomposition uses. For instance, the basis functions for the Fourier transform are unity amplitude sine and cosine functions

BER Bit Error Rate

biorthogonality

An orthogonality condition with the dual function

Bit Error Rate

The number of erroneous bits received divided by the total number of bits transmitted

BSC Base Station Controller

Carrier Frequency Error

A frequency difference between the transmitter and receiver caused by oscillator drift or Doppler effect

CDMA Code Division Multiple Access

CFE Carrier Frequency Error

Code Division Multiple Access

One of several "spread spectrum" techniques (see spread spectrum), which allows multiple users to share the same radio frequency spectrum by assigning each active user an unique code

correlation

see autocorrelation and crosscorrelation

crosscorrelation

The complex inner product of a first sequence with a shifted version of a second sequence. Sequences are considered to have good cross correlation properties when there is very little correlation between the sequences as they are shifted against each other.

DAB Digital Audio Broadcast

DFT Discrete Fourier Transform

Digital Audio Broadcast

Digital radio broadcast using MCM for transmission

Digital Subscriber Lines

A data communications technology that transmits information over the copper wires that make up the local loop of the public switched telephone network

Digital Video Broadcast

Digital television broadcast using MCM for transmission

Direct Sequence Code Division Multiple Access

A process of spectrum spreading where the digital information stream is multiplied, using an exclusive OR technique, by a high speed pseudorandom code (spreading sequence) and user's access is based on this orthogonal or nearly orthogonal code

Discrete Fourier Transform

Fourier transform of a periodic finite length time-series

Discrete Multi-Tone

A method of transmitting data on copper phone wires that divides the available frequency range into number of sub-channels or tones, and which is used for some types of DSL

Discrete Wavelet Multi-Tone

A variation of DMT modulation that improves performance by using wavelets rather than tones to provide additional isolation of sub-channels

diversity

A technique to reduce the effects of fading by using multiple spatially separated antennas to take independent samples of the same signal at the same time. The theory is that the fading in these signals is uncorrelated and that the probability of all samples being below a threshold at a given instant is low.

diversity combiner

A circuit or device for combining two or more signals carrying the same information received via separate paths or channels with the objective of providing a single resultant signal that is superior in quality to any of the contributing signals

DMT Discrete Multi-Tone

DMWT Discrete M-band Wavelet Transform

Doppler Shift

The magnitude of the change in the observed frequency of a wave due to the relative velocity of a transmitter with respect to a receiver

downlink

The transmission path from the base station down to the mobile station

downsampling

Sampling with the rate lower than the input signal rate

DS-CDMA Direct Sequence Code Division Multiple Access

DSL Digital Subscriber Lines

DVB Digital Video Broadcast

DWMT Discrete Wavelet Multi-Tone

DWT Discrete Wavelet Transform

EDGE Enhanced Data rates for GSM Evolution

EGC Equal Gain Combining

EIA Electronic Industries Association

EIA Interim Standard 95

The original digital mobile telephony standard based on CDMA technology.

EIA Interim Standard for U.S. Digital Cellular

Original TDMA digital standard. Implemented in 1992. This standard was the first to permit the use digital channels in AMPS systems. It used digital traffic channels but retained the use of analog control channels. This standard was replaced by the IS-136 digital standard in 1996.

Electronic Industries Association

A trade association and standards setting organisation in USA

ELS Early-Late Sample

Enhanced Data rates for GSM Evolution

A technology that gives GSMA and TDMA similar capacity to handle services for the third generation of mobile telephony. EDGE was developed to enable the transmission of large amounts of data at a high speed, 384 kilobits per second. (It increases available time slots and data rates over existing wireless networks.)

Equal Gain Combining

A diversity combiner in which the signals on each channel are added together and the channel gains are always made equal

ETSI European Telecommunications Standards Institute

European Telecommunications Standards Institute

The European standardisation body for telecommunications

fading

The variation in signal strength from it normal value. Fading is normally negative and can be either fast or slow. It is normally characterized by the distribution of fades, Gaussian, Rician, or Rayleigh

fast fading

The short term component associated with multipath propagation. It is influenced by the speed of the mobile terminal and the transmission bandwidth of the signal

Fast Fourier Transform

Popular fast algorithm used to implement discrete Fourier transform

FB-MC-CDMA Fourier-Based Multi-Carrier Code Division Multiple Access

FDMA Frequency Division Multiple Access

FFT Fast Fourier Transform

filter bank

A collection of individual filters designed to collectively achieve a desired effect

flat fading

A type of fading in a communications channel that attenuates or fades all frequencies in the channel the same amount

FM Frequency Modulation

Fourier transform

A family of mathematical techniques based on decomposing signals into sinusoids (or complex exponentials)

frequency diversity

The simultaneous use of multiple frequencies to transmit of information. This is a technique used to overcome the effects of multipath fading, since the wavelength for different frequencies result in different and uncorrelated fading characteristics

Frequency Division Multiple Access

Method of allowing multiple users to share the radio frequency spectrum by assigning each active user an individual frequency channel.

Frequency Modulation

A form of angle modulation in which the instantaneous frequency of a sine-wave carrier is caused to depart from the carrier frequency by an amount proportional to the instantaneous value of the modulating wave

frequency selective fading

A type of signal fading occurring over a small group of frequencies caused by a strong multipath component at those frequencies

Gaussian channel

An RF communications channel having the properties of wide-band uniform noise spectral density resulting in a random distribution of errors in the channel

Gaussian Minimum Shift Keying

A modulation technique involving Gaussian filtering of the input data prior to its application to the phase modulator. This results in a narrow occupied spectrum and better adjacent channel interference performance

General Packet Radio System

A packet-linked technology that enables high-speed (115 kilobit per second) wireless Internet and other data communications over a GSM network. It is

considered an efficient use of limited bandwidth and is particularly suited for sending and receiving small bursts of data

Global System for Mobile communications

Originally developed as a pan-European standard for digital mobile phone, GSM has become the world's most widely used mobile system. It is used on the 900 MHz and 1800 MHz frequencies in Europe, Asia and Australia, and the MHz 1900 frequency in North America and Latin America.

GMSK Gaussian Minimum Shift Keying

GPRS General Packet Radio System

GSM Global System for Mobile communications

guard band

A set of frequencies or band-width used to prevent adjacent systems from interfering with each other. Guard bands are typically used between different types of systems at the edges of the frequency allocations.

guard time

A redundant period of time allocated for alleviating intersymbol interference

IC Interference Canceler

ICI Inter-Channel Interference

IDMWT Inverse Discrete M-band Wavelet Transform

IFFT Inverse Fast Fourier Transform

IMT-2000 International Mobile Telecommunications-2000

Inter-Channel Interference

An interference of a signal band mixed with another signal band

International Mobile Telecommunications-2000

The global standard for third generation (3G) wireless communications, defined by a set of interdependent ITU Recommendations.

Internet Protocol

A set of instructions defining how information is handled as it travels between systems across the Internet.

Inter-Symbol Interference

An interference effect where energy from prior symbols in a bit stream is present in later symbols. ISI is normally caused by filtering of the data streams.

IP Internet Protocol

IS-54 EIA Interim Standard for U.S. Digital Cellular

IS-95 EIA Interim Standard 95

ISI Inter-Symbol Interference

Least Mean Square

An algorithm for adaptively adjusting the tap coefficients of an equaliser based on the use of (noise-corrupted) estimates of the gradients

LMS Least Mean Square

MAI Multiple Access Interference

matched filter

The receiver filter with impulse response equal to the time-reversed, complex conjugate impulse response of the combined transmitter filter-channel impulse response

Maximum Ratio Combining

A diversity combiner in which the signals from each channel are added together and the gain of each channel is made proportional to the rms signal level and inversely proportional to the mean square noise level in that channel

M-band wavelets

A wavelet system with 1 scaling function and M-1 wavelet functions

MC-CDMA Multi-Carrier Code Division Multiple Access

MC-DS-CDMA Multi-Carrier Direct Sequence Code Division Multiple Access

MCM Multi-Carrier Modulation

Minimum Mean-Square Error

An algorithm to minimise the mean-square error between the desired and the estimated signals

ML Maximum Likelihood

MMSE Minimum Mean-Square Error

MRC Maximum Ratio Combining

MUD Multi-User Detection

multi-carrier

A transmission where the information signal is transmitted with a number of subcarrier signals

Multi-Carrier Code Division Multiple Access

A combination of multi-carrier and CDMA where the spreading is performed in frequency domain

Multi-Carrier Modulation

see multi-carrier

multipath

A propagation phenomenon characterized by the arrival of multiple versions of the same signal from different locations shifted in time due to having taken different transmission paths of varying lengths

multiple access

The process of allowing multiple radio links or users to address the same radio channel on a coordinated basis. Typical multiple access technologies include FDMA, TDMA, CDMA.

Multiple Access Interference

An interference caused by other users utilising the same transmission channel

multiplexer

A device that combines multiple inputs into an aggregate signal to be transported via a single transmission channel

multi-user

A transmission where the transmission channel is used by a number of users

NMT Nordic Mobile Telephone

OFDM Orthogonal Frequency Division Multiplexing

Orthogonal Frequency Division Multiplexing

Frequency division multiplexing or multi-carrier modulation using orthogonal DFT basis

PAPR Peak to Average Power Ratio

PCM Pulse Code Modulation

Peak to Average Power Ratio

Parameter used to determine the robustness of a modulated signal against nonlinear distortion (usually expressed in decibels [dB])

Perfect Reconstructed

A condition where the signal can be reconstructed without destruction and aliasing after being transmitted (or other processed)

Perfect Reconstructed Quadrature Mirror Filter

A filter bank capable of perfectly reconstructing a signal from its component parts

Phase Shift Keying

Angle modulation in which the phase of the carrier is discretely varied in relation to a reference phase in accordance with data being transmitted.

PIC Parallel Interference Canceler

pilot (synchronising pilot)

In FDMA, a reference frequency used for achieving and maintaining synchronisation of the oscillators of a carrier modulation system or for comparing the frequencies or phases of the signals generated by those oscillators.

In TDMA, a reference time slot used for achieving and maintaining the time synchronisation between users.

In CDMA, a reference logical channel containing an unmodulated DS-SS signal continuously monitored by each base station which allows the mobile stations to acquire the timing of the forward channel, serves as a phase reference for demodulation, and allows the mobile to search out the best (strongest) base stations for acquisition and hand-off.

PR Perfect Reconstructed

PRQMF Perfect Reconstructed Quadrature Mirror Filter

PSK Phase Shift Keying

Pulse Code Modulation

Modulation in which a signal is sampled, and the magnitude (with respect to a fixed reference) of each sample is quantised and digitised for transmission over a common transmission medium

QPSK Quadrature Phase Shift Keying

Quadrature Phase Shift Keying

A type of phase modulation using 2 pairs of distinct carrier phases, in quadrature, to signal ones and zeros

Recursive Least-Squares

An adaptive algorithm to compute the optimal filter coefficients which requires much more computation (as opposed to the least squares) [see 134,198,199]

RLS Recursive Least-Squares

scaling function

A localised function with mean nonzero and satisfy the dilation equation (equation 2.21)

SFN Single Frequency Network

Short-Time Fourier Transform

DFT of a aperiodic time-series over short temporal intervals which assume signal stationarity

SIC Serial Interference Canceler

Single Frequency Network

A network of DAB transmitters sharing the same radio frequency to achieve a large-area coverage

single-carrier

A transmission where the information signal is transmitted with one carrier signal

single-user

A transmission where the transmission channel is used by one user only

SLD Square Law Detector

spread spectrum

A transmission system where the occupied spectrum of the signal is much higher than the required bandwidth to transmit the information signal.

spreading code

A bit sequence (which is also a user's unique code in CDMA) used to spread the spectrum of the baseband signal according to the processing gain which helps the signal resist interference and also enables the original data to be recovered if data bits are damaged during transmission

SS Spread Spectrum

STFT Short-Time Fourier Transform

subband

A subset of the transmission band where a carrier signal occupy

synthesis filter

A filter for reconstructing a signal from a number of subband signals

TACS Total Access Communication System

TDMA Time Division Multiple Access

Telecommunications Industry Association

One of the Telecommunications standards setting bodies in the United States

Third Generation Partnership Project

A global cooperative project in which standardisation bodies in Europe, Japan, South Korea and the United States, as founders, are coordinating W-CDMA issues. See also W-CDMA.

TIA Telecommunications Industry Association

Time Division Multiple Access

Method of allowing multiple users to share the radio frequency spectrum by assigning each active user an individual time slot for transmission.

Total Access Communication System

British analog cellular system

training sequence

transmitted data bits, already known by the receiver to provide a reference signal for synchronisation, channel estimation, detection or other process.

transmultiplexer

Equipment that transforms signals derived from FDM equipment, such as group or supergroups, to TDM signals having the same structure as those derived from PCM multiplex equipment, such as primary or secondary PCM multiplex signals, and vice versa.

upsampling

Sampling with the rate higher than the input signal rate

wavelet

A special representation of a signal in time and scale (frequency) which obeys a number of mathematical properties

wavelet function

A localised function with mean zero and satisfy equation 2.27

WB-MC-CDMA Wavelet-Based Multi-Carrier Code Division Multiple Access

W-CDMA Wideband Code Division Multiple Access

wideband

The property of any communications facility, equipment, channel, or system in which the range of frequencies used for transmission is greater than 0.1 % of the midband frequency

LIST OF SYMBOLS

$c_{k,m}$: m^{th} chip of k^{th} user spreading code

F_m : m^{th} subband synthesis filter (at the transmitter)

G_m : m^{th} subband analysis filter (at the receiver)

r : the received signal at the receiver

s_k : the transmitted signal of k^{th} user

T_s : data symbol period

t_L : late sample instant

t_E : early sample instant

α_m : m^{th} subchannel equalisation amplitude factor

δ : half of normalised time difference between late and early sample.

τ : time error input

T_b : data symbol period

T_c : code chip period

f(t) : function in time domain

F(w) : function in frequency domain

ω : angular frequency

Ψ : wavelet function

Φ : scaling function

$h_0(n)$: scaling coefficient

$h_1(n)$: wavelet coefficient

M : number of subbands

N : filter length

K : number of active users

$f_k(n)$: scaling coefficient

$h_k(n)$: wavelet coefficient

F(z) : synthesis filters

G(z) : analysis filters

a : data input signal

C : user's spreading codes matrix

H : channel matrix

E : the effective spreading sequence

y : decision variable (combining output) signal

$\beta_{k,m}$: multiplication of subband gain factor ($\alpha_{k,m}$) and code chip ($c_{k,m}$)

α_m : m^{th} subband equalisation/combining factor

α_{opt} : optimal combining factor

w_{opt} : optimal MMSE-MUD coefficients

γ : total factor which relates output (**y**) and input (**a**) signals

$\mathbf{R}_{ab}$: correlation between signal **a** and signal **b**

$\mathbf{p}(n)$: inverse correlation matrix in RLS algorithm

λ : forgetting factor in RLS algorithm

P_e : probability of error

η : multiuser efficiency

Na : number of complex additions

Nm : number of complex multiplications

AUTHOR'S DECLARATION

At no time during the registration for the Degree of Doctor of Philosophy has the author been registered for any other university award.

This study was financed by University of Plymouth and STTTelkom, Indonesia.

Relevant scientific seminars and conferences were regularly attended and work was presented at some conferences. Four papers were prepared for publication and published.

Signed .....

Date 16 Dec 2013 .....

CHAPTER I

INTRODUCTION

1.1 Introduction to Wireless Cellular Systems

The concept of cellular wireless system comes from the need to cover a large area for subscribers who are mobile. The oldest approach to do that is by setting up a high power transmitter located at the highest point in the coverage area. Obviously the size of the coverage area is limited by line of sight horizon (typically with a radius of 40 miles from the base station). Moreover the number of simultaneous calls is limited by the number of the available radio channels for all over the coverage area, for instance Bell System in New York City in 1970 could support 12 calls only at the same time [1]. A cellular system divides the area into many smaller coverage areas, each of which is called *cell*. By doing this the radio channels can be reused in different cells. On the other hand this system needs so called handoff and central control to serve smoothly when a mobile phone moves from a cell to another one. Thus a cellular system will have the following elements: cell with low power transmitter, handoff and central control as well as frequency reuse.

The first generation cellular systems used analogue modulation (FM). Each standard of this generation was developed for its own country or zone. Advanced Mobile Phone System (AMPS) emerged in the late 1970s in USA for North America zone. United Kingdom used TACS (Total Access Communication System) from 1985, whereas Scandinavian countries used Nordic Mobile Telephone (NMT) [1, 2]. Each system used different frequency band and different signalling protocols between base station and mobile station.

The spectacular demand of mobile phones and the need to improve the signal quality, the battery performance, the security as well as the capacity lead the cellular system to fully digital technology. The second generation system emerged which constitutes narrow band digital cellular system. European countries grouped in ETSI (European Telecommunications Standards Institute) drafted GSM (Global System for Mobile communications) standard in 1987 whereas USA under Electronic Industries Association (EIA) and Telecommunications Industry Association (TIA) launched IS-54 (TDMA) standard in 1993. Qualcomm proposed CDMA-based system called IS-95 standard in 1993.

In order to determine an open standard for the second generation cellular system, all networks operators and all mobile phone manufacturers in Europe met together in a formal body called ETSI in 1982. ETSI issued a standard which they called GSM. It is a truly solid standard that makes it widely spread not only in Europe but also in Asia, Australia, Africa and South America. GSM uses TDMA (Time Division Multiple Access) with 200 kHz bandwidth and transmission rate of 270 kbps for each carrier. Each radio channel consist of 8 time slots, each of which can support a call. It uses GMSK (Gaussian Minimum Shift Keying) modulation and operates in 900 MHz band.

The GSM system supports mainly voice with low data communication at a data rate of 9.6 kbps. In order to meet a higher data rate demand, ETSI developed 2+ phase or 2.5G standard which they called GPRS (General Packet Radio System). Using packet switching method, GPRS can support up to 170 kbps data rate using all 8 time slots available in each carrier but this GSM data evolution path will require new network infrastructure and new handset.

In order to migrate to third generation by utilising the existing *GSM network, 3GPP (*Third Generation Partnership Project) which is a collaboration agreement between a number of telecommunications standards bodies including ETSI, developed EDGE (Enhanced Data rates

for GSM Evolution) standard which provides multimedia services at a data rate of 384 kbps. This data rate enhancement is achieved by changing the modulation from GMSK to 8 PSK [3].

As radio channel are limited and expensive, the design of a cellular system involves how to maximise the number of times each channel can be reused in different cells in the service area. The radius of cell can be chosen from 30 km (large cell) in rural area where there are only few subscribers down to 1 km (small cell) in city centre where it needs considerable frequency reuse. The available radio channels are classified into N groups, where N is frequency reuse factor. Each group is allocated to certain cell and then it can be reused in other cell with a certain pattern [4].

The number of calls in a cell is determined by signal quality, usually represented by S/I (signal to interference ratio) parameter. The interference signal actually comes from different terminals (multiple access interference = MAI) and thermal noise. The latter can be neglected in a small cell (typically in city centre).

In FDMA system, MAI signal comes from other terminals which use the same channel (co-channel interference) and the neighbour channel (adjacent channel interference). In TDMA system, MAI signal comes from the terminals which uses the same time slot and the neighbour time slots. GSM system is actually a combination of TDMA/FDMA system and therefore experiences the above interference.

In CDMA system, frequency reuse factor is one, meaning all cells use the same radio channels. The MAI signal arises due to imperfect autocorrelation and imperfect crosscorrelation

processes and it comes from the terminals in the same channel (internal cell interference) and the neighbour cells (external cell interference) [5].

Most operators and manufacturers as well as some universities are beginning to study and develop a future mobile communications system following IMT-2000 which will be called fourth generation mobile communications. This is dealing with the research and development of basic technologies such as microwave and milliwave bandwidths, software defined units, adaptive array antennas, adaptive interference cancelers and also multicarrier modulation.

One important step in preparing future mobile communications is time-space signal processing, in which an adaptive array antenna is combined with adaptive equalisation technology in order to increase interference resistance while gaining the required reception signal levels.

In addition, the software defined unit makes it possible to provide more advanced functions by using software, thereby allowing full flexibility in system structuring. For example, access methods can be selected in accordance with the specific utilisation purposes.

It is envisaged that the fourth generation mobile communications will utilise multicarrier modulation to increase the capacity and the spectral efficiency. This can be a combination of OFDM and CDMA or MC-CDMA systems.

1.2 CDMA Wireless Cellular Systems

The objectives to improve a mobile communication system performance (signal quality, battery performance, security as well as capacity) led to fully digital technology. For the same reason, the wireless technology moved from TDMA (Time Division Multiple Access) to CDMA (Code Division Multiple Access) system.

CDMA or more precisely DS-CDMA (Direct Sequence CDMA) is based on spread spectrum (SS) technique. SS system spreads the energy of transmitted signal over a spectrum of frequency much larger than the minimum bandwidth required to transmit the signal [6-15]. This is done by multiplying the data signal with a spreading code uniquely assigned for a user. In the receiver, the signal is cross-correlated with the same code and the original data signal will be obtained and ideally all other interference signal originated from other user's codes will be filtered out.

CDMA system offers higher capacity and higher spectral efficiency because of lower MAI (multiple access interference), no guard band or guard time protection needed. All cells can use the same radio frequency channels or in other words the frequency reuse factor is one. It will further increase the number of users on the same bandwidth. In FDMA or TDMA systems it is not feasible for adjacent cells to share the same frequencies because of the interference signal.

Another important factor for a mobile network is packet data services. All the CDMA mobile communication standards, i.e. IS-95A, IS-95B, W-CDMA or IMT2000 (CDMAOne (1x) and CDMA-MC (3X)) support packet data services and IP networks. Hence they strengthen the

convergence of voice, data services and packet-switch network which is the significant trend of present and future network services.

The first CDMA standard (IS-95), a second generation mobile communication system, operates in 800 MHz band and 1900 MHz band and uses QPSK modulation. The transmission bandwidth is 1.25 MHz with a chip rate of 1.2288 Mbps. Using Walsh-Hadamard code, this system provides 64 channels for traffic, pilot, sync and paging channels. IS-95A can support digital data communication up to 14.4 kbps whereas IS-95B can support up to 115 kbps by bundling 8 above channels. The evolution from IS-95A to IS-95B will just need a new chip in handset and a new software in BSC (Base Station Controller).

The second CDMA standard (IMT2000), a third generation mobile communication system, is a wideband system [16] and operates in 2 GHz band and uses QPSK modulation. The transmission bandwidth is 5, 10 or 15 MHz with a correspondent chip rate of 4.096, 8.192 or 12.288 Mbps respectively. Using Walsh-Hadamard code, this system provides 64 channels (for traffic, pilot, sync and paging channels). IMT2000 MC 1X can support digital data communication up to 307 kbps whereas IMT2000 MC 3X can support up to 2 Mbps. The evolution from IS-95B to IMT2000 1X will need a new chip in the handset and a new software in the backbone and new channel cards in the base station. The evolution from IMT2000 1X to 3X will need a new handset and a modification in the backbone and new channel cards in the base station.

1.3 Multi-Carrier Modulation Systems

The development of multicarrier modulation originated from the need to carry higher rate message signal. Using single carrier modulation system, the high rate data signal will be

susceptible to inter symbol interference (ISI) due to the short signal period and also produce high distortion due to the wide frequency band especially over a dispersive channel. The solution to these problems is using multi carrier system. The data signal is converted to parallel data stream, each of which will be transmitted by a subcarrier. These parallel data streams will have longer period and narrower band that makes this system more robust against ISI.

The oldest approach to such a system is building parallel transmitters and receivers. Obviously such a system will be highly expensive and also bandwidth inefficient due to guard bands between subcarriers. To attain higher bandwidth efficiency, Colin Radio Co. developed so called Kineplex system for data transmission over HF radio channel subject to severe multipath fading. In this system 20 tones are modulated by differential 4-PSK and like modern OFDM, the signal spectra are the Sin (kf)/f shape and overlap [17].

The significant progress of OFDM was achieved in 1971 when discrete transform Fourier (DFT) was implemented in the modulation and demodulation processes [18] using FFT digital signal processing (DSP) technique.

OFDM system has been successfully adopted as digital subscriber lines (XDSL) standard [19] for data transmission over copper cable. This system is also used for digital broadcasting system, digital audio broadcast (DAB) and digital video broadcast (DVB) [20,21]. OFDM is also used in several fixed wireless systems and wireless local-area network (LAN) [20,21]. Now the possibility to use OFDM in multiuser mobile communication system is being investigated [17,19,21].

The basic principle of OFDM system is as follows: the input data signal is assembled into blocks of N complex numbers (including cyclic prefix, coding etc.) one for each subchannel. Each block is fed into N-points IFFT and the output signal is transmitted serially. At the receiver, the original data signal is recovered by performing FFT on every received block signal samples. Using rectangular signal for waveform window, each subband signal is of the form Sin (kf)/f which nulls at the centre of the other subcarriers.

Multi-carrier communication systems are commonly employed to combat channel distortion and improves the spectral efficiency by dividing the available bandwidth into a number of subbands to make them much less distorted. The combination of multi-carrier modulation and CDMA into multi-carrier CDMA [22-36] appears to be very attractive in mobile communications. There are two types of multi-carrier CDMA schemes in the literature. The MC-CDMA [22-25,33-35] and MC-DS-CDMA [37,38] depending on the spreading process being performed in frequency domain or time domain respectively. Details of these two schemes of multi-carrier CDMA and a comparison of their simulated performance are given in [22,23], which show that the MC-CDMA outperforms the MC-DS-CDMA. The performance of MC-CDMA in fading channel was presented in many literatures [22,23,39-42]. The hybrid of MC-CDMA and MC-DS-CDMA was introduced [43] where the spreading was performed both in the time and frequency domains. The multi-carrier modulation can be implemented using discrete Fourier transform (DFT) [17,18,20,21] that provides orthogonal basis between subchannels.

1.4 Multicarrier Modulation using Wavelets

In order to be able to recover data signal carried by different subchannels, the subcarriers must be orthogonal to each other. As mentioned above originally it was realised using a bank of

Nyquist filters with guard band between filters. Recently DFT basis functions (like in OFDM) which can be implemented using a single digital signal processor are used for multicarrier modulation (MCM) [20,21].

MCM with DFT basis usually uses a rectangular function as windowing waveform which generates strong sidelobes. This Fourier-based MCM will get interchannel interference (ICI) when transmitted over non ideal channel. The other drawback in MCM using DFT basis is the need of guard time in the system signal to alleviate intersymbol interference (ISI) due to dispersive channel which therefore reduce the bandwidth efficiency.

The basic theory of wavelet transform can be seen in chapter II for more details. MCM using wavelets can be implemented in three ways, using either dyadic wavelet transform, wavelet packet or M-band wavelets (see section 3.1 for more detail). In this thesis MCM is implemented using M-band wavelets for three reasons. Firstly, the system has the same bandwidth for each subchannel and hence it carries the same data rate. Secondly, the system has the same spectrum shape for each subband unlike in wavelet packet system. Thirdly, the system provides the flexibility to choose the orthogonality or the biorthogonality degree, the overlapping factor, the filter length, and the sidelobe relative power.

From now on wavelet-based MCM means multicarrier modulation using M-band wavelets as biorthogonal basis functions and at the same time these basis functions act as windowing waveform. The period of these basis functions is chosen according to the sidelobe relative power and usually much longer than system signal period T_s. The longer the period, the smaller the sidelobe component will be. Thus the system signal has such a good energy concentration that will reduce ICI and does not require a guard time. It is this guard time that makes wavelet-based MCM more bandwidth-efficient than Fourier-based MCM..

The wavelet transform has been proposed as a flexible tool for the multiresolution decomposition of continuous time signal [44,45]. Both the mathematics and the practical interpretations of wavelets seem to be best served by using the concept of resolution [46,47]. The significant step which has relevance with this thesis was achieved when Daubechies showed the linkages between the subband filter bank and the wavelet transform [48]. Since then there has been an explosion of interest and activity of interdisciplinary research and development on wavelet and subband transform as well as these applications [45-47,49-57] in digital communication systems, among others: channel estimation [58], pulse shaping [59-61], excision of jammer from spread spectrum signal [62,63], PRQMF codes for CDMA [64-72], discrete multicarrier modulation [73-76]. The latter uses the biorthogonal basis so-called discrete wavelet multi-tone (DWMT) to create multi-carrier modulation in copper cable applications. Another wavelet system is proposed for adding another orthogonality beside the orthogonality between spreading codes and between subcarriers in MC-CDMA system [77].

Before an MCM receiver can demodulate the data signal, the receiver has to perform two synchronisation stages. During the first stage the symbol boundaries are determined together with the optimal timing instant (time synchronisation). This is carried out to minimise ISI. The second stage has to estimate the frequency offset of the received signal in order to minimise ICI (frequency synchronisation). This synchronisation can be done using data-aided method (training sequence) [78], by exploiting the redundant cyclic prefix [79-82] or by exploiting the redundant zero padding [83]. Another method in estimation of frequency offset in OFDM system were introduced using a so-called adaptive decorrelator [84] .

The received signal energy in the MC-CDMA is scattered in the frequency domain. The challenging task in the design of MC-CDMA receiver is to combine and optimise all these

signal energies in order to best recover the data signal. These received subcarriers may have different amplitudes and different phase shifts when the signal is transmitted through non linear channel. Some combining methods have been proposed, such as equal gain combining (EGC) [23,85,86], minimum mean square error combining (MMSEC) [23,87,88].

The other important factor to be considered in detection process is multiple access interference (MAI). The detection process which takes into account the MAI signal is called multiuser detection [89-91]. The optimal multiuser detection was first introduced by Verdu [90-93] that applies maximum likelihood sequence detection (MLSD) which then developed by others [94-96]. The less complex suboptimal schemes [90,97] have been investigated and can be classified into two types, the linear detection [90,97] and the interference cancellation techniques [89,98,99].

1.5 Thesis Overview

This section describes the contributions of each chapter.

Chapter II presents the connection between wavelets, filter banks and transmultiplexer systems. The mutual influence and interaction between signal processing and communication engineering have been reinforced in discrete time multirate signal processing. Using this perspective, we introduced a generalisation of all digital communication systems (multi-user and/or multicarrier system) into one model. The analysis and differentiation between them are performed based on the characteristic of the set of filters used. We also showed how to design these filters in order to qualify certain type of digital communication system (FDMA, TDMA, CDMA, OFDM etc.)

In Chapter III, we consider the problems of multiple access interference (MAI) and frequency selective fading channel in cellular systems. We then choose a multi-carrier code division multiple access (MC-CDMA) system to cope with those problems. We also consider the problems of interchannel interference (ICI) and spectral bandwidth efficiency in multicarrier modulation system using DFT basis. We use a wavelet system to deal with these problems. We then propose a wavelet-based MC-CDMA system to mitigate all the above problems, i.e. multiple access interference (MAI), frequency selective fading channel, interchannel interference (ICI) and bandwidth efficiency. The theoretical analysis shows that the proposed system (wavelet-based MC-CDMA) has lower side lobe components and higher bandwidth efficiency. The simulation further shows that a wavelet-based MC-CDMA system gives a lower ICI and better BER performance than that using DFT basis under multipath fading channel. In addition to that, the proposed system is more robust against narrow band interference signal.

In Chapter IV, we consider the problem of synchronisation in MC-CDMA system which is required to maintain the orthogonality property between subcarriers and establish both symbol timing and carrier frequency offset. We propose a maximum likelihood acquisition system for coarse timing synchronisation followed by early late sample tracking for fine time synchronisation. Both stages exploit the wavelet correlation properties on subbands. We propose a blind (non-data aided) frequency offset estimation based on the variation of the signal phase.

In chapter V, we consider the detection strategy in MC-CDMA system. There are two levels of orthogonality in MC-CDMA signal, i.e. along subband axis and user axis. We propose a new approach where the detection is performed using minimum mean-square error algorithm in both subband and user axis. The first one, called MMSE combiner exploits the frequency

diversity available in MC-CDMA signal. The latest one is called MMSE multiuser detection. We present the adaptive implementation of MMSE multiuser detection as well in this chapter.

In chapter VI, we present the theoretical analysis of system performance (in BER) of our designed system (WB-MC-CDMA system) and then compare its performance with the simulation results. This is performed for the system under AWGN and Rayleigh channels. We also analyse the near-far resistance of the MMSE multiuser detection for WB-MC-CDMA system to deal with the dissimilar users powers. We discuss the computation complexity of the multiuser detection system at the end of this chapter.

We summarise the contributions of the thesis, draw some conclusions and discuss the possibility of the future works related to this research in chapter VII.

CHAPTER II

WAVELETS AND

DIGITAL COMMUNICATION SYSTEMS

The theories of communications engineering and signal processing have mutual influence and interaction since a long time. Just to name a few examples of this interrelation are signal filtering, modulation theory and Fourier transform. Recently this interaction reinforced in discrete time multirate signal processing with which one can see the linkage between wavelet transform, filter bank and transmultiplexer. Indeed using this perspective, all digital communication systems can be described and analysed in terms of synthesis/analysis configuration of filter bank (transmultiplexer system). This will be discussed in more detail at the end of this chapter.

2.1 Fourier Transform

Fourier transform is a linear transformation which maps the signal $f(t)$ into frequency domain $F(w)$ [24]. It has been popular in signal processing for numerous applications for many years. However for some cases, it is not well suited. Just take a simple example, a square pulse. In order to represent this signal one needs to extend the component's frequency from $-\infty$ to ∞. There has been a partial solution for this problem by using so-called short-time Fourier transform (STFT). STFT uses a time window and then apply the Fourier transform. Another more elegant solution is using wavelet transform. Fourier transform actually can be viewed as a special case of the larger class of wavelets [24].

Wavelet-based analysis is an interesting and powerful tool for mathematicians, scientists and engineers. It suits perfectly the modern calculation using computer with its basis functions defined by summations not integral or derivatives.

Using Fourier series, a periodic function or signal can be represented by a superposition of complex exponential (or sines and cosines) as follows [24]

$$f(t) = \sum_{n=\infty}^{\infty} F(n)\, e^{jn\omega_0 t}, \tag{2.1}$$

where the coefficients $F(n)$ are calculated from [24]

$$F(n) = \frac{1}{t_0} \int_0^{t_0} f(t)\, e^{-jn\omega_0 t} dt \tag{2.2}$$

and t_0 is the signal period.

If the signal is not periodic or $t_0 = \infty$ then the above equation is replaced by Fourier transform

$$F(\omega) = \int_{-\infty}^{\infty} f(t)\, e^{-j\omega t} dt \,. \tag{2.3}$$

The Fourier transform is useful due to its ability to analyse a signal for its frequency characteristic. This transform works by first translating a function in the time domain into a function in the frequency domain. The characteristic of the signal can then be analysed for its frequency content because the Fourier coefficients of the transformed function represent the contribution of each exponential (or sine and cosine) function at each frequency.

Here the complex exponential (or sines and cosines) are used as *orthogonal basis functions.* They are orthogonal to each other but extend over all time. Consequently, the transformed function is not time localised and loses its time-dependent property.

An inverse Fourier transform does just the inverse transformation, i.e. mapping the function from frequency domain into time domain

$$f(t) = \frac{1}{2\pi} \int_{-\infty}^{\infty} F(\omega)\, e^{j\omega t} d\omega \,. \tag{2.4}$$

The Fourier transform constitutes a process of analysis or decomposition, whereas the inverse Fourier transform is a process of synthesis or composition.

Fourier transform does not suit nonstationary signals (i.e. signals whose frequency characteristics are time-varying such as music, images etc.) because of its poor time localisation.

The classical solution to this problem is to use short-time (or windowed) Fourier transform (STFT) [45,100-104]. STFT uses a time window g (t) positioned at $t=\tau$ and the windowed function is applied with Fourier transform

$$F(\omega, \tau) = \int_{-\infty}^{\infty} f(t)\, g^{*}(t-\tau)\, e^{-j\omega t} dt \,. \tag{2.5}$$

The signal needs only be stationary during the window duration. The result is the transformed function tends to be localised in time. Since the duration of the window function is fixed, STFT gives a fixed time-frequency resolution. The following figures depict some window functions to get the localisation in time, Hamming function, Hanning function,

Blackman function and Kaiser function [105] in Figure 2.1 (a), (b), (c) and (d) respectively. In order to get the frequency resolution, one can take the Fourier transform of these window functions.

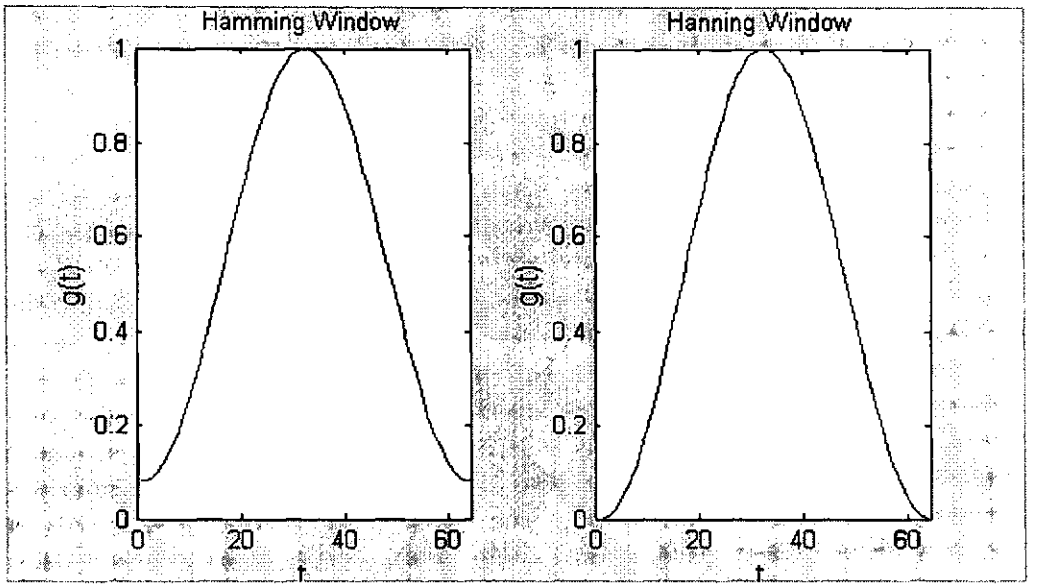

(a). (b).

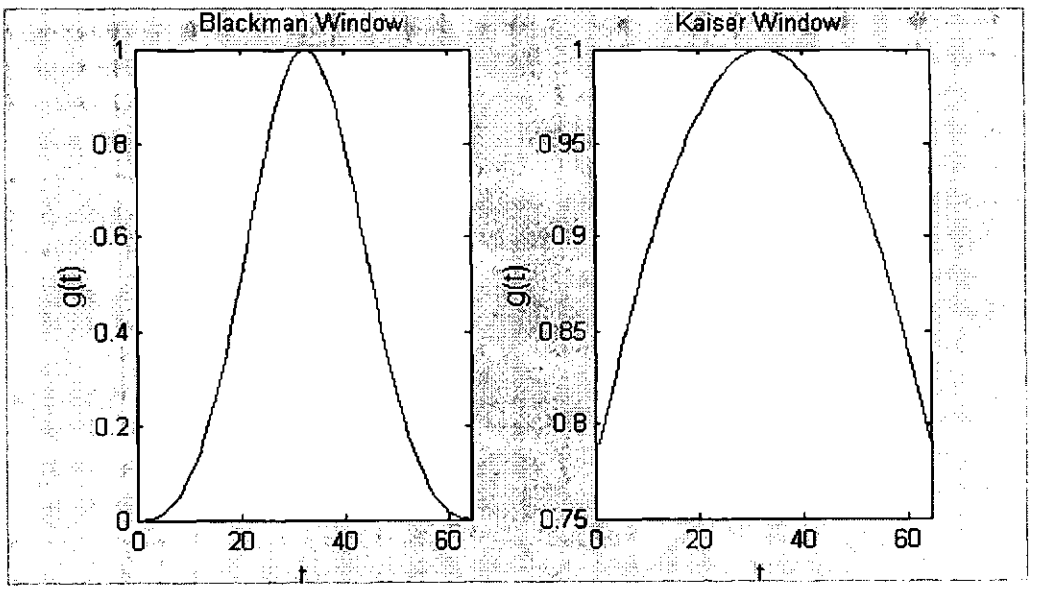

(c). (d).

Figure 2.1 STFT windows

a. Hamming window b. Hanning window

c. Blackman window d. Kaiser window, $\beta = 1$

2.2 Wavelet Transform

A wave refers to an oscillating function in time or space like a sinusoid. It usually extends over all time from $-\infty$ to $+\infty$. Fourier series analysis is a wave analysis. It can represents a function or a signal with infinite terms of sinusoid (or complex exponential) which has been proven to be very valuable in some applications (mathematics, science, engineering etc.) especially for periodic, time-invariant or stationary phenomena.

The wavelet term comes from the French word 'Ondelette' which means a small wave. It still have a wave characteristic but it does not extend to infinity. Its energy concentrated in some interval of time that makes it suitable for analysis of transient, time-varying, non-stationary phenomena.

Generalising Fourier series analysis, a function or signal $f(t)$ can be better analysed or processed if it is expressed in linear decomposition form

$$f(t) = \sum_k d_k \, \Psi_k(t) \,, \tag{2.6}$$

where k is index, d_k is a set of coefficients and $\Psi_k(t)$ is a set of orthogonal basis. In Fourier analysis, this basis is complex exponential or sinusoid. These basis are orthogonal to each other

$$< \Psi_k(t), \Psi_l(t) > = \int \Psi_k(t) \, \Psi_l(t) \, dt = 0 \quad , k \neq l \,. \tag{2.7}$$

The coefficients can be calculated from the inner product

$$d_k = < f(t), \Psi_k(t) > = \int f(t) \, \Psi_k(t) \, dt \,. \tag{2.8}$$

For wavelet analysis, two index parameters are needed, shift (translation) parameter k for covering time axis (from $-\infty$ to $+\infty$) R and scale (dilation) parameter j for covering different frequencies. The wavelet analysis becomes

$$f(t) = \sum_k \sum_j d_{j,k} \Psi_{j,k}(t) \quad . \tag{2.9}$$

The two-dimensional set of coefficients $d_{j,k}$ are called discrete wavelet transform (DWT) of $f(t)$. The *daughter wavelets* $\Psi_{j,k}(t)$ are derived from the mother wavelet $\Psi(t)$ by the following equation [64,66]

$$\Psi_{j,k}(t) = 2^{j/2} \Psi(2^j t - k) \quad j,k \in Z \quad . \tag{2.10}$$

Both the mathematics and the practical interpretations of wavelets are best served by using the concept of resolution [44,45,46101]. The multiresolution is obviously designed to represent signals where a single event is decomposed into finer and finer detail, but it turns out also to be valuable in representing signals where time-frequency or time-scale description is desired even if no resolution concept is needed [45,46].

2.2.1 Wavelets and Signal Space

In order to develop a multiresolution formulation of wavelet systems, the concept of *signal space*, an *expansion set* or bases set are needed.

The most basic signal space is called $L^2(R)$. It contains all functions f(t), which have a finite and well-defined integral of the square

$$f \in L^2 \Rightarrow E = \int |f(t)|^2 \, dt < \infty \quad . \tag{2.11}$$

It is actually a generalisation of normal Euclidean geometry and it gives a simple representation of the energy in a signal. **L** comes from *'Lebesque'* integral, the power '**2**'

means the integral of the square of the modulus of the function and **R** is the real number of which the independent variable of integration is a member.

Starting with the vector space of signals, S, if any function $f(t) \in S$ can be expressed as $f(t) = \sum_k d_k \Psi_k(t)$ then the set of functions $\Psi_k(t)$ is called an expansion set of the space S. When the representation is unique, the set is a basis.

Alternatively, starting with the expansion set or basis set, the space S, which is called the *span* of the basis set, is defined as the set of all functions that can be expressed by $f(t) = \sum_k d_k \Psi_k(t)$.

2.2.2 Scaling Function

The multiresolution concept defines the scaling function that then defines the wavelet function. A set of scaling functions is defined from the basic scaling function translated by shift parameter k

$$\Phi_k(t) = \Phi(t-k) \quad k \in Z \quad \Phi \in L^2 . \tag{2.12}$$

The subspace of $L^2(R)$ spanned by this function is defined as

$$V_0 = \overline{\underset{k}{Span}\{\Phi_k(t)\}} . \tag{2.13}$$

It means that any function $f(t)$ can be expressed by the following equation that is a member of the subspace V_0

$$f(t) = \sum_k d_k \, \Phi_k(t) \quad f(t) \in V_0 \, . \tag{2.14}$$

Similar to the definition of the daughter wavelet from the mother wavelet, the above definition can be expanded into two-dimensional set of functions using two parameters, shift parameter k and scale parameter j as expressed in (2.15):

$$\Phi_{j,k}(t) = 2^{j/2} \, \Phi(2^j t - k) \tag{2.15}$$

and the span over k is given by:

$$V_j = \overline{\underset{k}{Span}\{\Phi_k(2^j t)\}} = \overline{\underset{k}{Span}\{\Phi_{j,k}(t)\}} \quad \text{for all} \quad k \in Z \, . \tag{2.16}$$

Therefore, if $f(t) \in V_j$ then f(t) can be expressed as

$$f(t) = \sum_k d_{j,k} \, \Phi(2^j t - k) \quad . \tag{2.17}$$

The higher the scale parameter j, the larger the span and also the narrower the scaling function $\Phi_{j,k}(t)$ and ultimately the smaller step is translated which constructs finer details.

The definition of two-dimensional set of functions $\Phi_{j,k}(t)$ and the corresponding span V_j implicitly means that the space that contains high-resolution signal will contain the lower resolution signals as well. The nesting of spanned spaces is expressed as:

$$\cdots V_{-2} \subset V_{-1} \subset V_0 \subset V_1 \subset V_2 \subset \cdots \quad \subset L^2 \, . \tag{2.18}$$

In general, the nesting of the spanned spaces can be written as

$$V_j \subset V_{j+1} \quad j \in Z \tag{2.19}$$

with $V_{-\infty} = \{0\}$ and $V_{\infty} = L^2$.

The element in a space is simply scaled version of the elements in the next space

$$f(t) \in V_j \quad \Leftrightarrow \quad f(2t) \in V_{j+1} \, . \tag{2.20}$$

The relation between the spaces is illustrated in Figure 2.2.

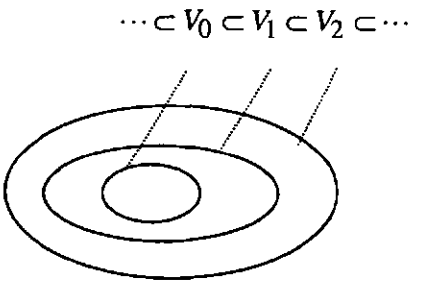

Figure 2.2 Nested spaces spanned by the scaling functions

If $\Phi(t) \in V_0$ which signifies that $\Phi(t)$ is in V_0, it is also in V_1 the space spanned by $\Phi(2t)$. This means $\Phi(t)$ can be expressed in terms of a weighted sum of shifted $\Phi(2t)$

$$\Phi(t) = \sqrt{2} \sum_n h_0(n)\, \Phi(2t - n), \tag{2.21}$$

where the coefficient $h_0(n)$ is a sequence of real or complex numbers called the scaling coefficients or low pass filter sequence and the factor $\sqrt{2}$ is to maintain the norm of the scaling function equal two. The above recursive equation is fundamental in wavelet theory regarding the scaling function and in multiresolution analysis. This equation is usually called *the dilation equation, the refinement equation* or *the multiresolution analysis (MRA) equation* [46,101,102,104,106-109].

2.2.3 Wavelet Function

The signal features can be better analysed or processed efficiently, not by using $\Phi_{j,k}(t)$ and changing j and k, but by using another set of functions $\Psi_{j,k}(t)$, which span the differences

between the spaces spanned by the various scales of the scaling function. This basis is the wavelet functions as used in equation 2.6.

The scaling functions and the wavelet functions have an orthogonal complement property [see section 2.3.8]. The orthogonal complement of V_j (the subspace spanned by $\Phi_{j,k}(t)$) is defined as W_j. Both of them are in V_{j+1}. This means that all members of V_j are orthogonal to all members of W_j. This relation can be written as follows

$$V_1 = V_0 \oplus W_0 . \tag{2.22}$$

It can be extended further to

$$V_2 = V_0 \oplus W_0 \oplus W_1 . \tag{2.23}$$

In general this gives the total space

$$L^2 = V_0 \oplus W_0 \oplus W_1 \oplus \cdots . \tag{2.24}$$

The above relation between subspaces (when it uses V_0 as initial space) is illustrated in Figure 2.3.

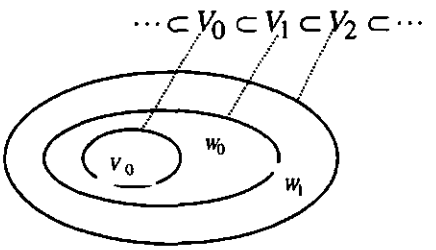

Figure 2.3 Spaces spanned by the scaling functions and the wavelet functions

The scale parameter j for the initial space is arbitrary and can be chosen according the resolution needed. For example $j=10$ will give

$$L^2 = V_{10} \oplus W_{10} \oplus W_{11} \oplus \cdots \tag{2.25}$$

or even $j = -\infty$ which gives

$$L^2 = \cdots W_{-2} \oplus W_{-1} \oplus W_0 \oplus W_1 \oplus W_2 \oplus \cdots . \tag{2.26}$$

Eliminating the scaling space altogether and it becomes the form as in equation 2.6.

Since $W_0 \subset V_1$, W_0 is the subspace spanned by $\Psi(t)$ and V_1 is the subspace spanned by $\Phi(2t)$ then the wavelet functions $\Psi(t)$ can be represented by a weighted sum of shifted scaling function

$$\Psi(t) = \sqrt{2} \sum_n h_1(n)\, \Phi(2t - n) , \tag{2.27}$$

where the coefficients $h_1(n)$ represent a sequence of real or complex numbers called the wavelet coefficients or high pass filter sequence and the factor $\sqrt{2}$ is to maintain the norm of the wavelet function equal two.

From the orthogonal complement property it can be shown [24,64] that the relation between the scaling coefficients and the wavelet coefficients $h_1(n)$ is the mirror image of $h_0(n)$

$$h_1(n) = (-1)^n\, h_0(1 - n) . \tag{2.28}$$

For a finite even length-N, this equation becomes

$$h_1(n) = (-1)^n\, h_0(N - 1 - n) . \tag{2.29}$$

Another important relation emerging from the orthonormality of the wavelet systems is the so-called double *shift orthogonality* [45,101,110]

$$\sum_n h_0(n)\, h_0(n + 2k) = \delta(k) . \tag{2.30}$$

Equation 2.27 gives the mother wavelet $\Psi(t)$ with which the equation 2.10 further gives the daughter wavelets.

The following figures depict some examples of scaling function and the correspondent wavelet function, the simplest wavelet, i.e. Haar wavelets [101-103] in Figure 2.4, Daubechies wavelets [101-103] in Figure 2.5, and biorthogonal wavelets (analysis and synthesis wavelets) [101] in Figure 2.6.

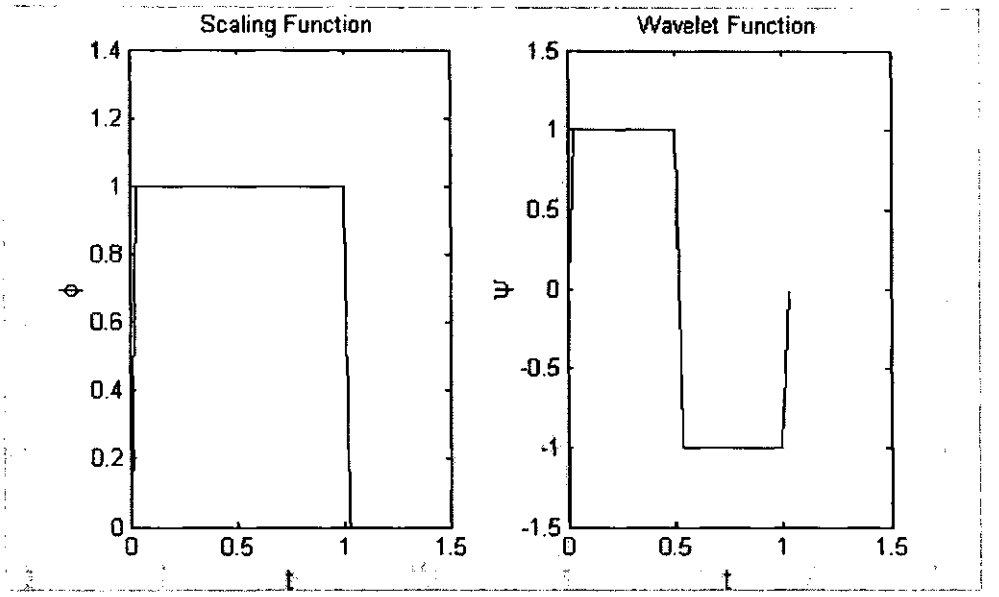

Figure 2.4 Haar scaling function and wavelet function

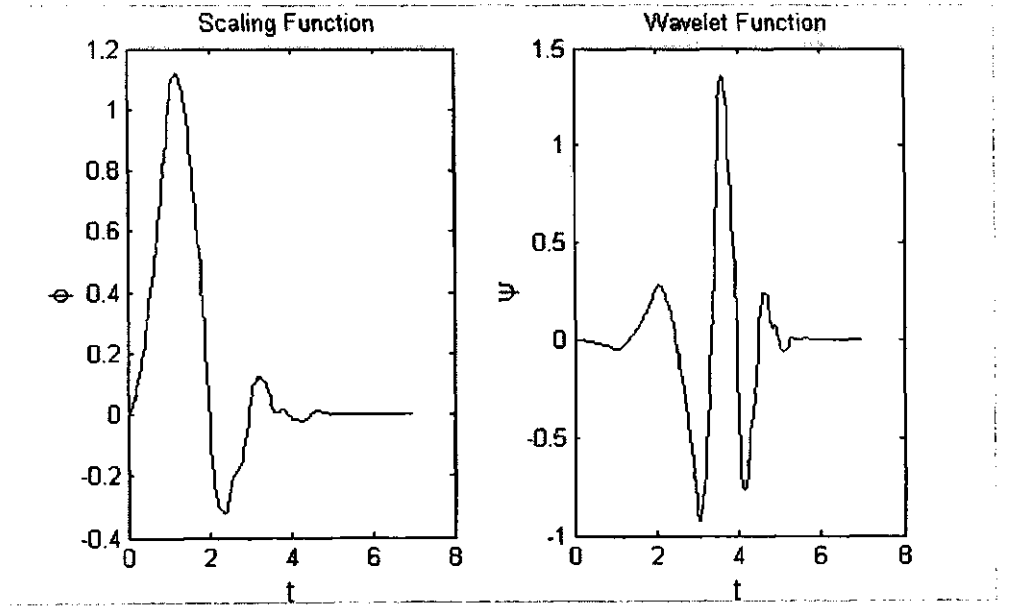

Figure 2.5 Daubechies-4 scaling function and wavelet function

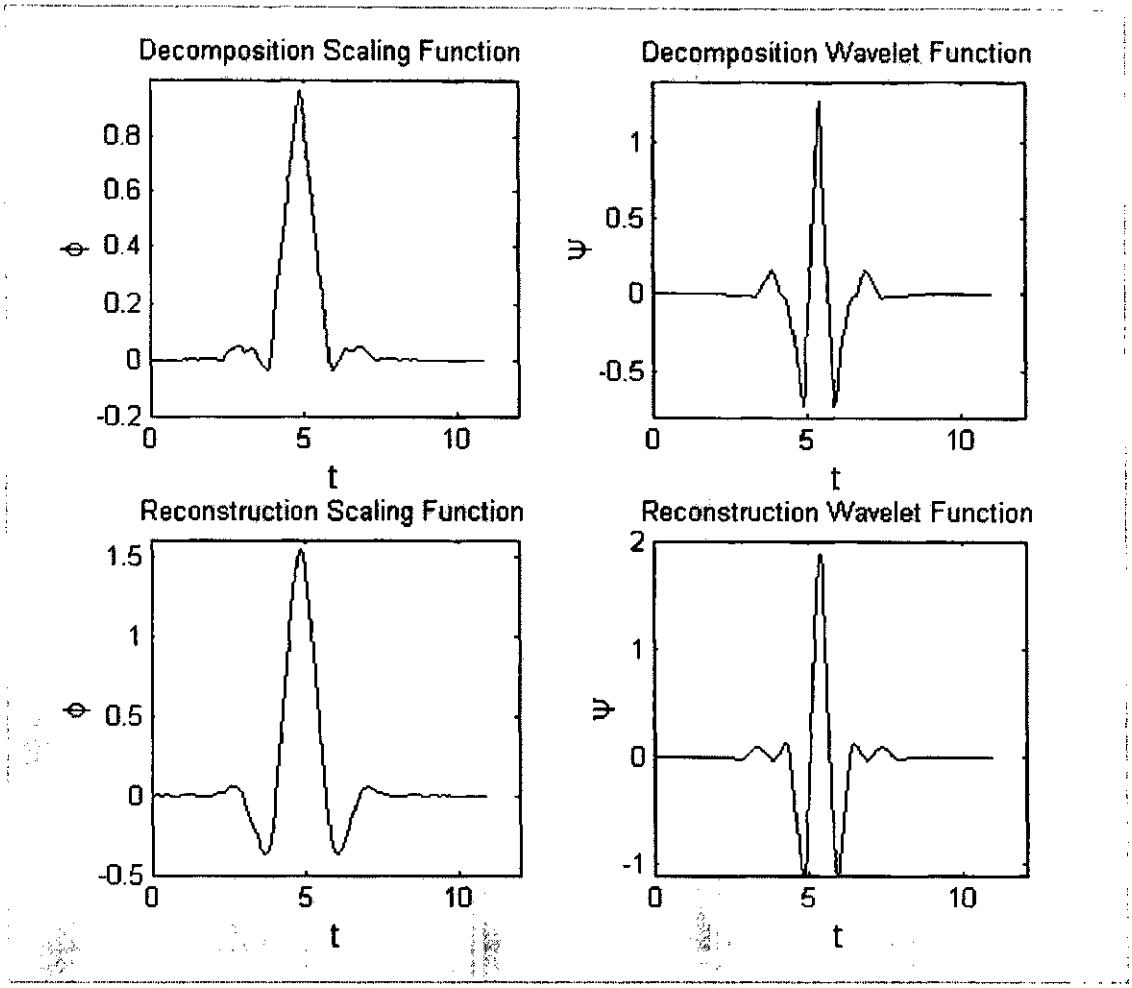

Figure 2.6 Biorthogonal 5.5 scaling functions and wavelet functions

2.2.4 Discrete Wavelet Transform

Analog to the Fourier series analysis, the discrete wavelet transform can be used for analysis, description, approximation and filtering of signals, but is more flexible and informative [101]. Unlike Fourier series analysis, it can be applied to non-periodic transient signals with a satisfying result.

As discussed in section 2.2.3, since $L^2 = V_{j_0} \oplus W_{j_0} \oplus W_{j_0+1} \oplus W_{j_0+2} \oplus \cdots$, (2.31)

any function $f(t) \in L^2$ can be decomposed into the elements of those subspaces $V_{j_0}, W_{j_0}, W_{j_0+1}, W_{j_0+2}, \cdots$. Therefore this function can be written as

$$f(t) = \sum_k c_{j_0}(k)\,\Phi_{j_0,k}(t) + \sum_k \sum_{j=j_0}^{\infty} d_j(k)\,\Psi_{j,k}(t), \tag{2.32}$$

or in a complete form

$$f(t) = 2^{\frac{j_0}{2}} \sum_k c_{j_0}(k)\,\Phi(2^{j_0}t - k) + 2^{\frac{j_0}{2}} \sum_k \sum_{j=j_0}^{\infty} d_j(k)\,\Psi(2^{j_0}t - k). \tag{2.33}$$

The parameter j_0 could be any integer according to the coarsest scale needed. If j_0 zero then the above equation becomes

$$f(t) = \sum_k c_0(k)\,\Phi(t-k) + \sum_k \sum_{j=0}^{\infty} d_j(k)\,\Psi(2^j t - k). \tag{2.34}$$

The coefficients of this wavelet analysis are called *discrete wavelet transform (DWT)*. If the wavelet systems are orthogonal, these coefficients can be calculated from the inner products

$$c_{j_0}(k) = \langle f(t), \Phi_{j_0,k}(t) \rangle = \int f(t)\,\Phi_{j_0,k}(t)\,dt, \tag{2.35}$$

$$d_j(k) = \langle f(t), \Psi_{j,k}(t) \rangle = \int f(t)\,\Psi_{j,k}(t)\,dt. \tag{2.36}$$

If the scaling and wavelet functions form an orthonormal basis, the signal energy is spread into its components without any loss as stated by *Parseval's theorem* [101,107,108]

$$\int |f(t)|^2\,dt = \sum_{k=-\infty}^{\infty} |c_{j_0}(k)|^2 + \sum_{j=j_0}^{\infty} \sum_{k=-\infty}^{\infty} |d_j(k)|^2. \tag{2.37}$$

It can be seen from the right side of the above equation, that the energy in the wavelet analysis domain is partitioned in time by k and in scale by j.

Here orthonormal basis means (see section 2.5 for more detail):

1. The scaling functions are orthonormal to each other:

$$\int_{-\infty}^{\infty} \Phi(t-k)\,\Phi(t-l)\,dt = \delta(k-l) \tag{2.38}$$

2. The wavelet at all scales are orthonormal:

$$\int_{-\infty}^{\infty} \Psi(2^i t-k)\,\Psi(2^j t-l)\,dt = \delta(i-j)\,\delta(k-l) \tag{2.39}$$

3. The scaling function are orthogonal to the wavelets:

$$\int_{-\infty}^{\infty} \Psi(2^i t-k)\,\Psi(2^j t-l)\,dt = \delta(i-j)\,\delta(k-l) \tag{2.40}$$

2.2.5 Time-Frequency Tiling

As stated by Parseval's theorem, if the basis functions are orthogonal and a signal is decomposed into some terms of these basis functions, the signal energy is partitioned into these terms in its transformed domain.

On the other hand, in multiresolution analysis (MRA) theory there is a time-frequency uncertainty principle that states [50,111]:

$$\Delta_t \Delta_\omega \leq \frac{1}{2} \tag{2.41}$$

where $\Delta_t = \sqrt{\overline{(t-\bar{t})^2}}$ is time resolution and $\Delta_\omega = \sqrt{\overline{(\omega-\bar{\omega})^2}}$ is frequency resolution. It is clear that there is always trade-off between time resolution and frequency resolution associated with a given basis.

Therefore each function can be represented as a tile in the time-frequency plane where its energy is concentrated. Non-overlapping tiles show an orthogonality between basis functions.

Under this assumption, the time-frequency tiles for standard basis in time domain (Dirac delta function, time division multiplexing (TDM) systems) and in frequency domain (Fourier series analysis, frequency division multiplexing (FDM) systems) are shown in Figure 2.7 (a) and (b) respectively. As can be seen, both standard bases give either time localisation or frequency localisation only.

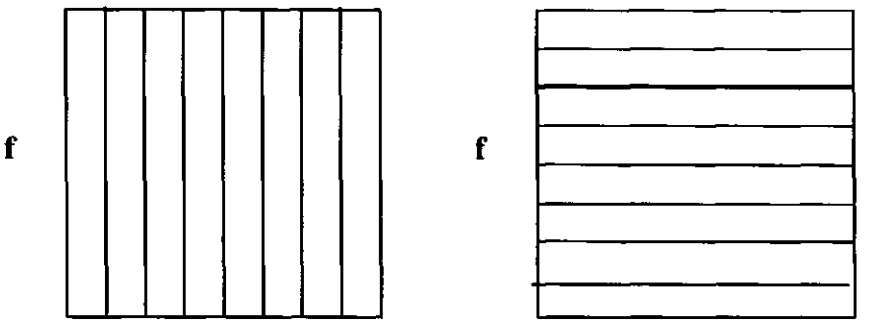

(a) (b)

Figure 2.7 Standard basis for (a) time domain basis (b) frequency domain basis

STFT (short-time frequency transform) which uses a window function partially fixes the lack of time localisation of Fourier transform [45,100,101]. However since the duration of window function is fixed, the STFT provides a fixed time-frequency resolution. This is illustrated in Figure 2.8 (a) and (b) for a narrow window and a wide window respectively.

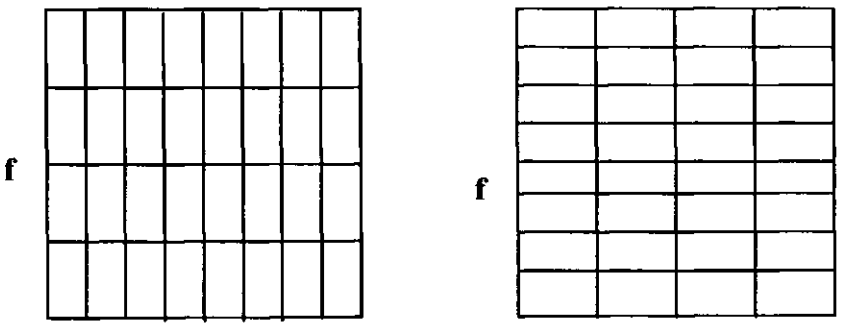

(a) (b)

Figure 2.8 STFT basis a. narrow-window b. wide-window

Discrete wavelet transform basis is generated by dilation and translation of a mother Wavelet as discussed earlier. The utilisation of the scale parameter leads to non-uniform or multiresolution tiles in the time-frequency plane. This two-band wavelet basis characteristic is shown in Figure 2.9.

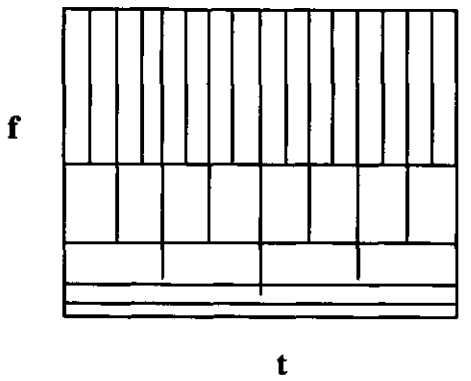

Figure 2.9 Two-band wavelet basis

2.2.6 Orthogonal Wavelet Functions

There are several advantages emerged by the orthogonality between the scaling function and the wavelet function. Orthogonal basis functions allow simple calculation of decomposition coefficients as defined in equation 2.6. It also allows partitioning the signal energy in the wavelet transform domain according to the Parseval's theorem [see section 2.2.4].

This orthogonality property covers three types of orthogonality characteristic as follows:

1. Intrascale orthonormality of scaling functions: $<\Phi_{j,k}(t),\Phi_{j,k'}(t)>=\delta_{kk'}$ (2.42)

2. Intra and interscale orthonormalities of wavelet functions:

$$<\Psi_{j,k}(t),\Psi_{j',k'}(t)>=\delta_{jj'}\delta_{kk'} \quad (2.43)$$

3. Complementary property of wavelet and scaling functions:

$$<\Psi_{j,k}(t),\Phi_{j',k'}(t)>=0 \quad (2.44)$$

where j is the scale parameter and k is the shift parameter.

2.2.7 Biorthogonal Wavelet Functions

Introducing dual basis (dual scaling function and dual wavelet function) beside original basis (scaling function and wavelet function) with certain conditions change the system from orthogonal system into biorthogonal system. Using the structure model as in Figure 2.11, the dual scaling function and the dual wavelet function with the corresponding scaling function and wavelet function are as follows

$$\Phi(t) = \sqrt{2} \sum_n h_0(n)\, \Phi(2t-n)\,, \tag{2.45}$$

$$\tilde{\Phi}(t) = \sqrt{2} \sum_n f_0(n)\, \tilde{\Phi}(2t-n)\,, \tag{2.46}$$

$$\Psi(t) = \sqrt{2} \sum_n h_1(n)\, \Phi(2t-n)\,, \tag{2.47}$$

$$\tilde{\Psi}(t) = \sqrt{2} \sum_n f_1(n)\, \tilde{\Phi}(2t-n)\,. \tag{2.48}$$

The conditions are cross-related between the filters as follows

$$h_1(n) = (-1)^n\, f_0(1-n)\,, \tag{2.49}$$

$$f_1(n) = (-1)^n\, h_0(1-n)\,. \tag{2.50}$$

For a finite even length-N, these equations become

$$h_1(n) = (-1)^n\, f_0(N-1-n)\,, \tag{2.51}$$

$$f_1(n) = (-1)^n\, h_0(N-1-n)\,, \tag{2.52}$$

and the biorthogonality involves both the filters and their dual filters

$$\sum_n h_0(n) f_0(n+2k) = \delta(k) \tag{2.53}$$

or in a more complete form

$$\sum_n h_i(n) f_j(n+2k) = \delta(k)\,\delta(i-j)\,. \tag{2.54}$$

2.3 M-Band Wavelet Systems

The original wavelet systems have a scale multiplier M = 2 to give two-band division in each stage (the concept of octave), a binary tree for Mallat fast algorithm, constant-Q or logarithmic frequency bandwidth [45,46,101,112]. It can be extended into general scale multiplier of M to meet some specific applications which need a more flexible tiling rather than two-band, for example, a multicarrier modulation system which needs a uniform bandwidth division rather than logarithmic bandwidth division.

The dilation equation for general M-band wavelet system is as follows [112].

The scaling function $\Psi_0(t)$ is given by Steffen et al [112]

$$\Psi_0(t) = \sqrt{M}\sum_{k=0}^{N-1} h_0(k)\,\Psi_0(Mt-k), \tag{2.55}$$

and the corresponding wavelet functions $\Psi_l(t), l = 1,\ldots\ M-1$ are as follow [112]

$$\Psi_l(t) = \sqrt{M}\sum_{k=0}^{N-1} h_l(k)\,\Psi_0(Mt-k). \tag{2.56}$$

Figure 2.10 presents an example of M-band wavelet system with the number of subbands M=16 for subband l = 0, 2, 7 and 15 in Fig. 2.11 (a), (b), (c) and (d) respectively. The corresponding power spectral densities are depicted in Figure 2.11.

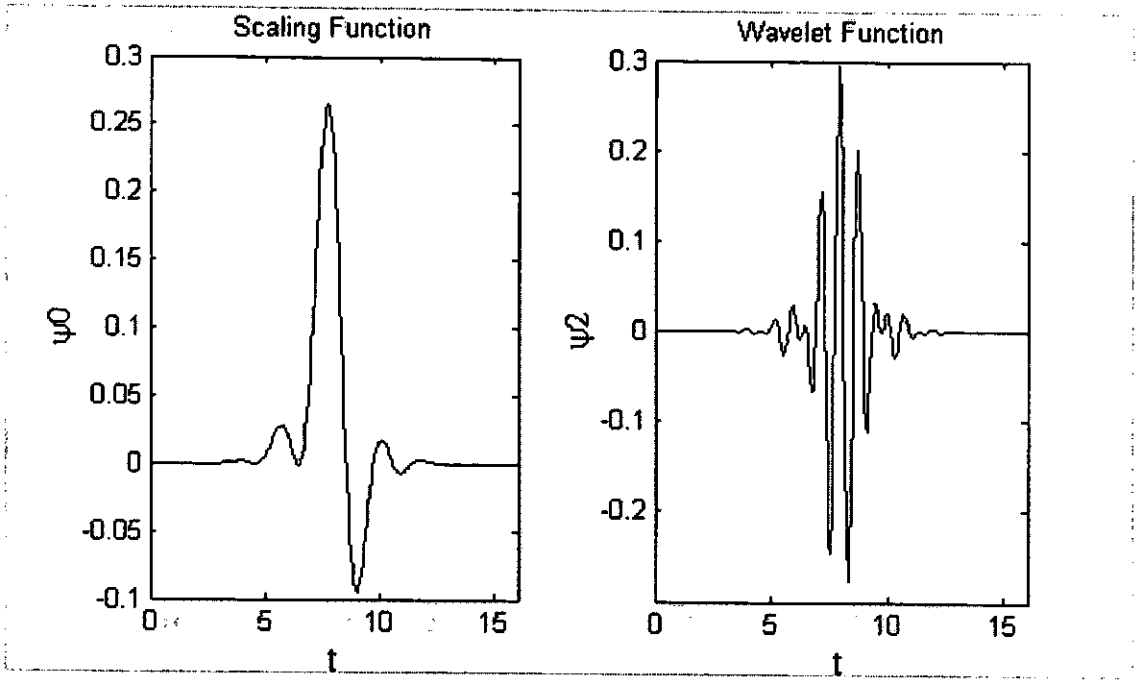

(a)

(b)

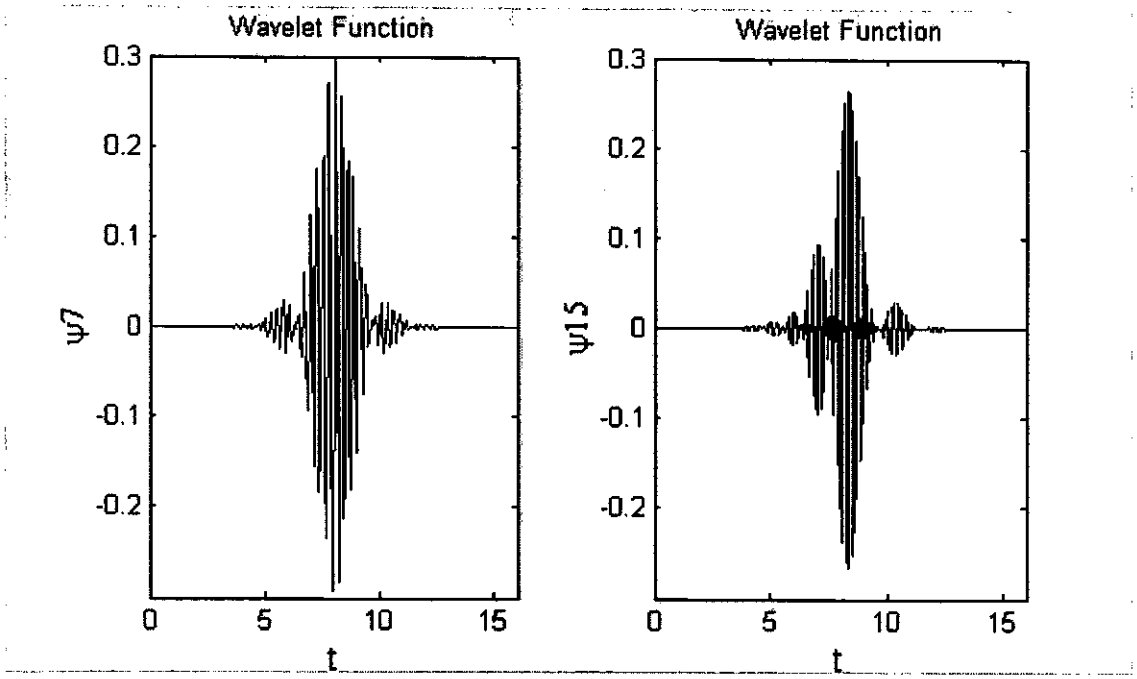

(c)

(d)

Figure 2.10 M-band wavelet system with M=16 for

(a) l = 0, (b) l = 2, (c) l = 7 and (d) l = 15

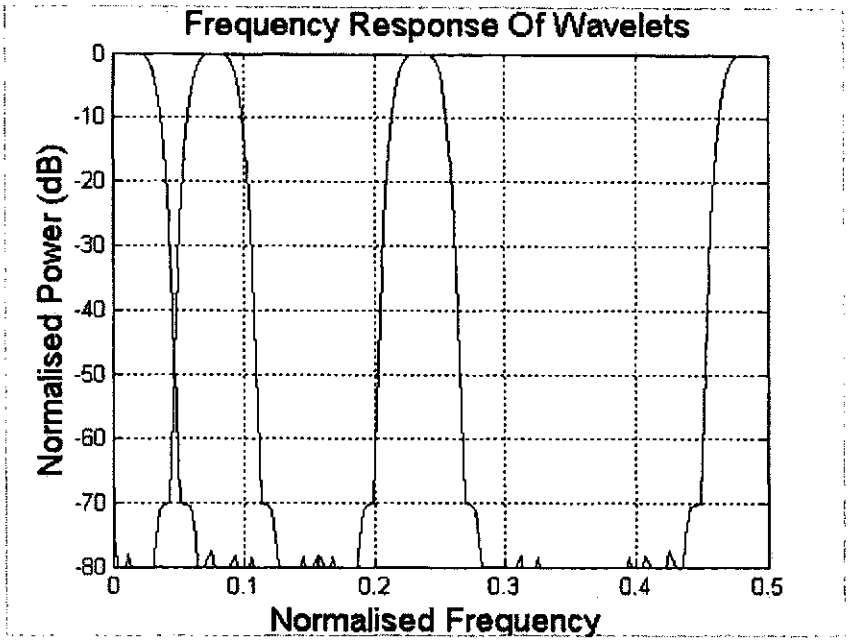

Figure 2.11 The power spectral densities of the M-band wavelets

2.4 Filter Banks

A filter bank is a structure that decomposes a signal into subsignals (or subband signals). After some processing which depends on the applications (transmission, signal compression etc.), these subband signals should be well reconstructed. A filter bank consists of a set of filters and down samplers at the analysis part and a set of up samplers and filters at the synthesis part. A two-band filter bank which has two filters, LPF and HPF for both analysis and synthesis sides is illustrated in the following figure.

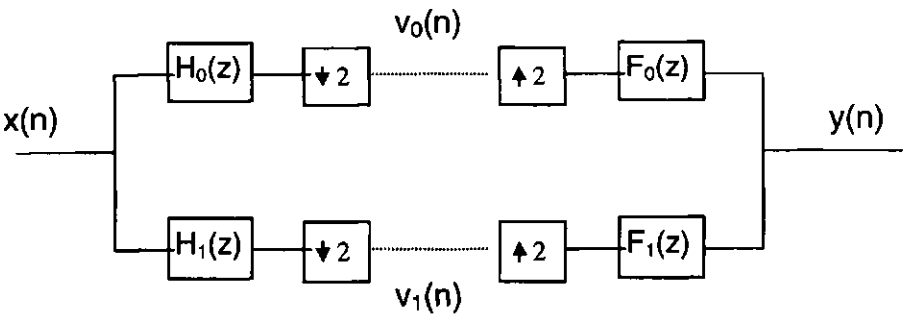

Figure 2.12 2-band filter bank

The problem of this structure involves the design of the analysis filters and the synthesis filters with the goals :

1. Perfect Reconstruction (i.e. $y(n)=x(n)$)

In order to retrieve the original signal at the output so that the filter bank meets perfect reconstruction condition or biorthogonal, there are two conditions: [45,110]

- No distortion: The output signal has the same amplitude as the original input signal or it is the same signal with a certain delay.

$$F_0(z)\,H_0(z)+F_1(z)H_1(z)=2\,z^{-l} \tag{2.57}$$

- Alias cancellation : There is no interference between subchannels

$$F_0(z)\,H_0(-z)+F_1(z)H_1(-z)=0 \tag{2.58}$$

Further calculation is done leading to the following results [45,110]

$$H_0(z)\,H_0(z^{-1})+H_0(-z)\,H_0(-z^{-1})=2 \tag{2.59}$$

$$H_1(z)=z^{-(N-1)}\,H_0(-z^{-1}) \tag{2.60}$$

$$F_0(z)=H_1(-z) \tag{2.61}$$

$$F_1(z)=-H_0(-z) \tag{2.62}$$

2. It meets the desired frequency characteristic. It should satisfy some constraints imposed by certain applications.

It can be further shown that equations (2.59), (2.61) and (2.62) constitute the z-transform of equations (2.53), (2.49) and (2.50), respectively, which indicate the linkage between wavelet systems and filter banks.

In many applications one does not have to deal directly with the scaling functions and the wavelet functions. Only the coefficients $h_0(n), h_1(n)$ and $c(k), d_j(k)$ need to be

considered. Indeed in this filter bank structure those coefficients are viewed as digital filters and digital signals respectively. Further discussion about filter bank can be found in [45,46,53,110,113,114].

2.5 Transmultiplexer Systems

A transmultiplexer is a structure that combines a collection of signals into a single signal by expanding the rate and/or the bandwidth. It can be regarded as the reverse of filter bank. The upsampling and the synthesis process come first in the transmitter side and the analysis and the downsampling process come later on in the receiver side.

The problem in transmultiplexer systems is how to design the synthesis filters and the analysis filters with the following goals :

1. Ensuring perfect reconstruction (i.e. $y_i(n)=x_i(n)$)
2. The frequency response of the filters meets the constraints imposed by certain applications.
3. Simple to design and to implement.

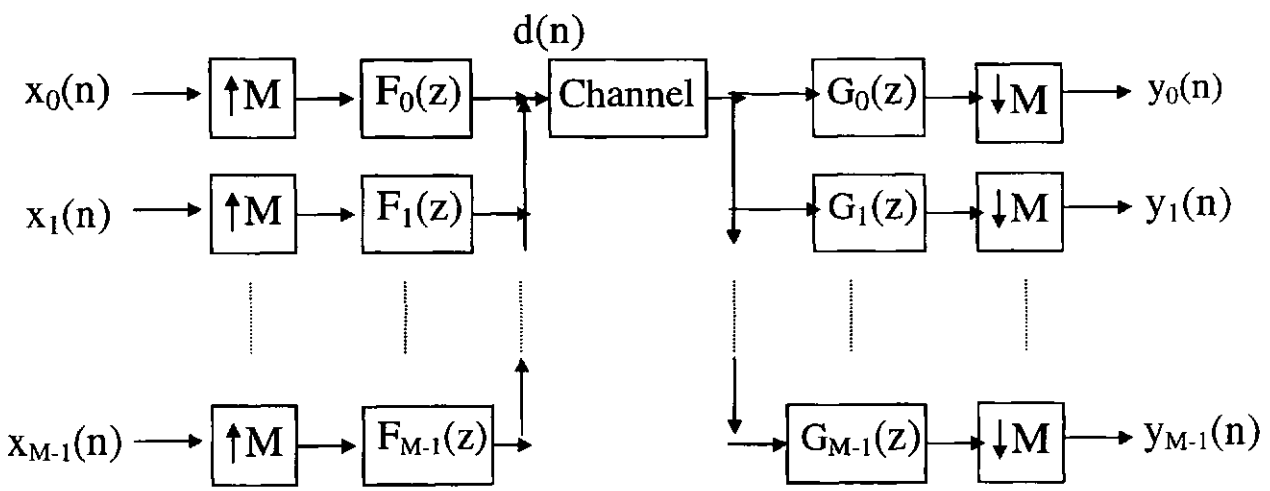

Figure 2.13 a transmultiplexer system

There are three ways to see whether the transmultiplexer is perfectly reconstructed or not, i.e. direct characterisation, matrix characterisation, z-transform domain [110,112,115]. In order to give an idea, just take an example in time domain or some say direct characterisation.

Since an arbitrary signal is a linear superposition of impulses, the input signal can be taken as

$$x_i(n) = \delta(n)\,\delta(i-j) \tag{2.63}$$

for all i and j then the output of synthesis part is

$$d(n) = f_j(n) \tag{2.64}$$

and the output of analysis part is

$$y_i(k) = \sum_n g_i(n) d(Mk-n) = \sum_n g_i(n) f_j(Mk-n). \tag{2.65}$$

In order to be perfect reconstructed (PR), the following equation has to be satisfied:

$$y_i(k) = \delta(k)\,\delta(i-j). \tag{2.66}$$

Hence a transmultiplexer is PR if and only if

$$\sum_n g_i(n) f_j(Mk-n) = \delta(k)\delta(i-j). \tag{2.67}$$

On the other hand, the concept of orthogonality is important in communication systems especially when some users utilise the same media of communications (multiple access) so that each user can be distinguished by an orthogonal function from the other users.

Conventional digital communication systems can be described using the above transmultiplexer structure, which consists of a synthesis part and an analysis part. The element that plays an important role to characterise the system is the filter set used in both synthesis and analysis parts. The time-frequency properties of these filters, i.e. time spread and frequency spread, determine the type of communication systems. The other factors which also involve are the number of users accessing the system simultaneously (single or multi

user), and the number of carriers used (single or multi carrier). Considering all these factors, digital communication systems can be categorised as described in the following sections.

2.5.1 Multi-User Single-Carrier Communication Systems

If each input branch has a signal comes from a user using single carrier system and the other branches that fed with some signals come from different users then the system becomes a multi-user single-carrier communications system. Here the filter used in each branch is also known as *user code*. It can be further distinguished as very well-known systems as follows:

2.5.1.1 FDMA (Frequency Division Multiple Access)

When the filter used is like a brick-wall shaped band pass filter in ideal case or the time spread is large and the frequency spread is small then the system tends to be an FDMA system. Here the communication channel is divided into disjoint frequency subchannels that are allocated for users. A user has its own frequency subband.

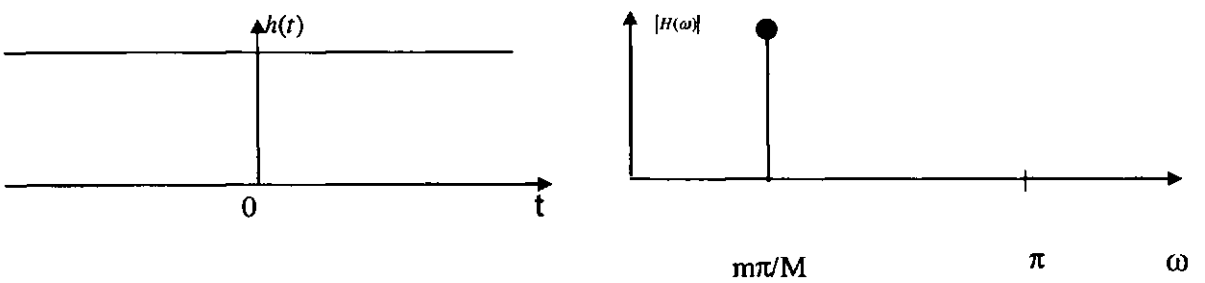

(a) (b)

Figure 2.14 The ideal filters (codes) for FDMA case

a. Filter response in time domain b. filter response in frequency domain

Those filters can be written as

$$f_m(t) = e^{j2\pi f_m t}, \tag{2.68}$$

where f_m is carrier frequency.

2.5.1.2 TDMA (Time Division Multiple Access)

When the user code is like a unit sample function (Dirac delta function) in ideal case or in other words the time spread is small and the frequency spread is large then the system tends to be a TDMA system. In this system, a user has its own dedicated time slot for communication with other user and uses the whole communication channel during the given time slot.

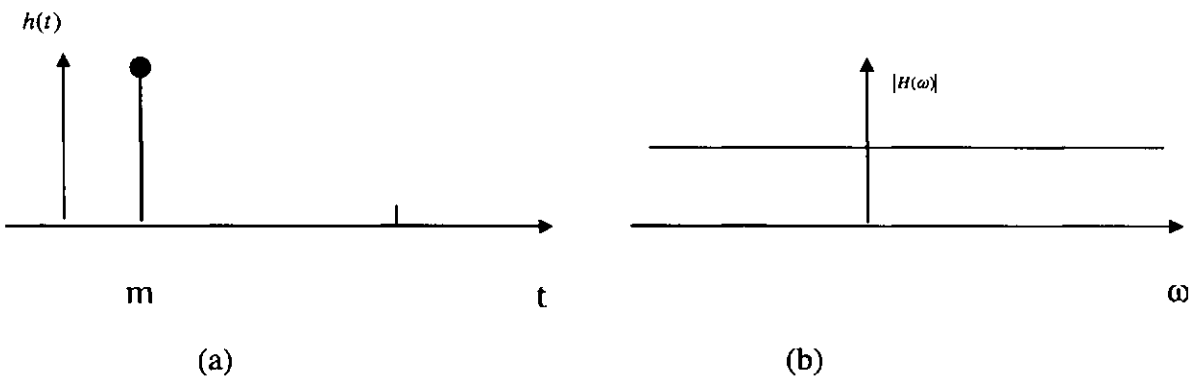

Figure 2.15 The ideal filters (codes) for TDMA case

a. filter response in time domain b. filter response in frequency domain

The filter can be written in time domain as follows:

$$f_m(t) = \delta(t-m) \qquad m = 0, 1, \cdots, M-1 . \tag{2.69}$$

2.5.1.3 CDMA (Code Division Multiple Access)

The emerging research in CDMA communication systems employs user codes or filters which are spread both in time domain and in frequency domain. In a CDMA communication system, the desired user code should jointly satisfy the following time-frequency condition [45,116] :

- The orthogonal user codes can not be unit sample functions in the time domain. This prevents the system from becoming a TDMA system.
- The orthogonal user codes should be allpass like spread spectrum functions with minimised intercode and intracode correlations. This condition assures that the communications scheme can not become an FDMA type.

The filter used can be modelled as:

$$f_m(t) = c_m(t) \tag{2.70}$$

where $c_m(t)$: user's code

2.5.2 Single-User Multi-Carrier Communication Systems

When all input branches come from a user but with different carriers or different frequency responses of filters then the system becomes a single-user multi-carrier communication system. Here the filter used in each branch tends to be a FDMA type to serve as a single subcarrier. As mentioned before in section 2.5.1, the filter used is a band pass filter or in other words the time spread is large and the frequency spread is small. A well-known system that can be categorised in this single-user multi-carrier communication system is discrete multitone (DMT) or orthogonal frequency division multiplexing (OFDM). DMT is used in asynchronous digital subscriber lines (ADSL) and high-bit-rate digital subscriber lines (HDSL) for copper cable transmission which can increase the transmission rate up to 8 Mbps. OFDM is used for digital audio broadcasting (DAB) and digital video broadcasting (DVB) [20,21].

This multicarrier modulation system can be interpreted as a transmultiplexer that takes time division multiplexed (TDM) data and transforms it to frequency division multiplexed (FDM) [64]. Discrete Fourier transform (DFT) is used to implement this multicarrier modulation

technique because it exhibits the desired orthogonality and can be implemented with fast algorithm using a single integrated circuit (IC). Another advantage is decreasing the effect of channel delay spread due to its longer symbol period.

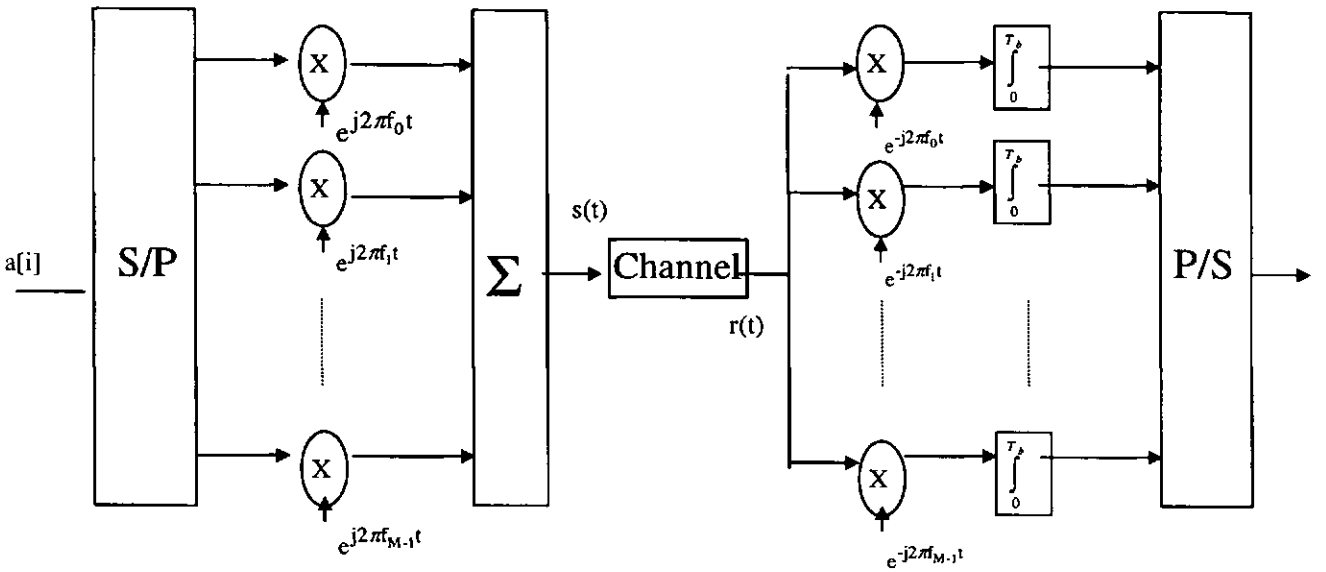

Figure 2.16 The simple model of OFDM transceiver systems

The filter used for OFDM system that is based on Fourier transform can be written as:

$$f_m(n) = e^{j2\pi \frac{mn}{M}} \tag{2.71}$$

$$x_m(n) = a(nM + m) \tag{2.72}$$

where a(n) is data signal.

Another transform, namely the so-called discrete wavelet multitone (DWMT) was proposed by Tzannes et al for multicarrier modulation [73-76] applied for cable transmission. DWMT uses a set of cosine modulated filters possessing an inherent robustness against intersymbol interference (ISI) and narrow band channel noise [73-76]. Daneshgaran et al proposed

another form of wavelets which is wavelet packet transform for multicarrier modulation [117,118].

Multi-carrier modulation in conjunction with coding and interleaving is powerful for combating severe wireless channel impairments [31,119,120]. For instance in broadcasting system (audio and video), it is possible for all transmitters to use the same frequency (single frequency network (SFN)). In this case, it can be viewed as an extreme form of multipath environment.

This system is also suitable for high bit rate data signal because it is a parallel transmission. The incoming high bit rate data stream will be divided into a number of subcarriers each of which has much smaller bit rate.

Using a certain bit allocation algorithm, this system can enhance the capacity. When the channel's quality changes with time and not flat for all frequency, this system can tailor the data rate according to the subchannel's quality. In this way, this system can handle higher data rate like the case in DSL (digital subscriber line) system for copper cable transmission. The MCM also has higher spectrum efficiency because it allows the spectra of subchannels overlap.

The disadvantages of MCM system are as follows. First, it needs a rigid synchronisation in time and frequency. This is to preserve the orthogonality between subchannels. Second, there is a problem with peak to average power ratio (PAPR) parameter [20,21,121]. This parameter is important to measure the degree of harmonic effect when the signal is fed through non linear power amplifier.

2.5.3 Multi-User Multi-Carrier Communication Systems

In this system there are two stages of orthogonality, firstly orthogonality between users by using different spreading codes and secondly orthogonality between subcarriers or subchannels using orthogonal transform like DFT, DWT etc. Basically this system is a combination of CDMA and multicarrier modulation. It can also be seen as two stages transmultiplexers where the first stage gives an orthogonality between users by using different spreading codes or a set of filters and the second stage gives an orthogonality between subcarriers or subchannels by another set of filters.

This combination of CDMA and multicarrier modulation mainly has two schemes. The first scheme spreads the original data stream using a given spreading code and each chip modulates its own subcarrier or in other words *the spreading is performed in frequency domain*. This system is called multi-carrier code division multiple access (MC-CDMA) [22-25,33-35].

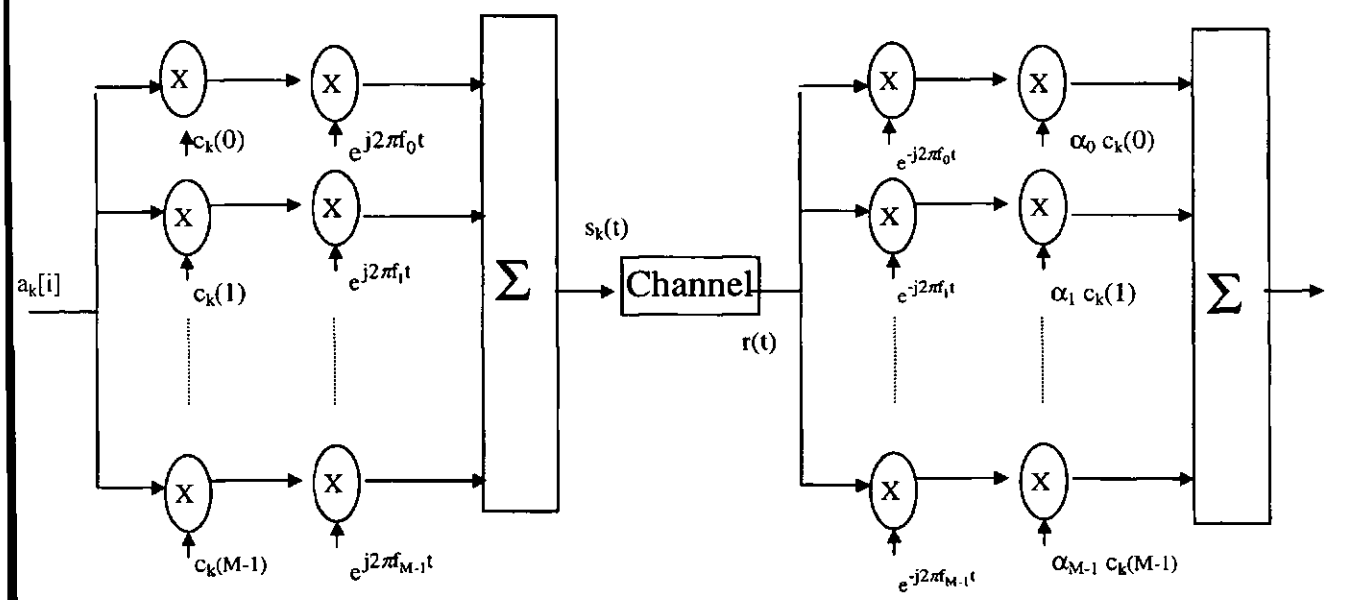

Figure 2.17 The model of MC-CDMA transceiver systems

The filters used in these MC-CDMA systems, for Fourier-based, are

$$f_m(n) = e^{j2\pi\frac{mn}{M}}, \tag{2.73}$$

and the branch signal is $x_{k,m}(n) = a_k(n)\, c_k(m)$, (2.74)

where a_k is k^{th} user's input data signal, k denotes k^{th} *user* and m denotes m^{th} subchannel. The second scheme of multi user multi carrier system spreads the serial-to-parallel converted data streams by multiplying its with user's code and then each spread data stream modulates its own subcarrier or in other words *the spreading is performed in time domain.* This system is called multi-carrier direct sequence code division multiple access (MC-DS-CDMA) [23,37,38].

The filter used for this MC-DS-CDMA is

$$f_m(n) = e^{j2\pi\frac{mn}{M}} \tag{2.75}$$

and the branch signal is

$$x_{k,m}(n) = a_k(nM + m)\, c_k(n), \tag{2.76}$$

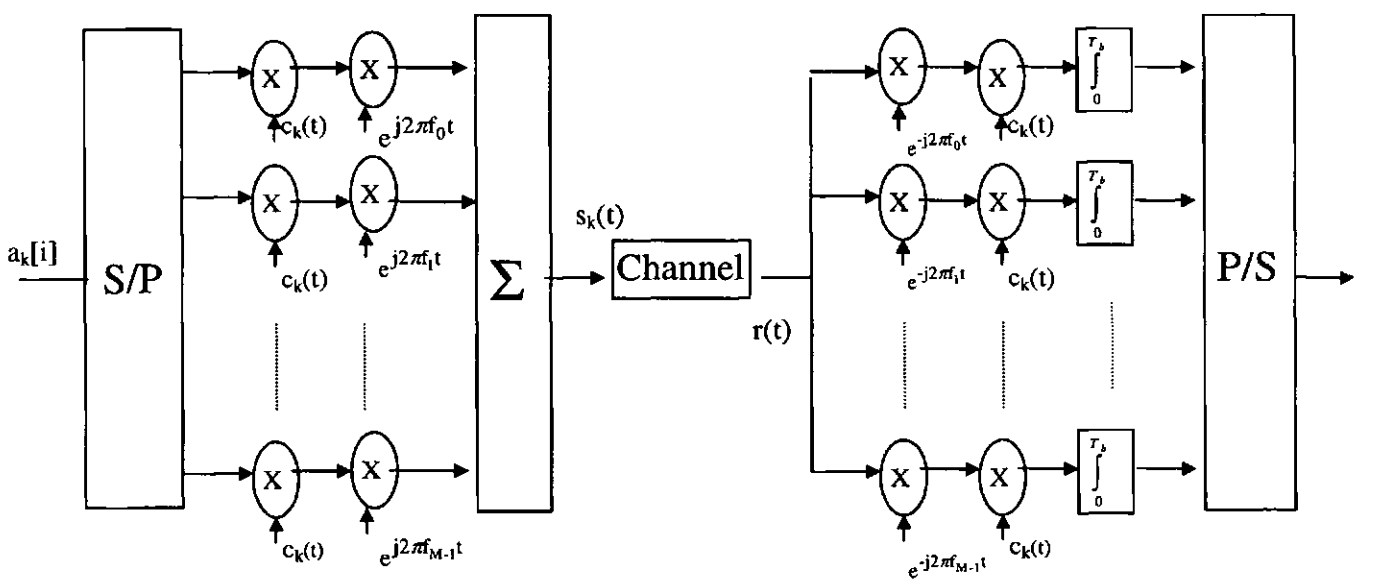

Figure 2.18 The model of MC-DS-CDMA transceiver systems

where a_k is the k^{th} user's input data signal, k denotes the k^{th} *user* and m denotes the m^{th} subchannel.

In practice it is easier to exploit the received signal scattered in frequency domain than in time domain. That is why MC-CDMA with appropriate detection strategy outperforms the other systems (DS-CDMA, MC-DS-CDMA) [22,23,39-42].

In an MC-CDMA system the user's data signal is copied and then multiplied by the corresponding chip of user's code to all available subchannels. So the transmitted signal gains a diversity in frequency domain. When the signal is transmitted over frequency selective fading channel, only some of the subband signals will be affected and also not entirely destroyed. Using an appropriate combining method and detection strategy the original data symbol still can be recovered.

The spreading of the data signal is performed in frequency domain using the user's code, the chip period (T_c) is equal to the data signal period (T_b) unlike in DS-CDMA where $T_c << T_b$. It is therefore easier to implement for MC-CDMA than DS-CDMA especially when the user's data signal has very high bit rate. It also makes the time synchronisation process easier.

Practically in DS-CDMA it is impossible to get full capacity (i.e. the number of users is equal to the processing gain) because of multiple access interference (MAI) and self interference (SI). MAI appears as a result of imperfect cross correlation between user's code when the signal is transmitted through non ideal channel. Self interference is a result of imperfect auto correlation of the corresponding user's code. As MC-CDMA has frequency diversity, practically it is easier to recover the data signal using appropriate combining

method and detection strategy. Therefore the effect of MAI and SI is considerably reduced which in turn enhances the performance.

CHAPTER III

WAVELET-BASED MULTICARRIER CDMA SYSTEMS

The first generation (1G) mobile communication system is analogue system offering only voice services. The second generation (2G) mobile communication system is narrow band digital system offering digital voice, messaging and low rate data services so that this 2G is more spectrum-efficient than 1G. The third generation (3G) mobile communication systems (UMTS, CDMA2000) [3] offer high bit rate data services such as video on demand, video communications and interactive games. The next generation mobile communication system that is currently discussed in some international telecommunication bodies (ETSI, ITU, American PCIA, etc) provides even higher rate data services. This system also requires an enhanced spectrum efficiency and a higher capacity. This thesis is trying to design a new system for cellular air interface in term of multiple access and which fulfil these requirements. Other important issue is the wireless channel impairment.

MC-CDMA system can provide the solution for those issues. This system can maximise the capacity (i.e. the number of users is equal to the processing gain). The system symbol period is larger than conventional CDMA which makes this system suitable for high bit rate data service. MC-CMDA has also frequency diversity to combat the severe multipath channel and it has been shown that MC-CDMA system with appropriate detection method outperforms the other systems (DS-CDMA, MC-DS-CDMA) [22,23,39-42]. The spectra of MC-CDMA is also overlap that makes this system is bandwidth-efficient.

In order to enhance the spectrum efficiency and also to reduce the effect of interchannel interference (ICI) we propose to use M-band wavelet basis instead of DFT basis conventionally used. We call this system wavelet-based multi-carrier CDMA (WB-MC-CDMA) system.

3.1 Wavelet-based Multicarrier System

There are at least three ways to implement a transmultiplexer structure described in section 2.5 or a multicarrier system with wavelet basis:

1. Using 2-band discrete wavelet transform (DWT) [45,122]

Two-band discrete wavelet transform with pyramid algorithm will give dyadic or logarithmic band division. In order to get M-band division, this wavelet method needs $\log_2(M)$ stages or levels. This method is given in Figure 3.1.

The 2-band wavelet analysis filter bank decomposes a broadband signal into a collection of successively more bandlimited components or subband signals. A 3-level filter bank structure is shown in Figure 3.1 which gives 4 non uniform subband signals. In order to build a transmultiplexer or a multicarrier modulation system, the synthesis filters are used in the transmitter and the counter part analysis filters are applied in the receiver side. The transmitter composes the subband signals into a more broadband signal ready to be transmitted through the channel.

In the analysis filters shown in the figure, at each level, the low-frequency output of the previous level is decomposed into adjacent high and low frequency subbands by a high-pass (HP) and low-pass (LP) filter pair. Each of the two output subbands is half the bandwidth of the input signal to that level. The bandlimited output of each filter is maximally decimated by a factor of two to preserve the bit rate of the original signal.

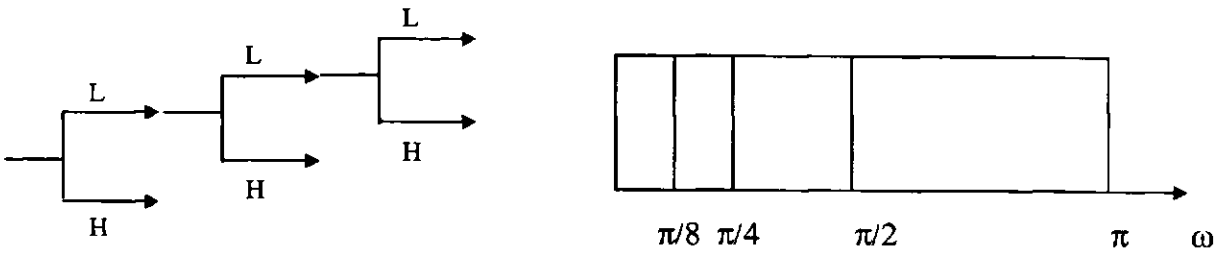

Figure 3.1 (a). 2-band fast wavelet transform with pyramid algorithm
(b). Dyadic bandwidth division

2. Using wavelet packet systems [60,117,118,123,124]

Wavelet packet transform (WPT) with the same two filters as 2-band DWT produces full subband tree instead of dyadic tree. In the analysis filters depicted in Figure 3.2, at each level, instead of the low-frequency in 2-band DWT, both low and high frequency outputs of the previous level is decomposed into other high and low frequency subbands by a high-pass (HP) and low-pass (LP) filter pair. The same as in 2-band DWT, each of the two output subbands is half the bandwidth of the input signal to that level. By doing so WPT provides M-equal bands division. A 3-level filter bank structure is shown in Figure 3.2 which generates 8 uniform subband signals.

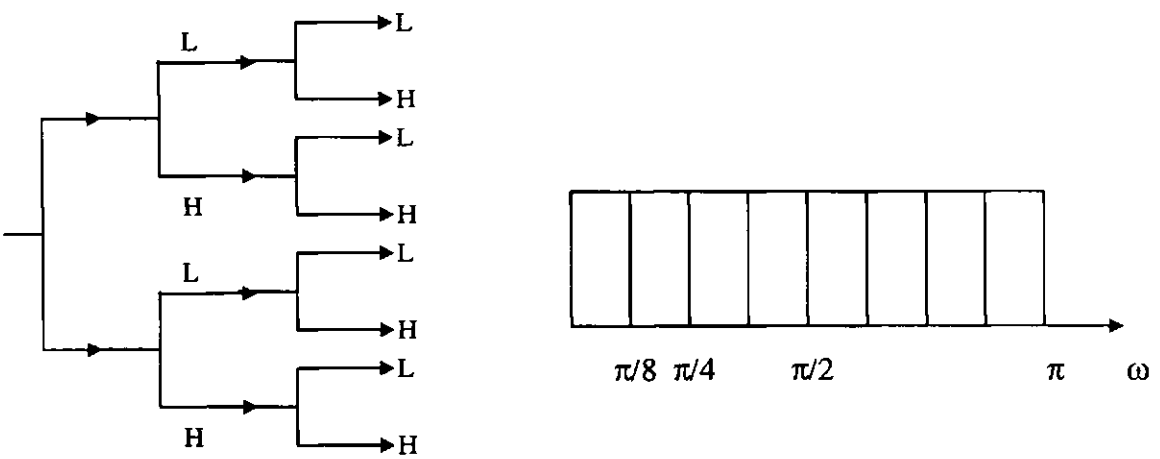

Figure 3.2 (a). Wavelet packet transform with full subband tree
(b). M-band uniform bandwidth division

3. Using M-band wavelet systems [45,101,125]

Another alternative technique is using M-band wavelet system that has M uniform band division. An 8-band uniform filter bank is depicted in Figure 3.3. Using this M-band wavelets to build a transmultiplexer or multicarrier modulation system, we need one level only. The transmitter composes the subband signals using the scaling filter (L_0) and the wavelet filters (H_0 ... H_{M-1}) into a broadband signal ready to be transmitted through the channel. More detail about this M-band wavelet system can be seen in section 2.3. One example of this type is cosines modulated filter bank. These filters can be obtained from a prototype low pass filter $H_0(z)$ by modulation to form M-band wavelet instead of conventional 2-band wavelet.

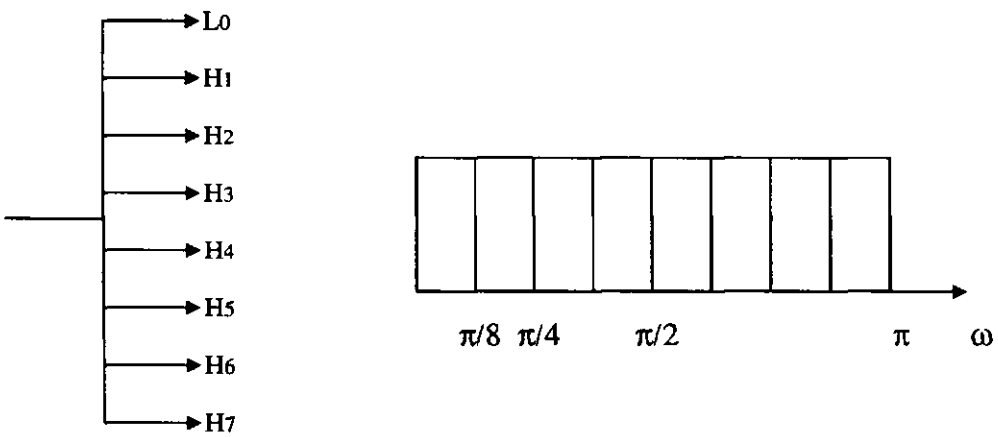

Figure 3.3 (a). M-band wavelet transform using M-band filters
(b). M-band uniform bandwidth division

In this thesis the multicarrier modulation (MCM) is implemented using M-band wavelets for three reasons. Firstly, these wavelets have the same bandwidth for each subchannel and hence provide the same data rate. Secondly, M-band wavelets can have the same spectrum shape for each subband unlike wavelet packet transform (WPT) system. Thirdly, this wavelet system provides the flexibility to choose the orthogonality

or the biorthogonality degree, the overlapping factor, the filter length, and the sidelobe relative power.

3.2 Filter Bank Design

Originally the theory of conventional transmultiplexer arose to perform a TDM-FDM conversion [64]. Recently the development of the theory of filter banks has provided a new tool for a transmultiplexer to span from an FDM version to a CDMA or multicarrier modulation version [64,116,125]. As discussed in section 2.5 this conversion strongly depends on the time-frequency properties of the filters used in the synthesis part in the transmitter and the analysis part in the receiver. The desired time spread and frequency spread are set as the design criteria for this optimisation purpose according the application needed. Many literatures discuss how to design a filter bank [126-133].

The time spread of the discrete time function *{h(n)}*, that is a measure of the localisation in time domain, is defined as:

$$\sigma_n^2 = \frac{1}{E}\sum_n (n-\bar{n})^2 \left|h(n)\right|^2, \tag{3.1}$$

where the energy E is

$$E = \sum_n \left|h(n)\right|^2 = \frac{1}{2\pi}\int_{-\pi}^{\pi} \left|H(e^{j\omega})\right|^2 d\omega \tag{3.2}$$

and time centre $\bar{n}$ is

$$\bar{n} = \frac{1}{E}\sum_n n\left|h(n)\right|^2. \tag{3.3}$$

Analog to the above criteria which is in time domain, the measure of localisation in frequency domain is the frequency spread that is defined as follows:

$$\sigma_\omega{}^2 = \frac{1}{2\pi E}\int_{-\pi}^{\pi}(\omega-\bar{\omega})^2\left|H(e^{j\omega})\right|^2 d\omega \tag{3.4}$$

where $H(e^{j\omega})$ is Fourier transform of discrete time function {h(n)}

$$H(e^{j\omega}) = \sum_n h(n)\, e^{-jn\omega} \tag{3.5}$$

and frequency centre $\bar{\omega}$ is

$$\bar{\omega} = \frac{1}{2\pi E}\int_{-\pi}^{\pi}\omega\left|H(e^{j\omega})\right|^2 d\omega\,. \tag{3.6}$$

Now using the above time-frequency parameters and, some other constraints according to the application, we consider the following examples of optimisation procedure.

3.2.1 PR-QMF Code for CDMA Systems

For simplicity consider a 2-band system. As discussed in chapter 2, the perfect reconstruction (PR) condition for this system can be summarised as

$$\sum_n h_0(n)\,h_0(n+2k) = \delta(k) \tag{3.7}$$

$$h_1(n) = (-1)^{n+1}\, h_0(N-1-n)\,. \tag{3.8}$$

In order to serve as a spreading code in a CDMA system, these filters must obey the following constraints:

- The spreading the perfect reconstructed-quadrature mirror filter (PR-QMF) codes in both frequency and time domains as evenly as possible or in other words maximising the frequency spread and the time spread.

- The intracode correlation is minimum

$$R_{00}(k)=\sum_{k} h_0(n)\,h_0(n+k) \quad k>0, k\in Z \,. \tag{3.9}$$

- The intercode correlation is minimum

$$R_{01}(k)=\sum_{k} h_0(n)\,h_1(n+k) \quad \forall k, k\in Z \,. \tag{3.10}$$

Therefore the objective function can be set as follows [64,116]

$$O=\max\left[\alpha{\sigma_n}^2+\beta{\sigma_\omega}^2-\gamma\sum_{k}\left|R_{00}(k)\right|-\eta\sum_{k}\left|R_{01}(k)\right|\right], \tag{3.11}$$

where α, β, γ, and η are the weight coefficients to adjust time spread, frequency spread, intracode correlation and intercode correlation.

3.2.2. PR-QMF for Multicarrier Modulation Systems

The filters used in this system tend to be of FDMA type, like a band pass filter or in other words the time spread is large and the frequency spread is small.

One of the choices for multicarrier systems, that simplifies the implementation, is using discrete Fourier transform (DFT) filters as synthesis filters and analysis filters

$$g_k(t)=u(t)\,e^{-j2\pi f_k t} \qquad f_k=f_0+\frac{k}{MT_s} \quad k=0,1\cdots\cdots M-1 \,, \tag{3.12}$$

where u *(t)* is a rectangular window function to make the set $g_k(t)$ orthogonal bases, f_k is centre frequency of the k^{th} filter. The relation between output transmitted signal $s_k(n)$ and input signals $x_k(n)$ is [64]

$$s_k(n)=\frac{1}{\sqrt{MT_s}}\sum_{l=0}^{M-1} x_l(n-1)\,e^{\frac{j2\pi kl}{M}} \tag{3.13}$$

and using the square function for windowing

$$u(t)=\begin{cases}\dfrac{1}{\sqrt{MT_s}} & 0\le t\le MT_s\\ 0\end{cases}. \tag{3.14}$$

Therefore the synthesis filters can be replaced by an inverse discrete Fourier transform (IDFT).

Another choice for multicarrier systems is using biorthogonal filter bank, which leads to wavelet systems that give M-band division. For 2-band-based wavelet system, this is the case of 2-band filter bank discussed in section 3.1, which is relatively simple. For M-band systems it is a good news and a bad news. The good news is higher degree of flexibility and the bad news is complexity of design. To reduce the complexity of design and implementation, explicit relations discussed below with some constraints are imposed. Here are some examples:

- Paraunitary means the total transfer function is unitary for $|z|=1$. This relation imposes the synthesis filters become the time-reversed version of the analysis filters

$$F_k(z)=z^{-N}H_k(z). \tag{3.15}$$

- Linear phase relation will impose the following constraint

$$H_k(z)=\pm z^{-N}H_k(z^{-1}). \tag{3.16}$$

- DFT filters will give the condition that the filters come from one prototype filter with the following equations

$$H_k(z)=H_0(zW^k) \qquad \text{where} \quad W=e^{\frac{-j2\pi}{M}}. \tag{3.17}$$

- Cosine modulated filters

  $F_k(z)$ and $H_k(z)$ come from modulations of one prototype filter.

In order to be used as multi-carrier modulation, the filters should have the following characteristics:

1. They are biorthogonal to achieve perfect reconstruction condition.

2. They exhibit a frequency response approaching the ideal response shown in Figure 3.4.

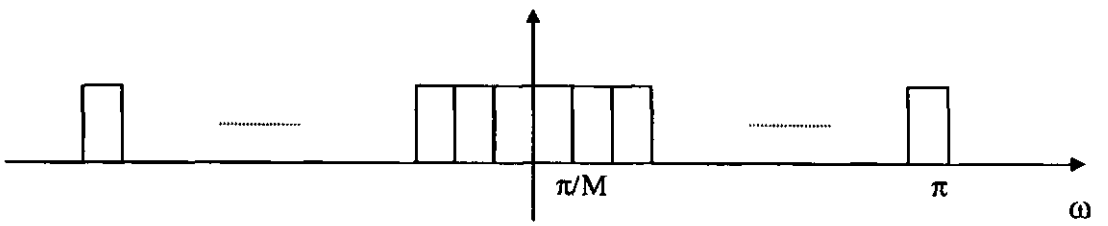

Figure 3.4 Ideal filter frequency response

The cosine modulated filters have the following characteristics that make them suitable for those conditions.

1. They can be biorthogonal or perfect reconstructed.

2. Their frequency response can be obtained by shifting the response of an ideal low pass filter as a prototype filter, from $\left[-\frac{\pi}{2M},\frac{\pi}{2M}\right]$ becomes

$$\frac{\pi}{M}(k+\frac{1}{2}) \quad 0 \le k \le M-1 . \tag{3.18}$$

3. This shifting is achieved by modulating in appropriate frequency and phase with a cosine function and is simple to design.

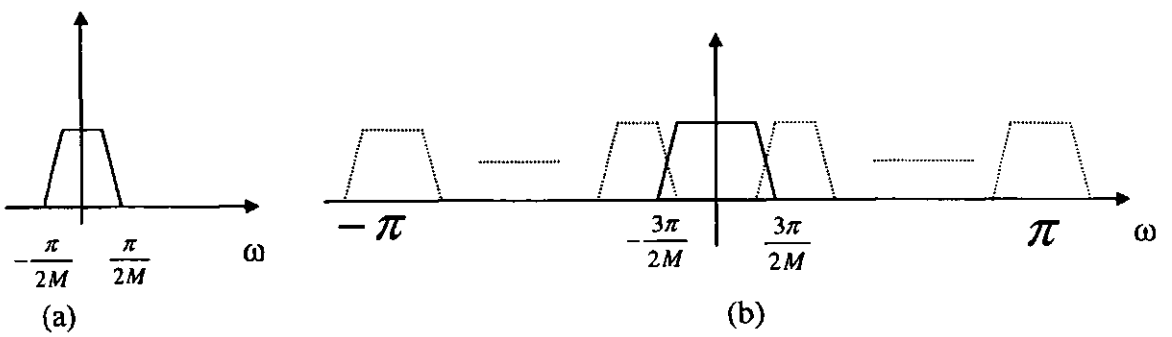

Figure 3.5 Frequency response of
(a) Prototype low pass filter (b). Cosines modulated filters

These filters are also used in multicarrier systems for DSL with a technique called discrete wavelet multitone (DWMT) which was proposed by Sandberg and Tzannes et. al. [73-76]. DWMT uses a set of cosines modulated filters and exhibits an inherent robustness against intersymbol interference (ISI) [73-76].

3.2.3. PR-QMF for Multiuser Multicarrier Modulation Systems

This system has two stages of orthogonality, firstly orthogonality between users by using orthogonal spreading *codes* and secondly orthogonality between subcarriers or subchannels. Hence this system constitutes a combination of CDMA and multicarrier modulation. It can also be interpreted as two stages transmultiplexers, where the first stage gives an orthogonality between users by spreading codes or a set of filters and the second stage gives an orthogonality between subcarriers or subchannels by another set of filters.

The first stage uses a set of filters, which is a CDMA type, and the second stage uses a set of filters, which is FDMA type. As discussed in section 2.5.3, there are two types of this system, MC-CDMA, which has spreading in frequency domain, and MC-DS-CDMA, which has spreading in time domain.

In this project, we design an MC-CDMA cellular system using both Fourier basis and wavelet basis. The spreading code used is Walsh-Hadamard code. The multi-carrier modulation is implemented using Fourier-based system, which employs tone subcarriers, and wavelet-based system, which employs cosines modulated filters. The performance of the two MC-CDMA systems are compared.

3.3 Multicarrier Modulation using M-band Wavelets

The cosine modulated filters, which build an M-band wavelet system, have the characteristics that make them suitable for multi-carrier modulation systems (see section 3.2.2).

The synthesis and the analysis filters come from the following equations [39,51]:

$$f_k[n] = 2\,p[n]\cos\left(\frac{\pi}{M}(k+\frac{1}{2})(n+\frac{1}{2}-\frac{N}{2})-(-1)^k\frac{\pi}{4}\right) \tag{3.19}$$

$$g_k[n] = 2\,p[n]\cos\left(\frac{\pi}{M}(k+\frac{1}{2})(n+\frac{1}{2}-\frac{N}{2})+(-1)^k\frac{\pi}{4}\right) \tag{3.20}$$

where $k = 0, 1, \ldots, M-1$ and $n = 0, 1, N-1$, while $p[n]$ is the prototype LPF filter. This prototype may be obtained from QCLS (Quadratic Constrained Least Squares) algorithm [110,128] to minimise the error between ideal and real frequency response over the pass band and the stop band.

3.3.1 QCLS Algorithm [110,128,129]

The Quadratic Constrained Least Squares (QCLS) algorithm is used to find the prototype filter $H(z)$ by minimising the integral error:

$$E = \int \left| D(\omega) - H(e^{j\omega}) \right|^2 d\omega, \tag{3.21}$$

where $D(\omega)$ is the desired frequency response and the integral is over the pass band and the stop band. The above equation then can be expressed in a quadratic form as

$$\mathbf{E} = \mathbf{h}^{\mathrm{T}}\mathbf{P}\,\mathbf{h} \tag{3.22}$$

where $\mathbf{P}$ is symmetric and positive definite matrix.

If $\mathbf{h}$ is a vector consisting all the filter coefficients $h_m(n)$, $0 \le m \le M-1$ and $0 \le n \le N-1$ then $\mathbf{h}=[h_0(0)\cdots h_0(N-1)\cdots h_{M-1}(0)\cdots h_{M-1}(N-1)]^T$.

The perfect reconstructed (PR) condition can be written as in the form $\mathbf{h}^T\mathbf{Q}_m\,\mathbf{h} = 0$ for no aliasing and $\mathbf{h}^T\mathbf{S}_m\,\mathbf{h} = 1$ for no distortion. The optimised filter $H_m(z)$ is

$$\mathbf{h}_{opt} = \min_{\mathbf{h}} \mathbf{h}^T\mathbf{P}\,\mathbf{h} \quad \text{subject to} \begin{cases} \mathbf{h}^T\mathbf{Q}_m\,\mathbf{h}=0 \\ \mathbf{h}^T\mathbf{S}_m\,\mathbf{h}=1 \end{cases}. \tag{3.23}$$

The design procedure is as follows

- Given the number of subbands M, the filter length N and the band edge of $H_m(z)$, compute $\mathbf{P}$ using the Eigen technique computation.
- Compute the corresponding matrices $\mathbf{Q}_m$ and $\mathbf{S}_m$.
- Design the filters with the same specifications as in $H_m(z)$ and use the coefficients as initial value of $\mathbf{h}$ in the quadratic-constrain minimisation problem.

3.3.2 Polyphase Implementation

Multi-carrier modulation systems can be realised with discrete M-band wavelet transform (DMWT) in receiver and inverse discrete M-band wavelet transform (IDMWT) in transmitter. IDMWT consists of upsamplers and synthesis filters, whereas DMWT consists of analysis filters and downsamplers. These filters are cosine modulated typed filters as discussed in section 3.3.

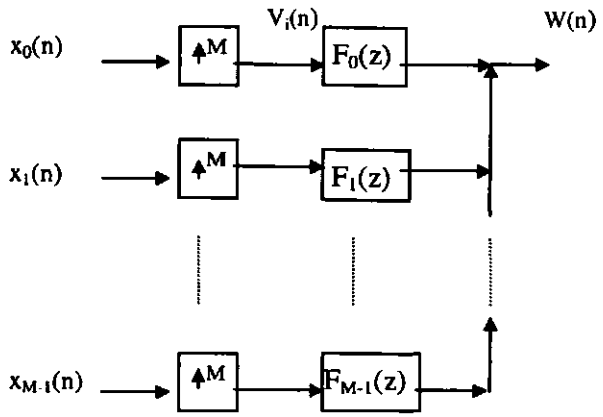

Figure 3.6 IDMWT in transmitter

The above structure can be implemented efficiently using polyphase structure, which then becomes as in Figure 3.7.

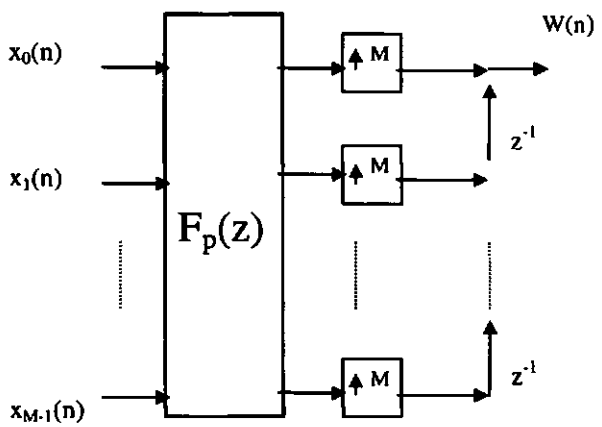

Figure 3.7 IDMWT with polyphase structure

In the above figure the polyphase matrix filter consists of the polyphase components of each subchannel filter. Therefore there are M x M polyphase filters, each with the length of N/M. One filter $F_k(z)$ can be replaced with M polyphase filters as follows:

$$F_k(z) = F_{k,0}(z^M) + z^{-1} F_{k,1}(z^M) + \cdots + z^{-(M-1)} F_{k,M-1}(z^M), \tag{3.24}$$

where $F_{k,i}(z) = \sum_{i=0}^{M-1} F_k(z^M) z^{-i}$. (3.25)

The output signal is given by:

$$W(z)=\begin{bmatrix}1 & z^{-1} & \cdots & z^{-(M-1)}\end{bmatrix}\begin{bmatrix}F_{0,0}(z^M) & F_{1,0}(z^M) & & F_{M-1,0}(z^M)\\ F_{0,1}(z^M) & F_{1,1}(z^M) & & F_{M-1,1}(z^M)\\ & & & \\ F_{0,M-1}(z^M) & F_{1,M-1}(z^M) & & F_{M-1,M-1}(z^M)\end{bmatrix}\begin{bmatrix}X_0(z^M)\\ X_1(z^M)\\ \vdots\\ X_{M-1}(z^M)\end{bmatrix}. \qquad (3.26)$$

If the length of each subchannel filter is $N = m\,M$, then the length of each polyphase filter is m. As all subchannel filters come from one prototype and with the symmetric property of each of these filters, the above structure can again be minimised as follows:

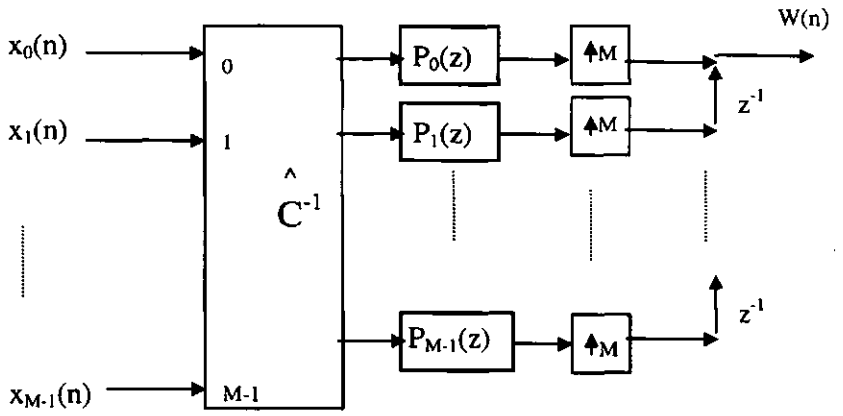

Figure 3.8 IDMWT with polyphase structure (further optimisation)

where the modulation matrix is

$$[C^{-1}]_k = 2\cos\left(\frac{\pi}{M}(k+\frac{1}{2})(n+\frac{1}{2}-\frac{N}{2})-(-1)^k\frac{\pi}{4}\right), \qquad (3.27)$$

and $P_k(z)$ is the polyphase filters of prototype filter.

The upsamplers and the delays then just can be replaced by a multiplexer.

The same principle is applied for DMWT in receiver side.

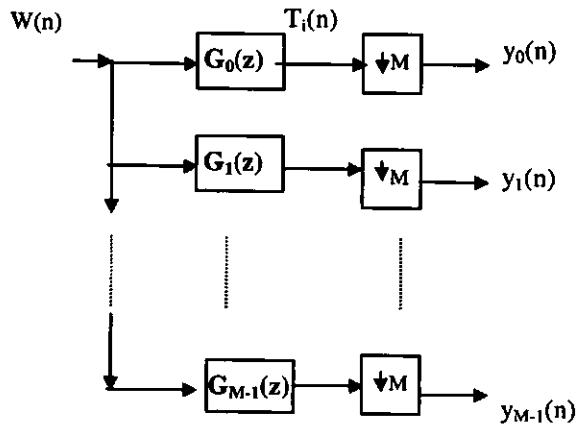

Figure 3.9 DMWT in receiver

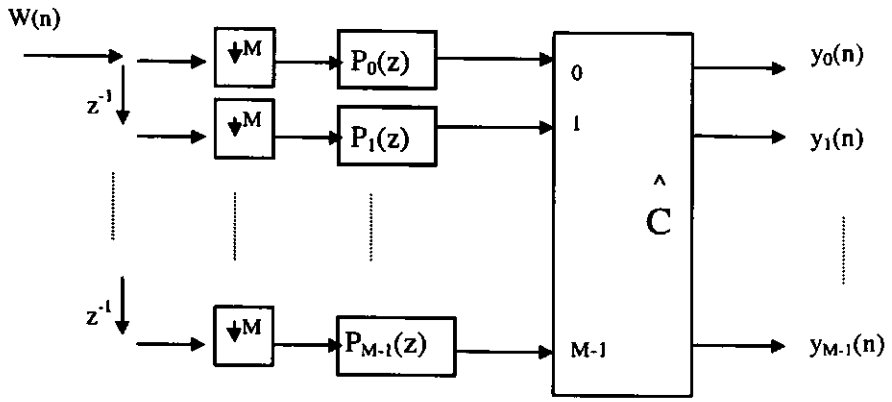

Figure 3.10 DMWT with polyphase structure

where the modulation matrix is

$$[C]_k = 2\cos(\frac{\pi}{M}(k+\frac{1}{2})(n+\frac{1}{2}-\frac{N}{2})+(-1)^k\frac{\pi}{4}) \tag{3.28}$$

3.4 Channel Model

In mobile communication there are two sources of interference which cause signal distortion. Those interference sources are *multipath interference* and *multiple access interference.*

Multipath interference is caused by propagation of the transmitted signal through several paths towards the receiver. These signals, originated from the same source but arrived with the different paths, are combined at the receiver to produce variation of amplitude and phase called signal fading. There are two parameters to measure in order to specify the multipath channel. The first parameter is the coherence bandwidth of the channel. When the coherence bandwidth is larger than the transmitted signal bandwidth, the fading is called *frequency non-selective fading* or *flat fading*. But when the coherence bandwidth is smaller than the transmitted signal bandwidth, then the fading is called *frequency selective fading*. In the latter case the signal is severely distorted by the channel. The second parameter is the coherence time of the channel. The mobile terminal causes Doppler effect that in turn produces time variation of the channel characteristic. The channel is said to be *time non-selective* or *slow fading* if the attenuation and phase shift are essentially fixed over the symbol duration. In other words, the coherence time of the channel is larger than the symbol duration of the transmitted signal. If the contrary is the case or the coherence time of the channel is smaller than the symbol duration of the transmitted signal then the channel is *time selective* or *fast fading*.

Multiple access interference (MAI) is caused by the fact that there is more than one user utilising the same channel. In order to cancel or reduce this interference, the transmitted signal from one user must be orthogonal or nearly orthogonal to the other user's signals.

A mobile radio channel suffering from multipath propagation has both frequency selective and time selective fading [134-139]. In this research, the channel is assumed to be frequency non selective when using MC-CDMA signal. This is due to the fact that MC-CDMA signal has a period much larger than the delay spread unlike in CDMA

system and therefore MC-CDMA system does not suffer much of overlapping between adjacent symbols (ISI). This condition can be written as follows:

$$\frac{1}{T_b} << \quad B_c \tag{3.29}$$

and $$B_c \approx \frac{1}{T_d} \tag{3.30}$$

B_c = coherence bandwidth

T_b = system symbol period

T_d = time delay spread of the channel

Although the system works on wideband channel this condition is still held. Let us take a simple practical scenario for our system.

Channel bandwidth = 5 MHz

Number of subchannels, M = 16

Subchannel bandwidth = 5 MHz /16 = 0.3126 MHz

Symbol period = 1/0.3126 = 3.2 μs

The delay spread for indoor or urban environment is typically less than 1 μs [25,136,140]. Thus the coherence bandwidth for each subchannel = 1/1 μs = 1 MHz. Since the coherence bandwidth is greater than the subchannel bandwidth, the channel is subjected to frequency non-selective (flat) fading.

It is also assumed in this analysis that the amplitude and phase remain constant over symbol duration, which means that Doppler shift due to the transceiver motion is negligible.

$$\frac{1}{T_b} >> f_D \tag{3.31}$$

f_D = maximum Doppler frequency.

The downlink channel has a fading characteristic that can be modelled for each m^{th} subchannel as follows:

$$h_m(t) = h_m e^{j\Phi_m}, \tag{3.32}$$

which shows that there are two parameters to consider, amplitude distortion h_m and phase distortion Φ_m, both caused by the channel. As discussed above, it is assumed that these amplitude and phase distortions remain constant over symbol duration T_b.

The uplink channel will be discussed in chapter 5 when the discussion about multiuser detection is underway.

3.5 Tranceiver Model

The design of both Fourier-based and wavelet-based MC-CDMA systems are presented here.

3.5.1 Fourier-Based MC-CDMA Systems

In order to simplify the analysis, the system is assumed as a continuous-time transmitter model as illustrated in Figure 3.11. The input data symbols $a_k[i]$ are binary antipodal with equal probability, where k denotes k^{th} user, i denotes i^{th} symbol, frequency subcarrier

$$f_m = f_0 + \frac{m}{T_b} \quad m \in [0, M-1] \tag{3.33}$$

where M is number of subcarriers which is equal to the spreading factor in frequency domain and there is no spreading in time domain.

$$T_b = T_c \tag{3.34}$$

T_b is data symbol period, T_c is spreading sequence chip period

The transmitted signal is generated as follows. A single data symbol is copied into M branches and multiplied by m^{th} chip of user code $c_k[m]$ on m^{th} branch and then BPSK modulated on its own subcarrier frequency f_m. The sum of all branches outputs will become the transmitted signal which is a multicarrier signal with subcarriers containing chip-spread (in frequency domain) data symbol.

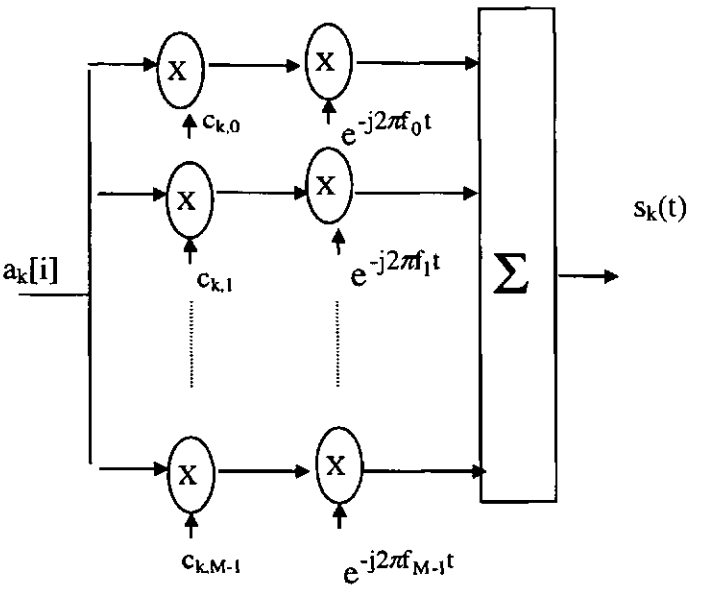

Figure 3.11 The model of Fourier-based MC-CDMA transmitter

The transmitted signal for k^{th} user is the real part of the following complex signal:

$$s_k(t) = \sum_{i=-\infty}^{\infty} \sum_{m=1}^{M-1} a_k[i]\, c_{k,m}\, p(t - iT_b)\, e^{-j2\pi f_m t} \tag{3.35}$$

where i denotes i^{th} data symbol, while $c_k[0]$, $c_k[1]$, ... , $c_k[M-1]$ represent the spreading code for k^{th} user and $p(t)$ is unit amplitude function which is non-zero in the interval of $[0,T_b]$.

If there are K active users, then the received signal in complex analytic representation is

$$r(t) = \sum_{k=0}^{K-1} \sum_{i=-\infty}^{\infty} \sum_{m=0}^{M-1} h_m a_k[i]\, c_{k,m} e^{-j(2\pi f_m t + \Phi_m)} + z(t)\,. \tag{3.36}$$

As can be seen, the received signal includes the effect of the channel, amplitude distortion h_m and phase distortion Φ_m, and additive white Gaussian noise (AWGN) $z(t)$ which has two-sided noise spectral density of *No/2*.

The receiver model with matched filter detection is illustrated in Figure 3.12.

The decision variable for 0^{th} user and i^{th} symbol is:

$$d_0[i] = \sum_{k=0}^{K-1} \sum_{m=0}^{M-1} \alpha_m h_m a_k[i]\, c_{0,m} c_{k,m} \frac{2}{T_b} \int_{iT_b}^{(i+1)T_b} \mathrm{Re}\left[e^{-j(2\pi f_m t + \Phi_m)}\right] \mathrm{Re}\left[e^{j(2\pi f_m t + \hat{\Phi}_m}\right] dt + \eta \tag{3.37}$$

where $\hat{\Phi}_m$ is estimated phase in the receiver

and $$\eta = \sum_{m=0}^{M-1} \alpha_m \frac{2}{T_b} \int_{iT_b}^{(i+1)T_b} z(t)\, \mathrm{Re}\left[e^{j(2\pi f_m t + \hat{\Phi}_m}\right] dt \tag{3.38}$$

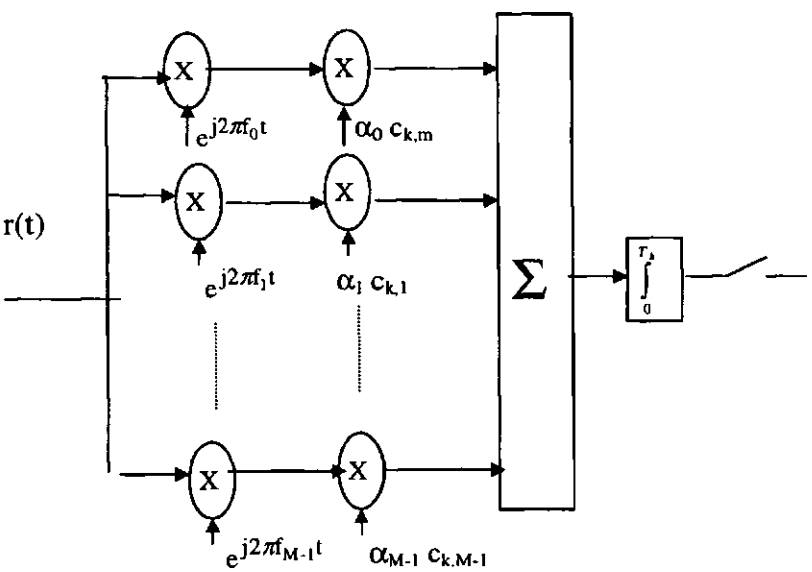

Figure 3.12 The model of Fourier-based MC-CDMA receiver

Assuming perfect phase estimation $\hat{\Phi}_m = \Phi_m$

$$d_0[i] = a_0[i]\sum_{m=0}^{M-1}\alpha_m h_m + \sum_{k=1}^{K-1} a_k[i]\sum_{m=0}^{M-1}\alpha_m h_m c_{0,m}c_{k,m}dt + \eta \tag{3.39}$$

From equation (3.39) there are three terms in the decision variable. The first term corresponds to the desired signal's component, the second one corresponds to the multiple access interference (MAI) and the last one is the noise term.

3.5.2 Wavelet-based MC-CDMA Systems

In wavelet-based MC-CDMA transmitter as illustrated in Figure 3.13, the transmitted signal for the k^{th} user is the following real signal in continuous form:

$$s_k(t) = \sum_{i=-\infty}^{\infty}\sum_{m=1}^{M-1} a_k[i]\, c_{k,m} f_m(t - iMT_b) \tag{3.40}$$

where $f_m(t)$ represents the waveform and modulator filter of m^{th} subchannel. This filter acts for waveform and subcarrier simultaneously and should be biorthogonal. In discrete form it is written as

$$\sum_n g_i(n) f_j(Ml - n) = \delta(l)\delta(i - j), \tag{3.41}$$

where $f_i(n)$ are the synthesis filters in the transmitter and $g_i(n)$ are the analysis filters in the receiver, $i=0,1, \ldots ,M-1$. These two set of filters can also be seen as matched filter process.

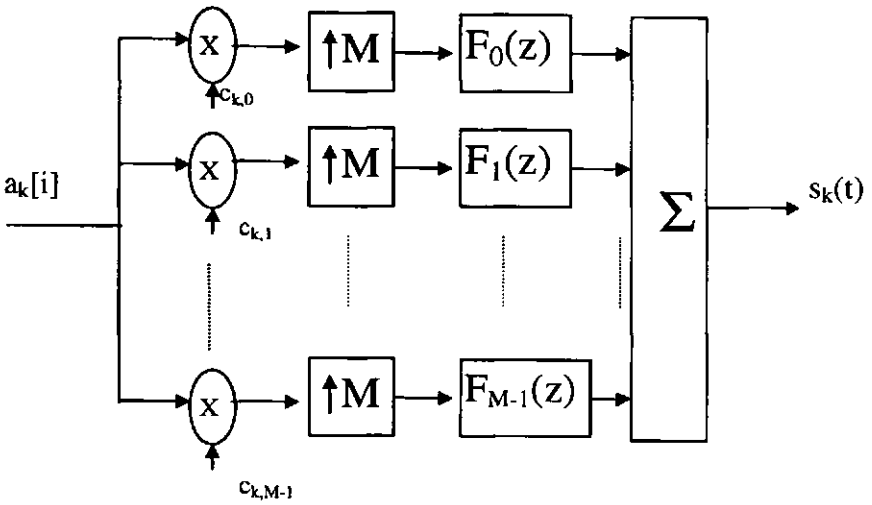

Figure 3.13 The model of wavelet-based MC-CDMA transmitter

If there are K active users, then the received signal in complex analytic representation is

$$r(t)=\sum_{k=0}^{K-1}\sum_{i=-\infty}^{\infty}\sum_{m=0}^{M-1}h_m a_k[i]\,c_{k,m} f_m(t-iMT_b-L_mT_b)+z(t). \tag{3.42}$$

The matched filter detection in the receiver is illustrated in Figure 3.14.

The decision variable for 0^{th} user and i^{th} symbol is

$$d_0[i]=\sum_{k=0}^{K-1}\sum_{m=0}^{M-1}\alpha_m h_m a_k[i]c_{0,m}c_{k,m}\frac{1}{T_b}\int_{iT_b}^{(i+v)T_b} g_m(t) f_0(iMT_b+(L_m-\hat{L}_m)T_b-t)dt+\eta, \tag{3.43}$$

where $\hat{L}_m$ is estimated delay in the receiver and v is the filter length $v=N$

and $\eta=\sum_{m=0}^{M-1}\alpha_m\frac{1}{T_b}\int_{iT_b}^{(i+v)T_b} g_m(t)\, z(iMT_b-t)dt.$ (3.44)

Assuming perfect delay estimation $\hat{L}_m=L_m$ and because of the biorthogonality of the filters

$$d_0[i]=a_0[i]\sum_{m=0}^{M-1}\alpha_m h_m+\sum_{k=1}^{K-1}a_k[i]\sum_{m=0}^{M-1}\alpha_m h_m c_{0,m}c_{k,m}dt+\eta. \tag{3.45}$$

As can be seen from equations (3.39) and (3.45), if synchronisation and delay estimation are perfect, both systems give almost the same bit error rate performance for the same

noise level. The imperfect of those processes will give different result for Fourier-based and wavelet-based systems. The wavelet-based system is expected to give better result because the averaging process in calculation of the decision variable is done both in frequency domain (by summation of all subchannels m) and time domain (by integration over v or summation over N).

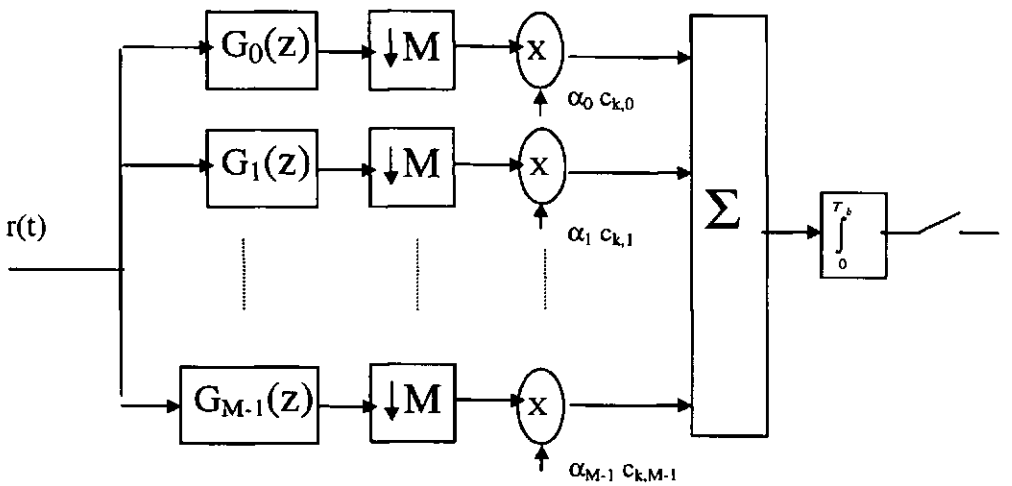

Figure 3.14 The model of wavelet-based MC-CDMA receiver

3.6 Numerical Results

The simulation, based on [141], is performed in m-file Matlab programming with the following specification:

- Number of subcarriers = spreading factor = M is 16
- Input signal is random data of 100 000 symbols
- The user codes are Walsh-Hadamard codes, each of which has 16 bits length
- The number of users is 4.
- The filters for wavelet-based system

The synthesis and the analysis filters come from the equations 3.19 and 3.20.

- AWGN channel

AWGN is generated from Gaussian (normal) distribution with the random variable x has the corresponding probability density function:

$$f(x) = \frac{1}{\sqrt{2\pi\sigma^2}} e^{-\frac{(x-\mu)^2}{2\sigma^2}} \tag{3.46}$$

- Multipath channel

Multipath channel is simulated using the resolvable path model [134,138,139] for 4 paths and the amplitude gain parameter B=[0.8 0.6 0.4 0.2], the time delay parameter tau=[1/16 2/16 3/16 4/16] of the data symbol period.

3.6.1 Sidelobe Component Power

The simulation result given in Figure 3.15 shows that in Fourier-based MC-CDMA (FB-MC-CDMA) systems, the first sidelobe component power is about -13 dB compared to the main lobe component, whereas in wavelet-based MC-CDMA (WB-MC-CDMA) systems the first sidelobe component power is about -80 dB compared to the main lobe component. This sidelobe suppression will improve in preventing interchannel interference when the signal is transmitted to the non ideal channel.

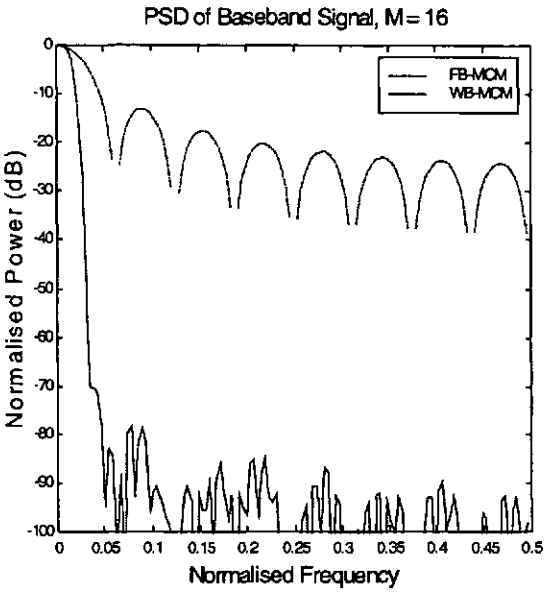

Figure 3.15 Frequency response of one subchannel baseband signal for FB-MC-CDMA and WB-MC-CDMA systems

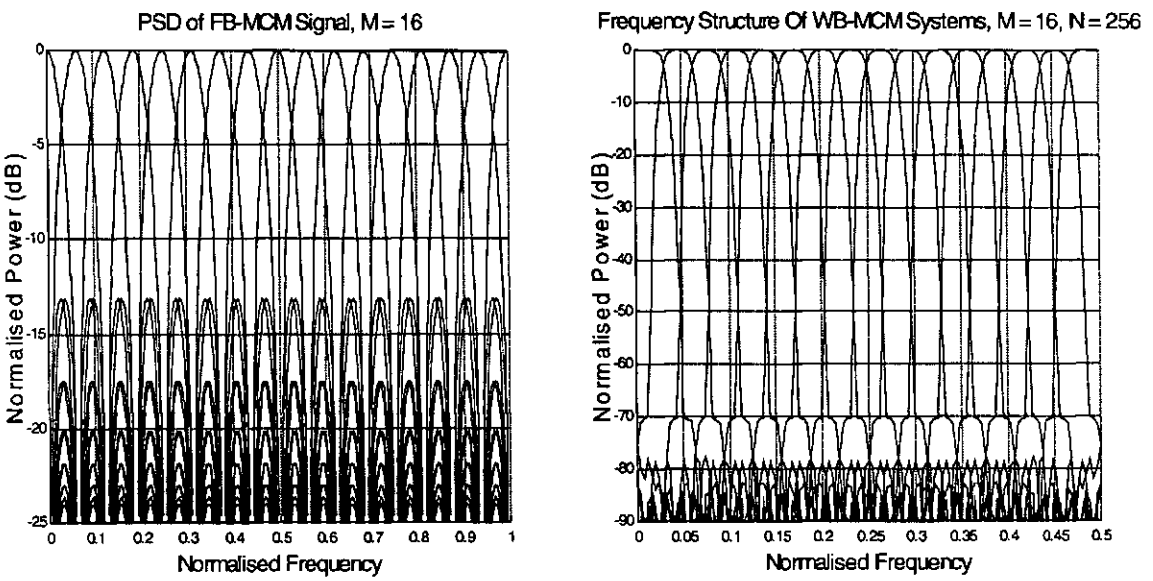

Figure 3.16 Frequency structure of MC-CDMA systems
a. Fourier-based b. Wavelet-based

It can also be seen from figure 3.16 that the same phenomenon happens when all subchannels are displayed together.

3.6.2 BER Performance

Under multipath channel with 4 synchronous users , WB-MC-CDMA system shows better BER (bit error rate) performance than FB-MC-CDMA.

As can be seen from equations (3.39) and (3.45), the wavelet-based system performs the averaging process of the decision variable in frequency domain (by summation of all subchannels m) and time domain (by integration over v or summation over N), therefore WB-MC-CDMA system is more robust against multipath signal than FB-MC-CDMA system as can be seen from the simulation result in figure 3.17. This result is generated by using the resolvable path model [134,138,139] for 4 paths with the amplitude gain parameter B=[0.8 0.6 0.4 0.2]. The time delay parameter tau=[1/16 2/16 3/16 4/16] of the data symbol period. All subbands are independently faded.

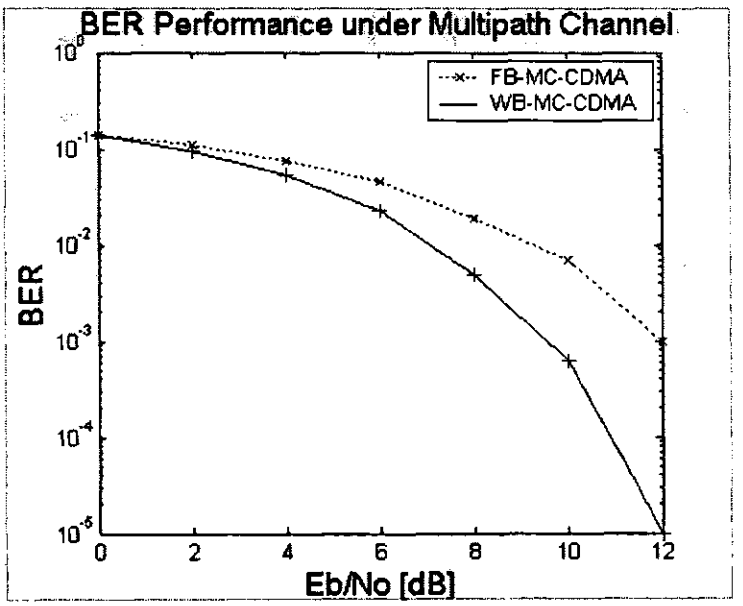

Figure 3.17 BER performance under multipath channel for FB-MC-CDMA and WB-MC-CDMA systems.

Under single frequency or tone interference or jamming signal, when the jamming signal ratio, i.e the ratio between jamming signal power and the desired signal power, is smaller than processing gain (Gp=16=12 dB), MC-CDMA wavelet-based system shows

better performance than MC-CDMA Fourier-based system. This wavelet-based superiority can be explained by the PSD of WB-MC-CDMA signal which has much lower sidelobe components. For this reason when the tone jamming signal disturbs the system, the disturbance effect is lower to WB-MC-CDMA system than that to FB-MC-CDMA system. When the jamming signal ratio is larger than processing gain, both systems show the same BER performance because the jamming rejection capability is out of the range which is within the processing gain.

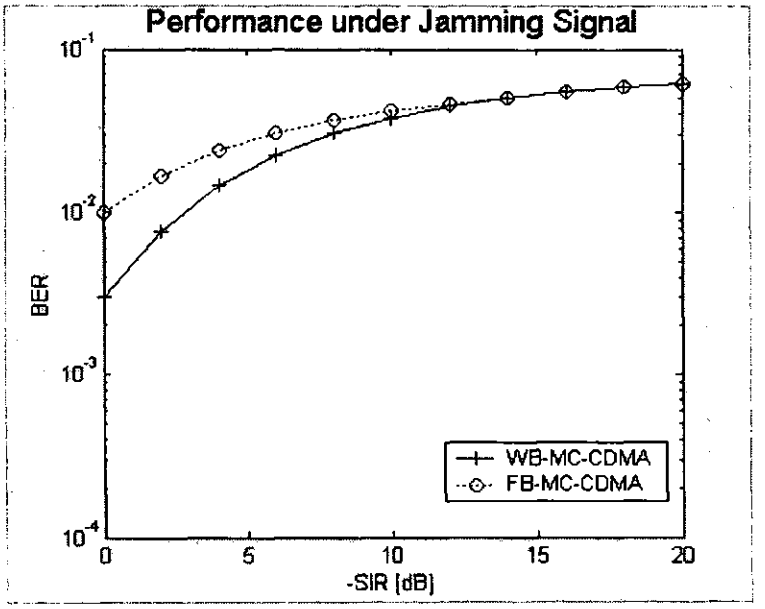

Figure 3.18 BER performance under single frequency jamming signal for FB-MC-CDMA and WB-MC-CDMA systems with matched filter detection and Eb/No=12 dB

CHAPTER IV

SYNCHRONISATION TECHNIQUES

In a single carrier modulation (SCM) system, the receiver usually performs frequency synchronisation included in carrier recovery circuit and time synchronisation in symbol synchroniser (see carrier and symbol synchronisation in [134,142]). In a multicarrier modulation (MCM) system, however the remaining carrier frequency error (CFE) and time error destroy the signal orthogonality which causes poorer performance.

First of all we discuss the synchronisation stages in multi-carrrier code division multiple access (MC-CDMA) systems. To implement the RF demodulation process (especially in coherent system), an MC-CDMA system needs a carrier reference with matched frequency and phase between transmitter and receiver. Therefore the system necessitates carrier frequency and carrier phase synchronisation process. Carrier (frequency and phase) synchronisation is always required in the coherent demodulation systems. Various methods of carrier synchronisation [134,142-143] have been proposed. This carrier synchronisation and performance analysis can be directly applied to wavelet-based multicarrier CDMA (WB-MC-CDMA) systems if carrier modulation is employed. We do not discuss these methods of carrier synchronisation in this thesis however we discuss the estimation of carrier frequency error and carrier phase offset in this chapter. Numerous techniques for frequency error estimation have been proposed [78-80,83-84,144-155]. The effect of this carrier frequency error in multicarrier modulation has also been discussed [156-159].

Once the baseband signal is recovered, then the receiver needs to synchronise the clock with the baseband sequence. This is usually called clock synchronisation or symbol

synchronisation. Various methods of symbol synchronisation [60,78-81,83,160-166] have been proposed.

The MC-CDMA system, unlike CDMA system, as we can see in the system model (see figure 3.13), has no timing information in user's code signal. This is because the sequence of the user code is along the frequency domain. So we cannot use the autocorrelation function of the user code to synchronise the system.

Wavelet-based multi carrier CDMA (WB-MC-CDMA) is a multicarrier system which has a number of subcarriers each of which is generated by a wavelet filter and will locate in its own subband. These wavelet waveform signals contain timing information. More than that these wavelets have good autocorrelation functions that make the time synchronisation easier.

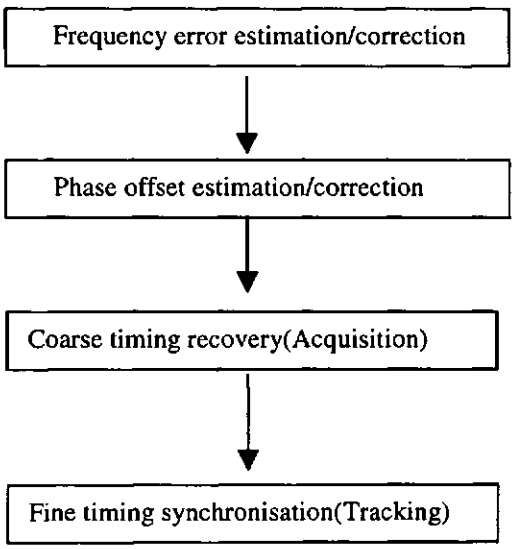

Figure 4.1: A synchronisation sequence in WB-MC-CDMA systems

There are two stages of synchronisation in WB-MC-CDMA cellular systems: frequency synchronisation and time (sampling clock) synchronisation. In frequency synchronisation, the phase and the frequency of local reference carrier is made as closely matching as

possible to that of the transmitter. In time synchronisation, the sampling clock oscillator of the receiver is made the same instant possible to that of the transmitter.

Carrier frequency error and carrier phase offset compensations are usually treated as sequential tasks. Carrier frequency error must be resolved prior to acquiring phase offset since sizeable carrier frequency errors will prevent successful estimation of the phase offset even if a phase-locked loop (PLL) is used.

The synchronisation sequence is illustrated in figure 4.1. The order is as follows:

1. frequency error estimation and correction
2. phase offset estimation and correction
3. coarse timing synchronisation (acquisition)
4. fine timing synchronisation (tracking)

The synchronisation in MC-CDMA system is essential to maintain the orthogonality property between subcarriers. The synchronisation method in MC-CDMA system requires finding of both symbol timing and carrier frequency error. We propose a maximum likelihood system for coarse timing synchronisation (ML acquisition) followed by early late tracking (ELT) for fine time synchronisation. Both stages take advantage of the correlation property of the wavelet waveforms on subbands. We propose a blind (non-data aided) frequency error estimation based on the variation of the signal phase. We also discuss a blind (non-data aided) phase offset estimation.

4.1 Time Synchronisation

In digital communication systems, with single carrier or multi-carrier systems, the receiver must derive carrier frequency and symbol timing from the received signal to demodulate and detect the data signal.

The received signal at the receiver can be written as follows:

$$r(t) = s(t,\varphi) + n(t)\,. \tag{4.1}$$

In order to estimate the parameter φ (frequency, phase or delay) of signal s(t,φ) perturbed by additive white Gaussian noise n(t), one can use the maximum aposteriori probability (MAP) method [53] where $\hat{\varphi}$ is considered to be an estimate of φ when the aposteriori probability $p(\hat{\varphi}|r)$ is maximum. In implementation, the MAP receiver generates a number of trial values, evaluates $\tilde{\varphi}$ for each value and then chooses $\hat{\varphi} = \tilde{\varphi}$ for which $p(\tilde{\varphi}|r)$ is maximal. Analytically this process can be expressed as

$$MAP \Rightarrow \hat{\varphi} = \arg\max_{\tilde{\varphi}} p(\tilde{\varphi}|r)\,. \tag{4.2}$$

The Bayesian rule relates the aposteriori probability $p(\hat{\varphi}|r)$ and the apriori probability $p(r|\tilde{\varphi})$ as

$$p(r,\tilde{\varphi}) = p(r)\; p(\tilde{\varphi}|r) = p(\tilde{\varphi})\; p(r|\tilde{\varphi})\,. \tag{4.3}$$

Assuming uniform apriori distribution of φ, maximising $p(\tilde{\varphi}|r)$ is equivalent to maximising $p(r|\tilde{\varphi})$ which can be determined more easily. The later method is known as maximum likelihood (ML) estimation and usually written analytically as

$$ML \Rightarrow \hat{\varphi} = \arg\max_{\tilde{\varphi}} p(r|\tilde{\varphi})\,. \tag{4.4}$$

Since the additive noise n(t) is white and zero-mean Gaussian, the pdf $p(r|\tilde{\varphi})$ can be written as follows:

$$p(r|\tilde{\varphi}) = \left(\frac{1}{\sqrt{2\pi}\sigma}\right)^{N} e^{-\left(\sum_{n=1}^{N}\frac{[r_n - s_n(\tilde{\varphi})]^2}{2\sigma^2}\right)}, \tag{4.5}$$

where r_n, n=1, ... ,N are expansion of r(t) using N orthonormal basis $f_n(t)$.

$s_n(\tilde{\varphi})$, n=1, ... ,N are expansion of $s(t,\tilde{\varphi})$ using N orthonormal basis functions

$$r_n = \int_{T_0} r(t)\, f_n(t)\, dt\,, \tag{4.6}$$

$$s_n(\tilde{\varphi}) = \int_{T_0} s(t,\tilde{\varphi})\, f_n(t)\, dt \tag{4.7}$$

T_0= observation interval for the expansion of r(t) and $s(t,\tilde{\varphi})$.

The argument in the exponent of equation 4.5 may be expressed in terms of signal waveforms r(t) and $s(t,\tilde{\varphi})$ as follows

$$\sum_{n=1}^{N} \frac{[r_n - s_n(\tilde{\varphi})]^2}{2\sigma^2} = \frac{1}{2\sigma^2} \sum_{n=1}^{N} \int_{T_0} (f_n(t))^2\, dt \int_{T_0} (r(t) - s(t,\tilde{\varphi}))^2\, dt \tag{4.8}$$

$$= \frac{1}{2\sigma^2} \frac{1}{T_0} \int_{T_0} (r(t) - s(t,\tilde{\varphi}))^2\, dt \tag{4.9}$$

and because $B = \frac{1}{2T_0}$ the above equation becomes

$$= \frac{1}{N_0} \int_{T_0} (r(t) - s(t,\tilde{\varphi}))^2\, dt\,. \tag{4.10}$$

Therefore maximising $p(r|\tilde{\varphi})$ with respect to the signal parameter $\tilde{\varphi}$ is equivalent to maximising the following log-likelihood function:

$$\lambda(\tilde{\varphi}) = -\frac{1}{N_0}\left(\int_{T_0} r^2(t)\, dt + 2\int_{T_0} r(t)\, s(t,\tilde{\varphi})\, dt + \int_{T_0} s^2(t,\tilde{\varphi})\, dt \right). \tag{4.11}$$

The first term does not involve the signal parameter $\tilde{\varphi}$. Given signal power, the third term is constant over observation interval. Therefore the maximisation is equivalent to the maximisation of the second term only which is given by:

$$\lambda(\tilde{\varphi}) = \int_{T_0} r(t)\, s(t,\tilde{\varphi})\, dt\,. \tag{4.12}$$

Replacing r(t) with equation 4.1, equation 4.12 becomes

$$\lambda(\tilde{\varphi}) = \int_{T_0} s(t,\varphi)\, s(t,\tilde{\varphi})\, dt + \int_{T_0} n(t)\, s(t,\tilde{\varphi})\, dt\,. \tag{4.13}$$

The second term which is the cross-correlation between n(t) and $s(t,\tilde{\varphi})$ is zero because both of them are independent, yielding

$$\lambda(\tilde{\varphi}) = \int_{T_0} s(t,\varphi)\, s(t,\tilde{\varphi})\, dt\,. \tag{4.14}$$

The above log-likelihood function reaches the maximum value for $\varphi = \tilde{\varphi}$ when that function becomes the autocorrelation function at zero delay. This maximum likelihood (ML) parameter estimation is depicted in figure 4.1. The algorithm is used to achieve the timing acquisition of wavelet-based multicarrier CDMA systems.

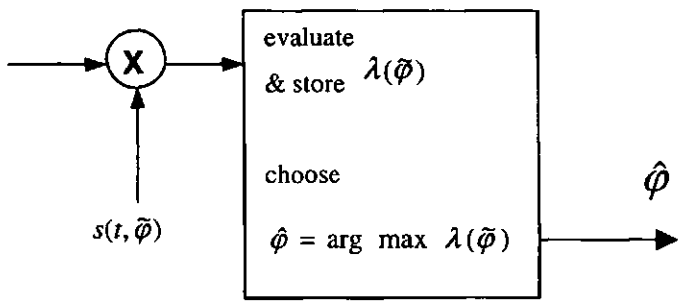

Figure 4.2 The basic maximum likelihood (ML) parameter estimation structure

4.1.1 Time Acquisition

The received signal at the wavelet-based multi-carrier CDMA receiver in discrete complex analytic representation is as follows:

$$r(n) = \sum_{i=-\infty}^{\infty} \sum_{m=0}^{M-1} h_m a_k[i] c_{k,m}\, f_m(n - iM - \tau_m) + z(n)\,. \tag{4.15}$$

As can be seen, the received signal includes the effect of the channel, amplitude distortion h_m and constant delay τ_m, and additive white Gaussian noise (AWGN) $z(n)$ which has noise spectral density of *No/2*.

The output signal at the analysis filter is

$$w_l(k) = \sum_{n=0}^{N-1} r(n)\, g_l(k+N-1-n)\,. \tag{4.16}$$

Substituting $r(n)$ and apply the biorthogonality principles to the filters, equation 4.16 becomes

$$w_m(k) = h_m a_k[i] c_{k,m} \sum_{n=0}^{N-1} f_m(n-\tau_m)\, g_m(k+N-1+\tilde{\tau}_m-n)+\eta(n) \tag{4.17}$$

Substituting for the analysis and the synthesis filters using equations (3.19) and (3.20) we get

$$\begin{aligned} w_m(k) = h_m a_k[i]\, c_{k,m} \sum_{n=0}^{N-1} 2p(n-\tau_m)\, \exp\left(-j\frac{\pi}{M}(m+\frac{1}{2})(n+\frac{1}{2}-\frac{N}{2})+(-1)^m\frac{\pi}{4}\right). \\ 2p(k+N-1+\tilde{\tau}_m-n)\exp\left(-j\frac{\pi}{M}(m+\frac{1}{2})(k+N-1+\tilde{\tau}_m-n+\frac{1}{2}-\frac{N}{2})-(-1)^m\frac{\pi}{4}\right)+\eta\,. \end{aligned} \tag{4.18}$$

In order to remove the modulation which gives multiple peaks in time domain, we can consider either the amplitude (modulus) or the power (square) of the signal. Let us take the power and ignore the noise term for the moment just to show how to get the time delay estimation.

$$(w_m(k))^2 = 16\,(h_m)^2 \left|\sum_{n=0}^{N-1} p(n-\tau_m)\; p(k+N-1+\tilde{\tau}_m-n)\right|^2 \tag{4.19}$$

It is this function that is used to get the estimation of time delay and to get the correct epoch for timing at the maximum value. Physically this function (see Figure 4.3 (b) as an example) is maximal at $\tilde{\tau}_m = \tau_m$ meaning the estimated delay equals to the delay which is then set as the objective point. This is performed by time acquisition algorithm for WB-MC-CDMA systems.

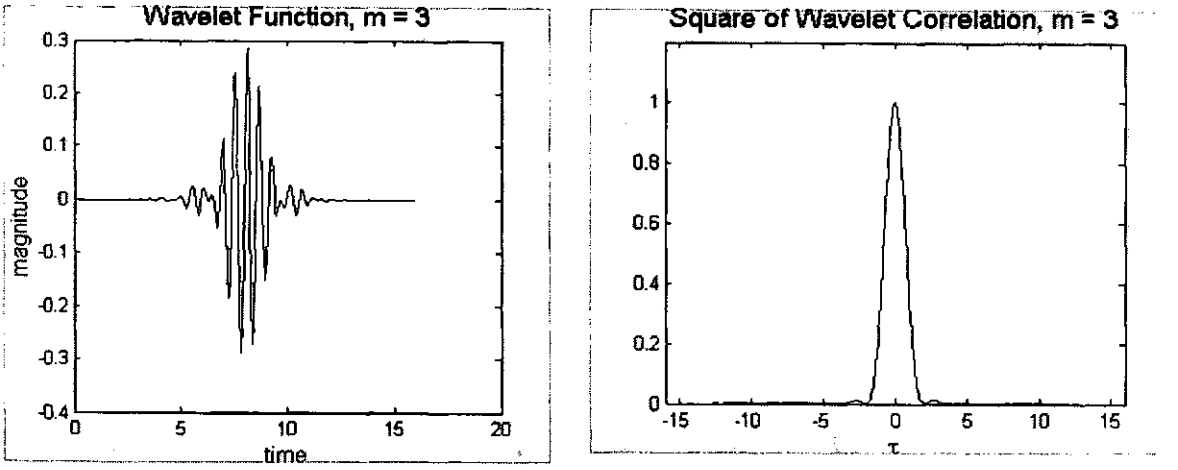

(a) (b)

Figure 4.3 (a) Wavelets function and (b) The square of wavelet autocorrelation; for m=3

Figure 4.3 displays the wavelet function (a) and the square of wavelet autocorrelation (b), both in subband m=3, that is typical on all subbands. As it can be seen, this function may be used for time synchronisation without ambiguity since it has a unique peak and it is an even function (symmetric at τ=0)

We consider serial implementation of maximum likelihood algorithm to perform the timing acquisition. The received signal is serially correlated with all possible times (phases) of the local wavelet signals. If the filter length is N, there will also be N possible time positions. So the number of cells to be searched or the uncertainty region is N, considering that the step size is one. There are other possibilities when the base station has information about cell radius and therefore the maximum possible delay of the transmitted signal as well. In that case, the uncertainty region maybe less than N.

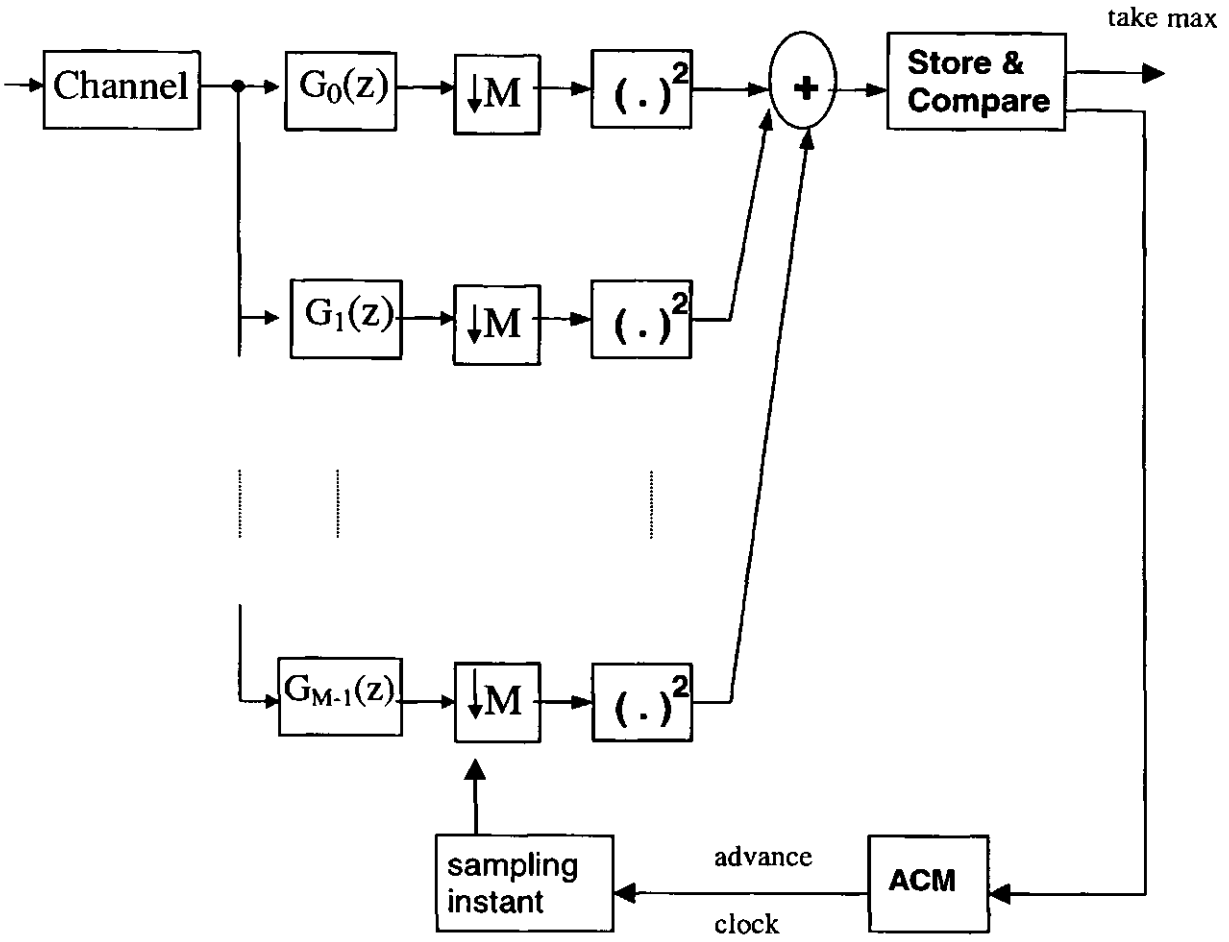

ACM : advance clock mechanism

Figure 4.4 Wavelets acquisition in wavelet-based MC-CDMA Systems

The acquisition circuit for wavelet-based MC-CMDA systems is shown in figure 4.4. The acquisition algorithm can be written as follows :

1. The complex low-pass received signal is correlated with the local wavelets using analysis filters G(z).
2. The output signals are then squared to remove the data signal and modulation. Here we apply the complex form of filters, i.e. complex modulated filter bank. We can still use the cosine form, i.e. cosines modulated filter bank, but we need a low pass filter after the square law detector (SLD)= $(.)^2$.
3. The SLD output signals are then combined together. We use equal gain combining (EGC) because the different wavelet basis functions carry the same timing information

in the correlations. Hence the EGC here does an averaging of the wavelet correlations along the subband axis.

4. The correlation result is stored and then the clock is advanced to get the wavelet correlations on the next acquisition cell.
5. The procedures 1 - 4 are repeated until the wavelet correlations in all cells are obtained and compared.
6. The time instant or the cell where the wavelet correlation is maximal is considered as the correct timing.

Let us write again the received signal in continuous form and include the channel effect

$$r_t(t) = A \sum_{k=0}^{K-1} \sum_{i=-\infty}^{\infty} \sum_{m=0}^{M-1} a_k[i]\, c_{k,m}\, f_{eq,m}(t - iT_b - \tau_{me}) + n(t), \qquad (4.20)$$

where A is the signal amplitude, τ_{me} denotes the timing delay on m^{th} subband to be estimated, K is the number of active users, and $n(t)$ is the AWGN noise signal, $f_{eq,m}(t)$ is the total impulse response resulting from the wavelet filter $f_m(t)$ at the transmitter and the low pass equivalent channel $h(t)$.

Firstly in order to reject multiple access interference signal and using the orthogonal spreading codes, the despreading in the frequency domain is performed so that equation (4.20) can be modified to

$$r(t) = A \sum_{i=-\infty}^{\infty} \sum_{m=0}^{M-1} a_k[i]\, f_{eq,m}(t - iT_b - \tau_{me}) + n(t). \qquad (4.21)$$

The log-likelihood function for each subband is given by [142]:

$$\Lambda_L(\tau_m) = \frac{2}{N_0} \int_{T_{obs}} r(t)\, s_m(t;\tau_m)\, dt \qquad (4.22)$$

The local signal is $s_m(t;\tau_m) = g_m(t - \tau_m)$, (4.23)

where $g_m(t)$ is the matched wavelet of $f_m(t)$ and τ_m is the local time delay on the m^{th} subband to be adjusted to estimate τ_{me}. Here in order to have a unique peak the signal must

have a clearance (filled with null symbols) of $\frac{N}{2}T_f$ where $T_f = \frac{T_b}{M}$ is the filter clock period and T_b is the symbol period. Therefore we need a sort of training sequence of

$$\underbrace{1,0,0 \cdots}_{\frac{N}{2M}} \; 1,0,0 \cdots$$

Averaging the log-likelihood function over the information symbols, we will get the following averaged log-likelihood function [134]

$$\overline{\Lambda}_L(\tau_m) = \sum_n \ln\cosh\left(C\, y_n(\tau_m)\right) \tag{4.24}$$

where the matched filter output is given by

$$y(\tau_m) = \int_{NT_f} r(t)\, g_m(t - nT_b - \tau_m)\, dt \tag{4.25}$$

and $C = \frac{2}{N_0}$. For small x, we have $\ln\cosh x \approx \frac{1}{2}x^2$ therefore

$$\overline{\Lambda}_L(\tau_m) = \frac{1}{2}\left(\frac{2}{N_0}\right)^2 \sum_n {y_n}^2(\tau_m). \tag{4.26}$$

Substituting r(t) of equation (4.21) into equation (4.26), assuming ideal AWGN channel (so that $f_{eq,m}(t) = f_m(t)$), exploiting the biorthogonality of the filters (so that $\sum_{m=0}^{M-1} \int_{NT_f} f_m(t - iT_b - \tau_{me})\, g_l(t - nT_b - \tau_m)\, dt = \delta(m - l)$), and omitting the noise signal (due to the averaging and independent of τ_m), we get:

$$\overline{\Lambda}_L(\tau_m) = \frac{2A^2}{{N_0}^2} \sum_n \sum_i (a_k[i])^2 \left(\int_{NT_f} f_m(t - iT_b - \tau_{me})\, g_m(t - nT_b - \tau_m)\, dt \right)^2. \tag{4.27}$$

The effects of the data signal are removed due to squaring, yielding

$$\overline{\Lambda}_L(\tau_m) = \frac{2A^2}{{N_0}^2} \sum_n \sum_i \left(\int_{NT_f} f_m(t - iT_b - \tau_{me})\, g_m(t - nT_b - \tau_m)\, dt \right)^2. \tag{4.28}$$

Substituting for f_m and g_m from equations (3.19) and (3.20), equation (4.28) becomes

$$\overline{\Lambda}_L(\tau_m)=\frac{2A^2}{{N_0}^2}\sum_n\sum_i\int_{NT_f}\Bigg(2p(t-iT_b-\tau_{me})\exp(-j\frac{\pi}{M}(m+\frac{1}{2})(t-iT_b-\tau_{me}+\frac{T_f}{2}-\frac{NT_f}{2})+(-1)^m\frac{\pi}{4}).$$

$$2p(t-nT_b-\tau_m)\exp(-j\frac{\pi}{M}(m+\frac{1}{2})(t-nT_b-\tau_m+\frac{T_f}{2}-\frac{NT_f}{2})+(-1)^m\frac{\pi}{4})\,dt\Bigg)^2 \qquad (4.29)$$

where $p(t)$ is the prototype impulse response.

The squarer will remove the modulation that gives multiple peaks. The averaged log-likelihood function becomes

$$\overline{\Lambda}_L(\tau_m)=\frac{32A^2}{{N_0}^2}\sum_n\sum_i\left(\int_{NT_f}p(t-iT_b-\tau_{me})\,p(t-nT_b-\tau_m)\,dt\right)^2 \qquad (4.30)$$

This function reaches maximum at $\tau_m=\tau_{me}$ which is the correct epoch for the system timing. This point is the objective in the time acquisition algorithm. The Cramer-Rao lower Bound of the acquisition variance $\sigma^2_{\hat{\tau}_m}$ is given in [134,167,168]

$$\sigma^2_{\hat{\tau}_m}=-\frac{1}{E\left[\frac{\partial^2}{\partial\tau_m^2}\overline{\Lambda}_L(\tau_m)\right]}. \qquad (4.31)$$

Figure 4.5 shows the performance of the acquisition circuit when the signal is transmitted through an AWGN channel. The performance is interpreted as the variance of the relative time delay error versus Eb/No values. It can be seen that the acquisition circuit performs close to the Cramer-Rao Bound calculated from equation (4.31).

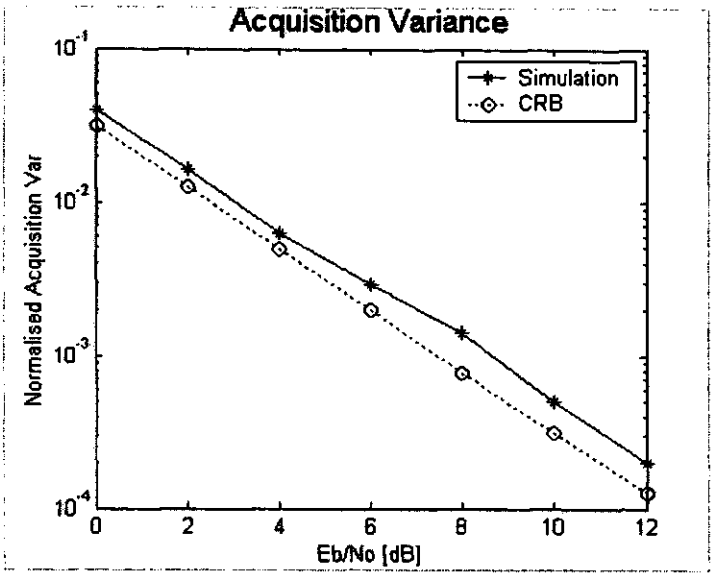

Figure 4.5 The timing acquisition performance under AWGN channel.

4.1.2 Time Tracking

The above ML acquisition searches for the maximum of $\lambda(\tilde{\varphi})$, which is actually achieved at $\varphi = \tilde{\varphi}$, when the ML function becomes the autocorrelation function at zero delay. Another equivalent structure called ML tracking (MLT) searches for the zero value of the first derivative of $\lambda(\tilde{\varphi})$ as follows

$$MLT \Rightarrow \hat{\varphi} = \arg \underset{\tilde{\varphi}}{zero} \frac{\partial \lambda(\tilde{\varphi})}{\partial \tilde{\varphi}} = \arg \underset{\tilde{\varphi}}{zero} \int r(t) \frac{\partial s(t,\tilde{\varphi})}{\partial \tilde{\varphi}} dt. \tag{4.32}$$

This algorithm can be replaced by another equivalent algorithm which takes the signal difference between early and late version of the local signal with respect to the parameter φ to be estimated

$$\frac{\partial s(t,\tilde{\varphi})}{\partial \tilde{\varphi}} = \frac{s(t,\tilde{\varphi}+\Delta\varphi) - s(t,\tilde{\varphi}-\Delta\varphi)}{2\Delta\varphi}. \tag{4.33}$$

So this early late tracking (ELT) algorithm can be written analytically as follows

$$ELT \Rightarrow \hat{\varphi} = \arg \underset{\tilde{\varphi}}{zero}[E(t,\tilde{\varphi}) - L(t,\tilde{\varphi})], \tag{4.34}$$

where the early signal is

$$E(t,\tilde{\varphi}) = \frac{\int r(t)\, s(t,\tilde{\varphi}+\Delta\varphi)\, dt}{2\Delta\varphi}, \tag{4.35}$$

and the correspondent late signal is

$$L(t,\tilde{\varphi}) = \frac{\int r(t)\, s(t,\tilde{\varphi}-\Delta\varphi)\, dt}{2\Delta\varphi}. \tag{4.36}$$

The basic structure of the early late tracking (ELT) system is illustrated in figure 4.6.

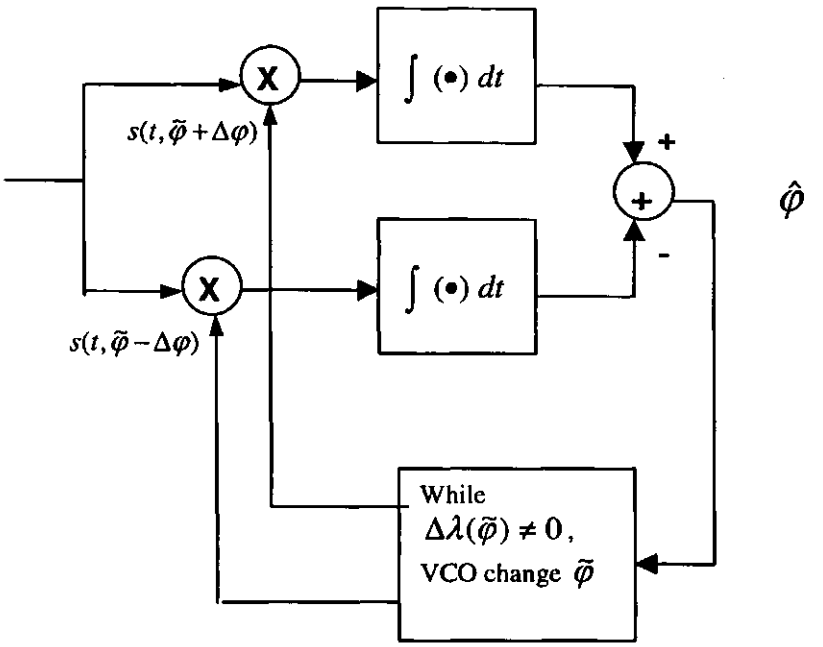

Figure 4.6 The basic early-late tracking (ELT) structure

The tracking circuit for wavelet-based MC-CDMA systems is shown in figure 4.7.

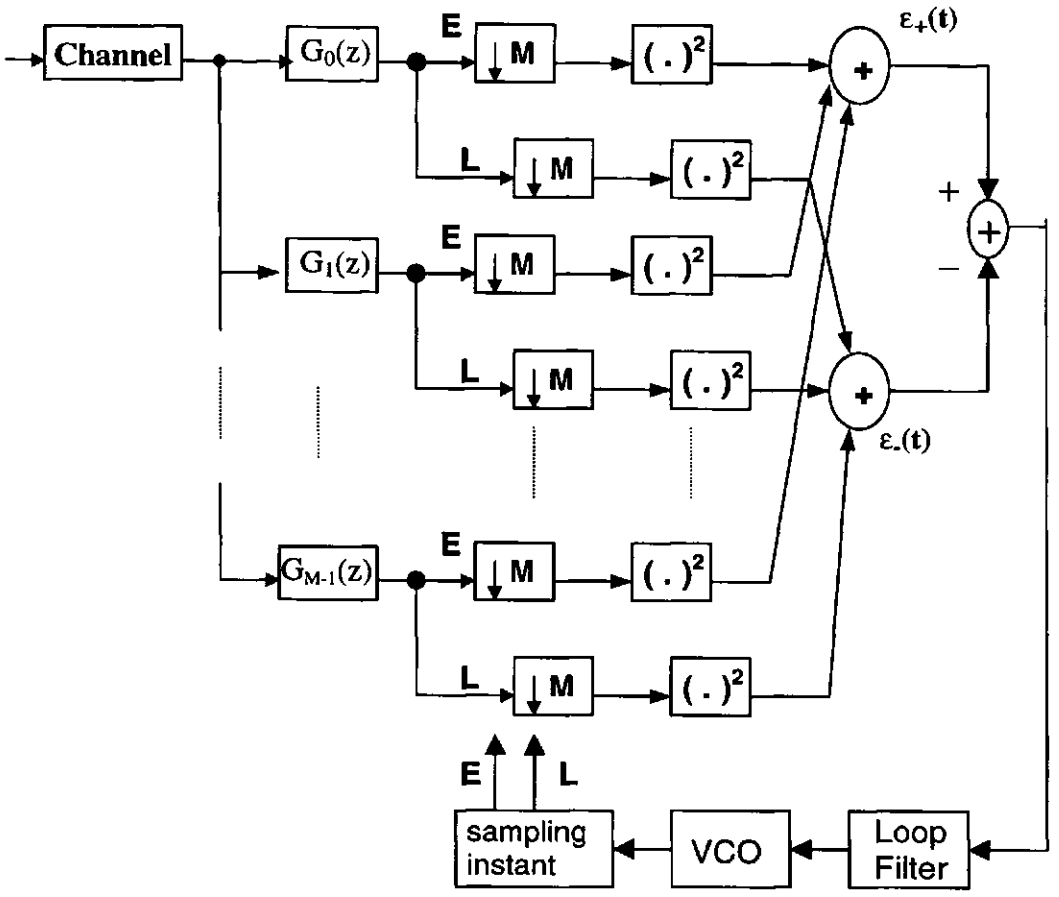

VCC: voltage controlled oscillator

Figure 4.7 Wavelets tracking in wavelet-based-MC-CDMA Systems

The tracking algorithm can be written as follows :

1. The received signal, after being corrected by the acquisition circuit, is correlated with the early and late versions of local wavelets.
2. The output signals on both the early and late versions are then squared to remove the effects of the data signal and modulation.
3. The SLD output signals are then combined together for both early and late versions. We apply equal gain combining (EGC) because they carry the same timing information in the correlations.
4. The wavelet correlation results are differentiated to get the error signal.

5. The error signal is low pass filtered. The loop filter is adjusted according to the bandwidth coverage and the response speed.
6. The filter output signal triggers the VCO. If it is positive the VCO will increase the frequency and hence advance the sampling instant. If it is negative the VCO will decrease the frequency and therefore retard the sampling instant.
7. The procedures 1 - 6 are repeated in a closed loop until the error signal is zero which is the steady state condition. The correct timing instant is the average time between the early timing and the late timing.

The derivative form $\frac{\partial \bar{\Lambda}_L}{\partial \tau_m} = 0$ is used in the tracking circuit to get the correct system timing.

The DC component of the error signal in the tracking circuit (plotted as S-Curve in Figure 4.8) is given by:

$$S_d(T_n) = R_t^2(T_n - \frac{\delta}{2}) - R_t^2(T_n + \frac{\delta}{2}) \qquad (4.37)$$

where $R_t = \sum_{m=0}^{M-1} \sum_{n=0}^{N-1} f_m(n+\tau)\, g_m(n)$ is the autocorrelation function, $T_n = \frac{\tau - \hat{\tau}}{T_b}$ is the normalised time error and $\delta = \frac{T_L - T_E}{2T_b}$ is the normalised tracking range.

Figure 4.8 presents the S-Curve characteristic of the tracking circuit, plotted using equation (14), and represents the signal error output versus the time error input (τ) for δ=0.5, 1 and 1.5 respectively. For $\delta \leq 1$ the slope in the linear zone does not change much although the locking range decreases proportionally to δ.

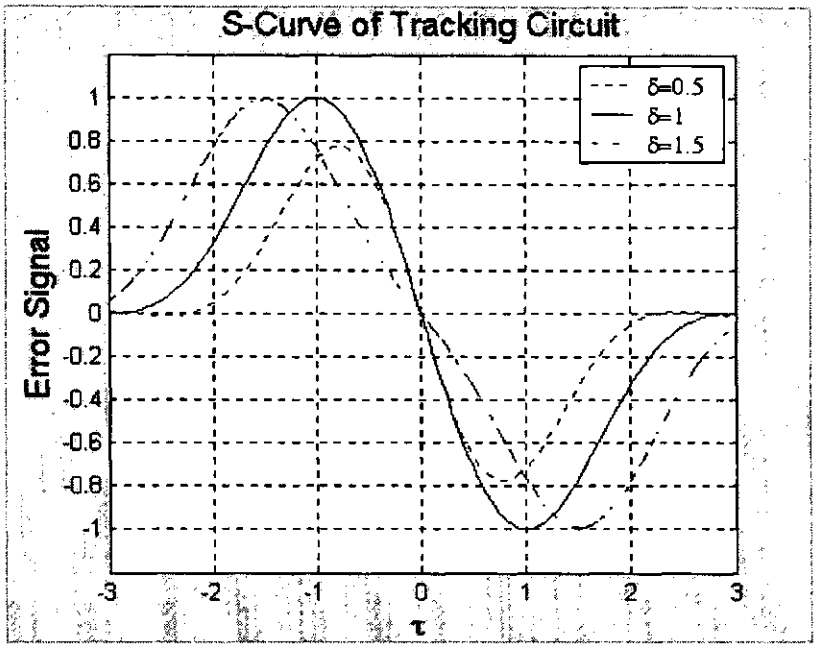

Figure 4.8 the S-Curve characteristic of the tracking circuit

The tracking timing jitter variance is given by [169]

$$\sigma_{T_n}^2 = \frac{N_0 B_L}{2A^2}\left(N_0 B_N + \frac{A^2}{2}\right) \tag{4.38}$$

where B_L is the loop bandwidth and B_N is the wavelet filter bandwidth.

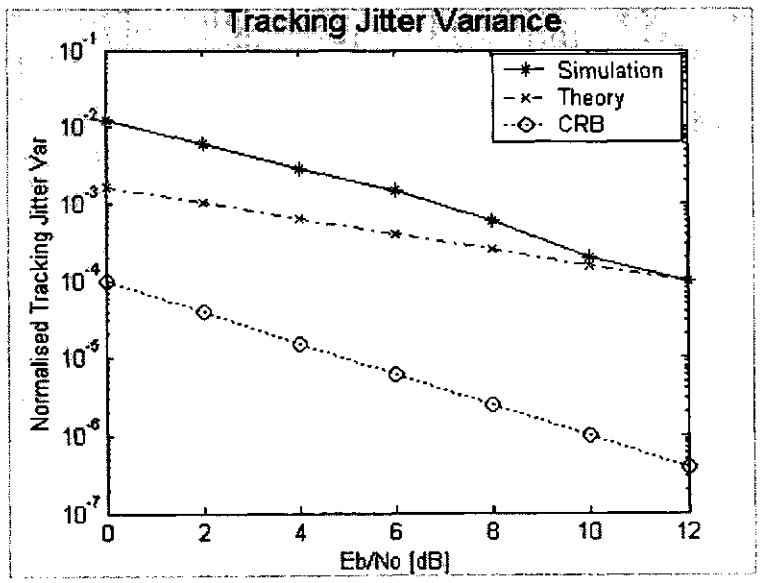

Figure 4.9 The tracking circuit performance under AWGN channel

Figure 4.9 shows the performance of the tracking circuit from simulation and from theory using equation (4.38) under AWGN channel and compared with the Cramer-Rao Bound which is the first term of the equation (4.38) and the other term is from data variation (self noise). In this graph, we have assumed $B_L T_b = 10^{-1}$ and $B_N T_b = 0.5$.

4.2 Frequency Error & Phase Offset Estimation

One of the advantages of multicarrier modulation systems is the reduced complexity of the equaliser at the receiver, which allows for inexpensive hardware implementation [23]. Multicarrier modulation transforms a frequency selective channel into parallel flat fading subchannels. Equalisation is therefore carried out by a bank of single-tap equalisers. Multicarrier systems are however more sensitive to carrier frequency error (CFE) than single carrier systems. The presence of CFE causes loss of orthogonality between the sub carriers in a multicarrier scheme and leads to increased bit-error-rate [159]. The effect of this CFE in MC-CDMA is also discussed in [156-159]. Accurate CFE compensation is therefore crucial for multicarrier systems including MC-CDMA systems.

A symbol clock and a frequency error estimate may be generated at the receiver with the aid of pilot symbols known to the receiver or by maximising the average log-likelihood function. Redundancy in the transmitted OFDM signal also offers the opportunity for synchronisation. JJ Van de Beek presented and evaluated the joint *Maximum Likelihood* (ML) estimation of the time and carrier-frequency error in OFDM systems [79,80]. The key element is that the OFDM data symbols already contain sufficient information to perform synchronisation. The algorithm exploits the cyclic prefix preceding the OFDM symbols, thus reducing the need for synchronising pilots [79,80].

Blind CFE synchronisation is attractive because it saves bandwidth, i.e., no training pilots are required. Consequently, there has been considerable work in the area of blind CFE estimation recently. A blind CFE estimator was recently proposed in [151] (see also [152] for more details). This estimator, designed to work with dispersive channels, exploits the fact that practical OFDM systems are not fully loaded, i.e., a few subcarriers are not modulated. The unmodulated subcarriers are referred to as virtual subcarriers (VSC) or null-subcarriers. This approach is extended in [153], by inserting a few extra null-subcarriers in order to improve performance and ensure identifiability. More recently, a blind CFE estimator was developed for PSK-OFDM by exploiting the constant modulus property of PSK constellation [154]. This algorithm was shown to greatly outperform the VSC-based method in [151]. Here this algorithm is generalised to include QAM constellations.

In this research we consider a frequency error estimator which takes advantage of the fact that the frequency error is the phase rotation rate of the signal. Therefore the frequency error is simply the derivative of the signal argument. We also consider a phase offset estimator which averages the signal argument over number of samples.

4.2.1 Frequency Error Estimation

Carrier frequency error and carrier phase offset compensation is usually treated as consecutive tasks. Carrier frequency error must be resolved prior to the phase offset acquisition because coarse carrier frequency errors will prevent successful estimation of the phase offset even if a phase-locked loop (PLL) is used. Besides, the coarse frequency error may shift the signal spectrum in a frequency band rejected by the receiver's passband filters. This spectral distortion will also destroy the received signal in the time domain. Thus, in order to accommodate a significant amount of frequency error, the receiver's passband

bandwidth must be increased. Unfortunately, this increases the receiver's noise bandwidth and the susceptibility to adjacent channel signals.

The total frequency error can be written as

$$\Delta f_t = \Delta f_c + \Delta f_f , \tag{4.24}$$

where Δf_c is the coarse frequency error which is an integer multiple of the subband spacing $\frac{1}{T_b}$ Hz and Δf_f is the fine frequency error which is a fraction of the subband spacing $|\Delta f_f| \le \frac{0.5}{T_b}$.

Carrier frequency error is introduced due to the unmatched oscillator's frequency between the receiver and the transmitter and also due to the Doppler effect arising because of the terminal's motion. The received signal in discrete form containing the frequency error and the phase offset can be written as follows:

$$r(n) = \sum_{k=0}^{K-1} \sum_{i=-\infty}^{\infty} \sum_{m=0}^{M-1} h_m a_k[i] c_{k,m} f_m(n - iM) e^{j(\Delta\omega n + \Delta\varphi)} + z(n) \tag{4.25}$$

As we can see in equation 4.25 there is an angular frequency error $\Delta\omega = 2\pi \Delta f$ and a phase offset $\Delta\varphi$.

The output signal before the detection process is expressed as

$$y_0[l] = \sum_{k=0}^{K-1} \sum_{m=0}^{M-1} \alpha_m h_m a_k[i] c_0[m] c_k[m] \sum_{n=0}^{N-1} g_m(n) f_0(lM - n) e^{j(\Delta\omega n + \Delta\varphi)} + \eta(l), \tag{4.26}$$

where N is the filter length, index $l = i + \delta$, the delay is $\delta = \frac{N}{M} - 1$

and the noise term becomes $\eta(l) = \sum_{m=0}^{M-1} \alpha_m \sum_{n=0}^{N-1} g_m(n)\, z(lM - n)$. (4.27)

Assuming the absence of multiple access interference (MAI), perfect equalisation and taking into account that the frequency error and phase offset do not change the amplitude of the received signal but only the phase, the equation 4.26 becomes

$$y_0[l] = a_0[i]\, e^{j(\Delta\omega\, l + \Delta\varphi)} + \eta(l)\,. \tag{4.28}$$

It is clear that if the frequency error and the phase offset are not rectified, they can severely damage the performance (i.e. increase the probability of error). As we are concerned with the phase parameter, we need a training sequence (known data symbols stream) that does not influence the phase. We use the following training sequence in the simulation

$$a_0[i] = 1 \quad for\ i = 0,1,\cdots M-1. \tag{4.29}$$

We consider the argument term only and therefore the output of the arg(.) block is as follows

$$p(n) = \Delta\omega\, n + \Delta\varphi + \varphi_n\,, \tag{4.30}$$

where φ_n is the phase variation due to noise, which depends on the SNR value.

The derivative of this parameter is

$$q(n) = \frac{dp}{dn} = \Delta\omega + \omega_n \tag{4.31}$$

where again ω_n is the drift of phase rotation rate due to noise, which depends on the SNR value.

The measurement must be performed in a number of experiments (in time or in ensemble) then averaged to minimise the effect of Gaussian noise.

$$\Delta\hat{\omega} = E(q) = \Delta\omega \tag{4.32}$$

It should be noted that the above procedure is valid to measure the fine frequency error, i.e. $\left|\Delta f_f\right| \le \frac{0.5}{T_b}$.

The frequency error estimator is depicted in Figure 4.10. After the wavelet demodulation, the argument of the combiner output signal is estimated. The frequency error is the slope of the phase variation and given by the derivative of arg(.) and averaged over a number of measurements.

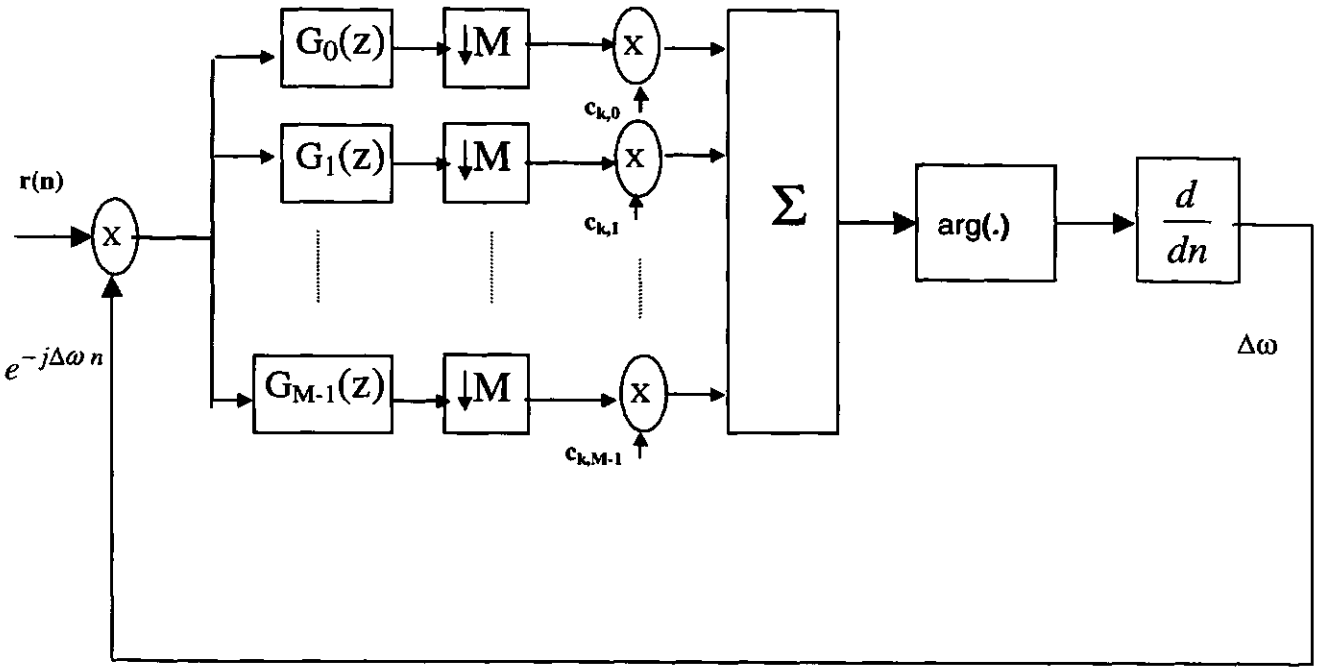

Figure 4.10 Frequency error estimator

Figure 4.11 shows the effects of the frequency error on the signal orthogonality using binary random input signal. Without frequency error, Figure 4.11 (a) demonstrates the perfect orthogonality of the combiner output signal. Signal '1' and '0' have the same magnitude and distinct phases to distinguish between them. With a fine frequency error ($\Delta f_f = \frac{0.01}{M}$) in Figure 4.11 (b), the signal phases become random like which cause the probability of error = 0.5 if it is not corrected. In an extreme case when a coarse frequency error ($\Delta f_c = 1$) in Figure 4.11 (c), the orthogonality is still maintained perfectly. Note that this is just to show the cyclic with the assumption of no band rejection which is not always the case.

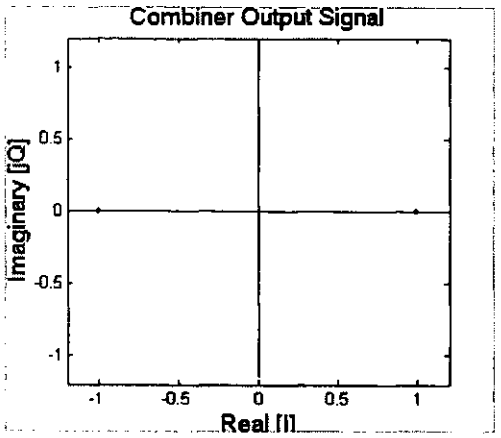

(a)

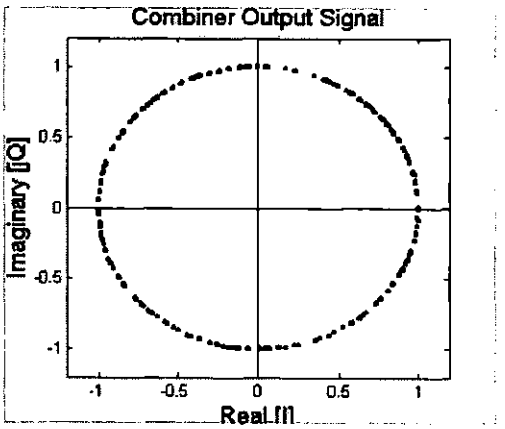

(b)

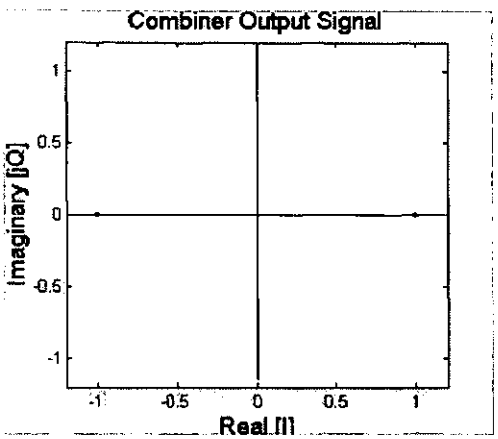

(c)

Figure 4.11 The diagram of the combiner output signal

(a) without frequency error ($\Delta f_c = 0$) (b) with a fine frequency error ($\Delta f_f = \frac{0.01}{M}$)

(c) with a coarse frequency error ($\Delta f_c = 1$)

Figure 4.12 demonstrates the effect of frequency error on the phase variation and this phase rotation rate is used to measure the fine frequency error. Figure 4.12 (a) shows the phase variation without frequency error which is zero mean random due to the noise. Figure 4.12 (b) shows the phase variation due to the frequency error and the noise. The fine frequency error is just the mean slope of the phase. The simulation yields the measured frequency error of 0.1010/M and the variance = 1.608×10^{-4} . The same phenomenon happens but with better results because higher Eb/No value in Figure 4.12 ((c) and (d). The simulation yields the measured frequency error of 0.0998/M and the variance = 1.951×10^{-5}.

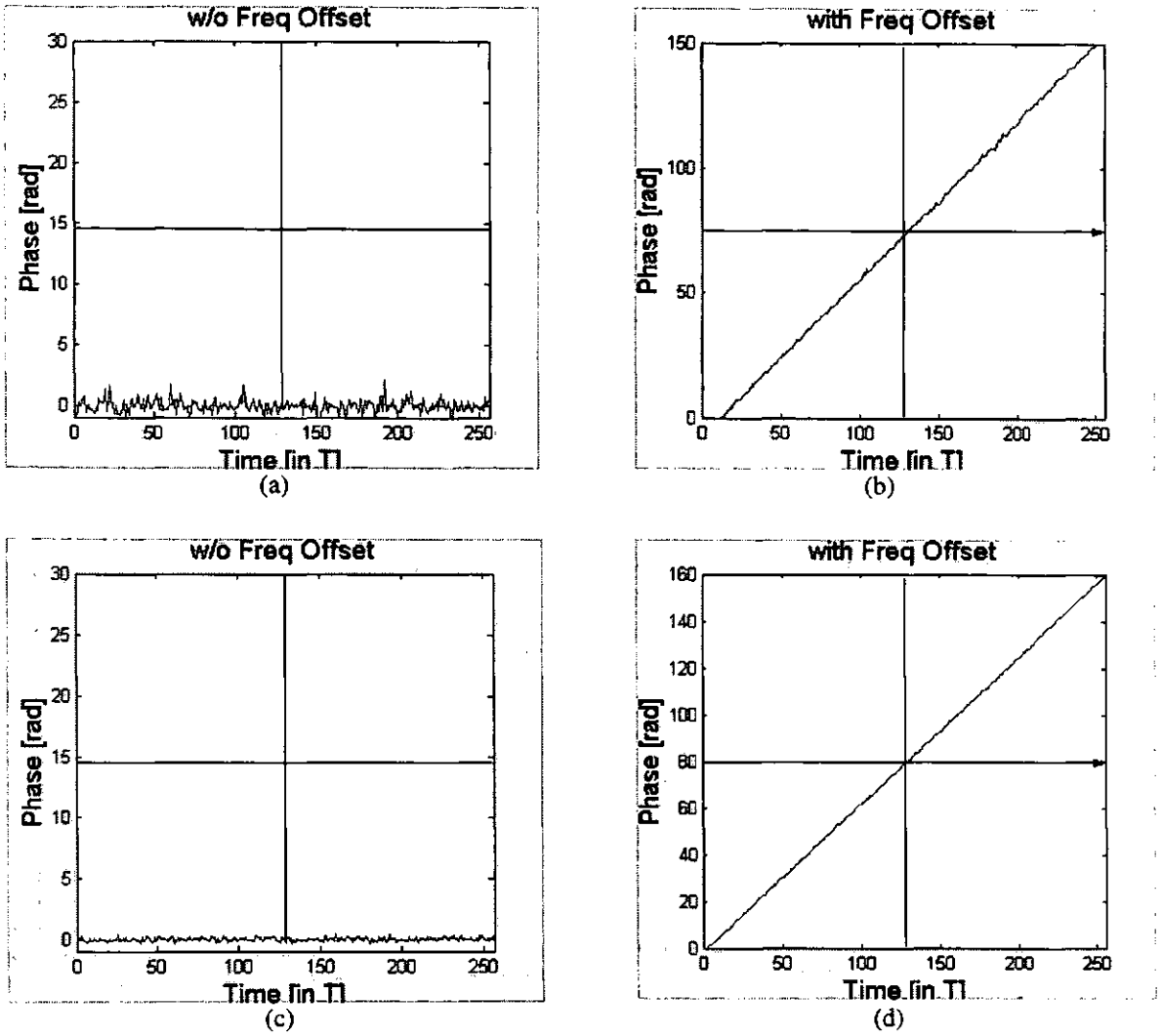

Figure 4.12 The effect and the estimation of frequency error

(a) without frequency error (Eb/No=0 dB) (b) with a fine frequency error ($\Delta f_f = \frac{0.1}{M}$ and Eb/No=0 dB)

(c) without frequency error (Eb/No=10 dB) (d) with a fine frequency error ($\Delta f_f = \frac{0.1}{M}$ and Eb/No=10dB)

The performance of the frequency error estimator as measured in variance of frequency error versus Eb/No is shown in Figure 4.13. The variance becomes smaller for higher Eb/No.

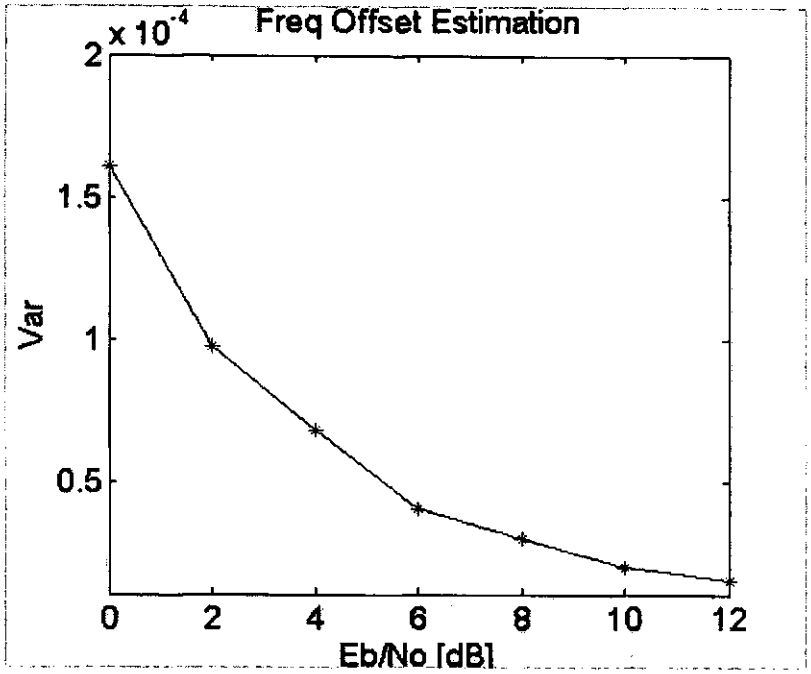

Figure 4.13 Variance of frequency error estimation error versus Eb/No

4.2.2 Phase Offset Estimation

After the frequency error correction, equation 4.25 becomes

$$r(n)=\sum_{k=0}^{K-1}\sum_{i=-\infty}^{\infty}\sum_{m=0}^{M-1}h_m a_k[i]c_{k,m}f_m(n-iM)e^{j\Delta\varphi}+z(n) \tag{4.31}$$

Again we apply the same procedure as described in the above section (4.2.1) we will get the following equation instead of equation 4.28.

$$p(n)=\Delta\varphi+\varphi_n \tag{4.32}$$

Carrying out the measurement in a number of experiments (in time or in ensemble) then averaging the results to minimise the effect of Gaussian noise we will get the following result

$$\Delta\hat{\varphi}=E(p)=\Delta\varphi \tag{4.33}$$

The phase offset estimator is depicted in Figure 4.14. After the wavelet demodulation, the argument of the combiner output signal is taken. In order to obtain the phase offset, this signal is measured in a number of samples.

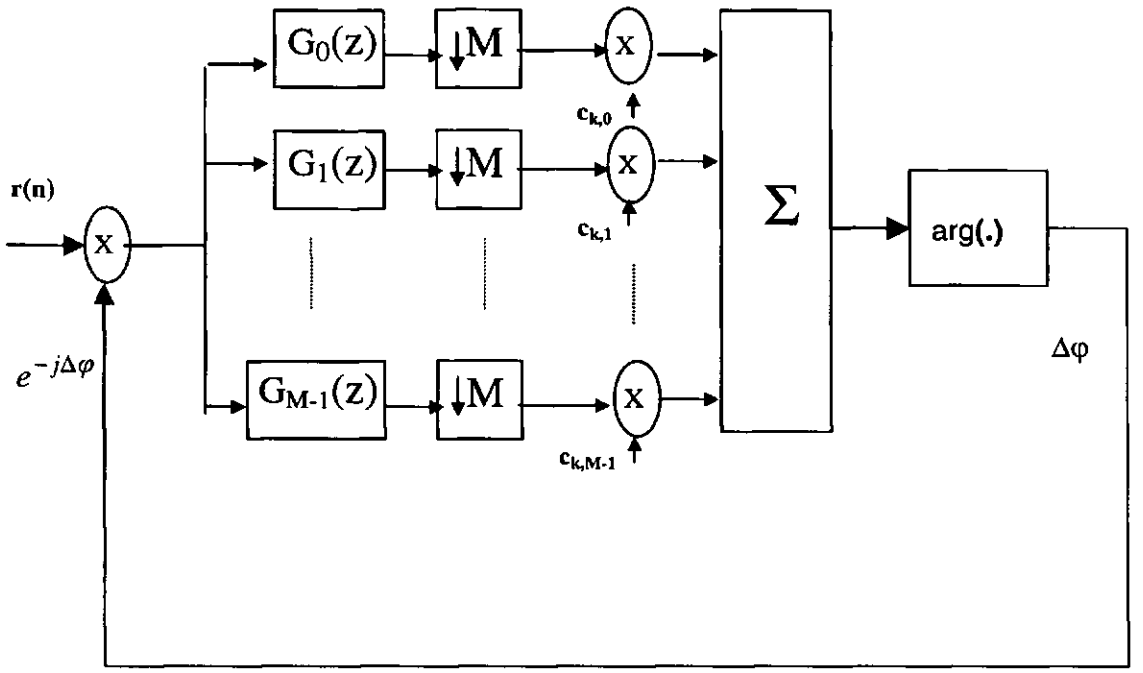

Figure 4.14 Phase offset estimator

Figure 4.15 shows the effect of the phase offset to the signal orthogonality using binary random input signal. For small phase offset ($|\Delta\varphi| < \frac{\pi}{2}$), Figure 4.15 (a) demonstrates the phase distortion of the combiner output signal, but this distortion does not cause error. On the other hand, for a large phase offset ($|\Delta\varphi| > \frac{\pi}{2}$), Figure 4.15 (b) shows that the phase distortion may cause error in symbol detection if it is not corrected.

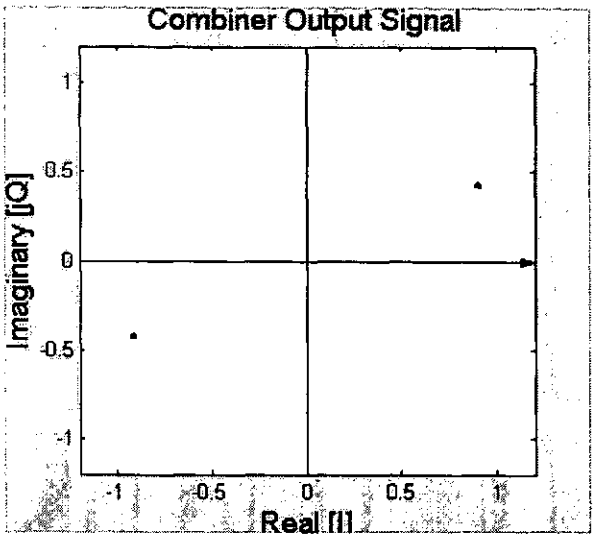

(a)

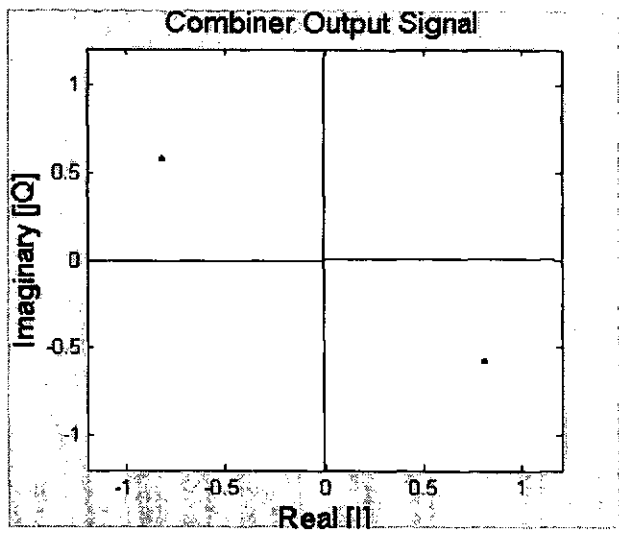

(b)

Figure 4.15 The diagram of the combiner output signal

(a) with a phase offset ($\Delta\varphi = 25$ deg) (b) with a phase offset ($\Delta\varphi = 145$ deg)

Figure 4.16 demonstrates the effect of phase offset on the combiner output signal. Figure 4.16 (a) shows the phase variation without phase offset which is zero mean random due to the noise. Figure 4.16(b) shows the phase variation due to the phase offset and the noise. The phase offset is just the mean of the signal argument. The simulation yields the measured phase offset of 45.0170 and the variance of 0.02910. The same phenomenon happens in Figure 4.16 (c) and (d) but with better results because higher Eb/No value. The simulation yields the measured phase offset of 44.9986 and the variance of 0.00321.

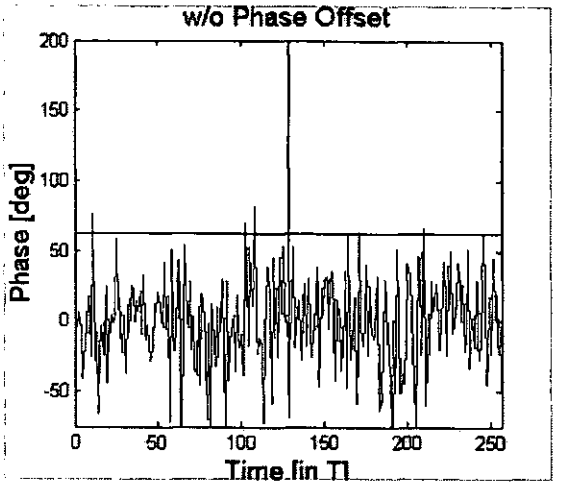

(a)

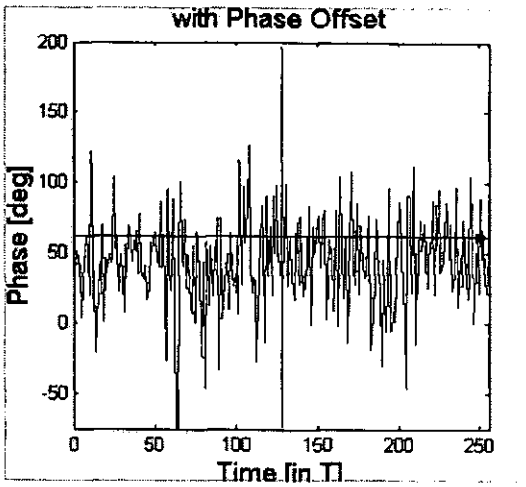

(b)

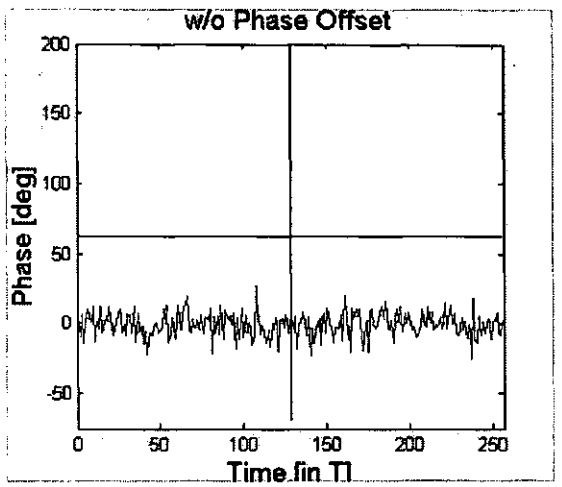

(c)

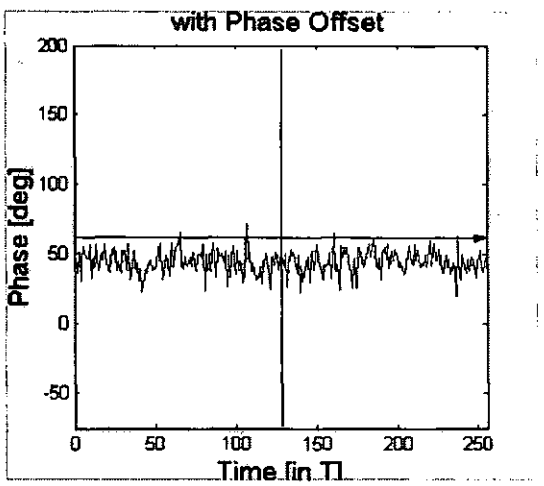

(d)

Figure 4.16 The effect and the estimation of phase offset

(a) without phase offset (Eb/No=0 dB) (b) with a phase offset ($\Delta\varphi = 45$ deg and Eb/No=0 dB)

(c) without phase offset (Eb/No=10 dB) (d) with a phase offset ($\Delta\varphi = 45$ deg and Eb/No=10dB)

The performance of the phase offset estimator, measured as variance of phase error versus Eb/No is shown in Figure 4.17. The results show better performance (meaning the variance is smaller) for higher Eb/No.

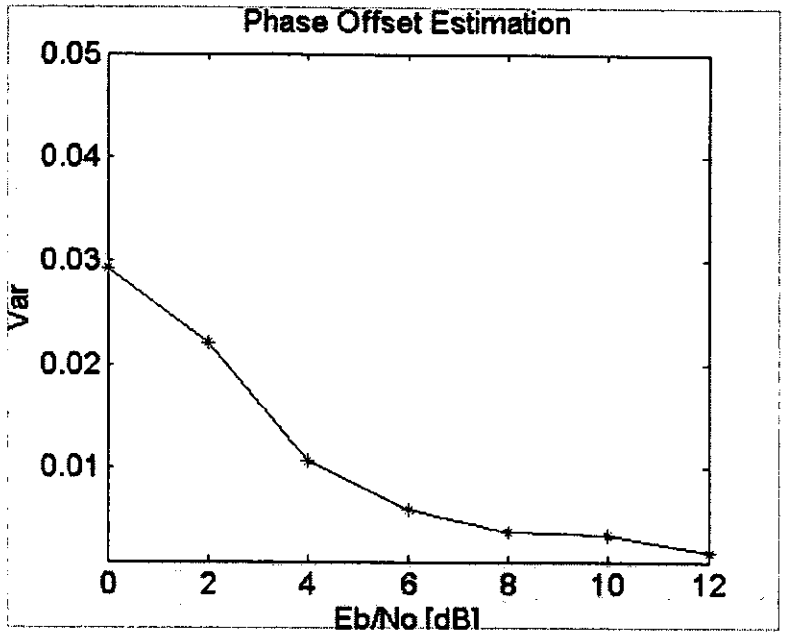

Figure 4.17 Variance of phase offset estimation error versus Eb/No

CHAPTER V

MULTIUSER DETECTION METHODS

The radio frequency spectrum is very limited and in order to use it efficiently the communication systems employs *multiple access* technique to share the communication channel between a number of users. The separation between user energies is carried out in the space domain or in the time-frequency domain. Examples of the multiple access technique in the space domain are polarisation division multiple access (PDMA) and space division multiple access (SDMA) [4]. Multiple access in the time-frequency domain allocates a signature waveform for each user to modulate the data signal. The receiver demodulates the data signal using user's unique signature waveform. Various signature waveform designs result in different multiple access techniques. The oldest one is frequency division multiple access (FDMA) where each user's signature waveform occupies its own frequency band. Then later on time division multiple access (TDMA) appears in digital communication systems, where each user's signature waveform is limited to a certain time interval. The more recent multiple access method is code division multiple access (CDMA) where users are separated neither in time nor in frequency domain, but all signature waveforms occupy the whole frequency band allocated for the transmission at all times. The users detect the desired data making use of the orthogonality or near orthogonality of the signature waveforms. CDMA can be implemented in numerous ways, such as direct sequence (DS), time hopping (TH), and frequency hopping (FH) spread spectrum systems [14,117] as well as using multicarrier (MC) techniques [15,19,21,23]. Design of CDMA signature waveforms based on wavelets [62,6365-68] or

overlapping signature waveforms (spread signature CDMA) [69-71] have also been proposed to improve system performance.

In a single user communication through AWGN channel, the optimal linear detector is matched filter [90]. It is implemented using a linear filter with impulse response $s(T-t)$ sampled at time T where $s(t)$ is the signature waveform and T is data signal period. It can also be implemented using a correlator that performs a multiplication of the received signal with the signature waveform $s(t)$ followed by integration.

It is this single user matched filter which was used originally for multi user CDMA channel. For this reason, it usually refers to the conventional detector. This type of detector is not optimal when used in multi user channel where there is multiple access interference (MAI). Each active user influences and distorts all other user signals and degrades the received signal quality which in turn increases the bit error rate (BER). This MAI is caused by :

- channel distortion
- near-far effects (not-ideal power control)
- cross correlation characteristics of codes for asynchronous users

Therefore, the design of conventional CDMA systems relies on accurate power control [7,170] to alleviate the near-far problem and spreading sequence design [10,43,67,68,70-72] to reduce cross-correlations between the signature waveforms of the users.

There are two levels of orthogonality in MC-CDMA signal, i.e. subband axis and user axis. On subband axis, the subband signals are orthogonal each other or between wavelet basis in the case of WB-MC-CDMA system . On user axis, the signal are orthogonal between users

using spreading code. For this reason, we perform the optimised detection based on both subband and user axis.

On subband axis, the detection task is how to combine all subband signal energies in order to best recover the data signal. These received subband signals may have different amplitudes and different phase shifts when the signal is transmitted through fading channel. Some combining methods have been proposed, such as equal gain combining (EGC) [23,85,86,171,172] and minimum mean square error combining (MMSEC) [23,87,88,173,174].

In order to improve the performance (BER) and the capacity of the system, the MAI signal must be taken into account. The detection process which takes into account the MAI signal is called *multiuser detection* [89-91] which works along user axis. The optimal multiuser detection was first introduced by Verdu [90-93] that applies maximum likelihood sequence detection (MLSD) which then developed by others [94-96]. The MLSD detects the most likely transmitted sequence by maximising the conditional joint a posteriori probability and then the sequence estimation can be performed by Viterbi algorithm. This multiuser detection is both interference and near-far resistant. The complexity of optimal multiuser detector is exponential with the number of users K that makes it difficult to implement for many practical applications. That is why numerous suboptimal [89,90,97] schemes have been investigated and can be classified into two types, the linear detection [89,90,97] and the interference cancellation techniques [89,98,99,175-183].

The multiuser detection methods that can be classified into linear are the decorrelation [184,185] and the minimum mean square error (MMSE) detection [89,90,186,187]. The

zero-forcing decorrelating detector was first proposed by Schneider [184]. Decorrelating detector applies a linear transformation by multiplying the matched filter output with the inverse cross correlation matrix. Decorrelating detector removes the MAI signal effects but it enhances the background noise effect. The MMSE detector, on the other hand, compromises the effects between the MAI signal and the background noise signal.

For the reasons of reducing the receiver burden in term of prior required parameters, or reducing the computation complexity or adapting with the channel variation, an adaptive version of multiuser detection can be an interesting solution. Many types of adaptive multiuser detection have been proposed [188-197].

In this thesis we apply decorrelating detector, MMSE detector and adaptive implementation to our wavelet-based multicarrier CDMA systems.

5.1 Transmission System Model

The transmission system comprises M branches, each consists of an up-sampler followed by a synthesis filter whose impulse response, derived from the wavelet function's orthogonality conditions, generates a specific wavelet signal. This system is conceptually similar to the familiar multi-rate system except for the use of the energy spreading technique and the order of synthesis and analysis filters. In this system, the synthesis filters come first in the transmitter and the analysis filters come later in the receiver whereas in the multi-rate system the order is the other way around. The block diagram of the baseband wavelet multicarrier CDMA system is shown in Figure 5.1.

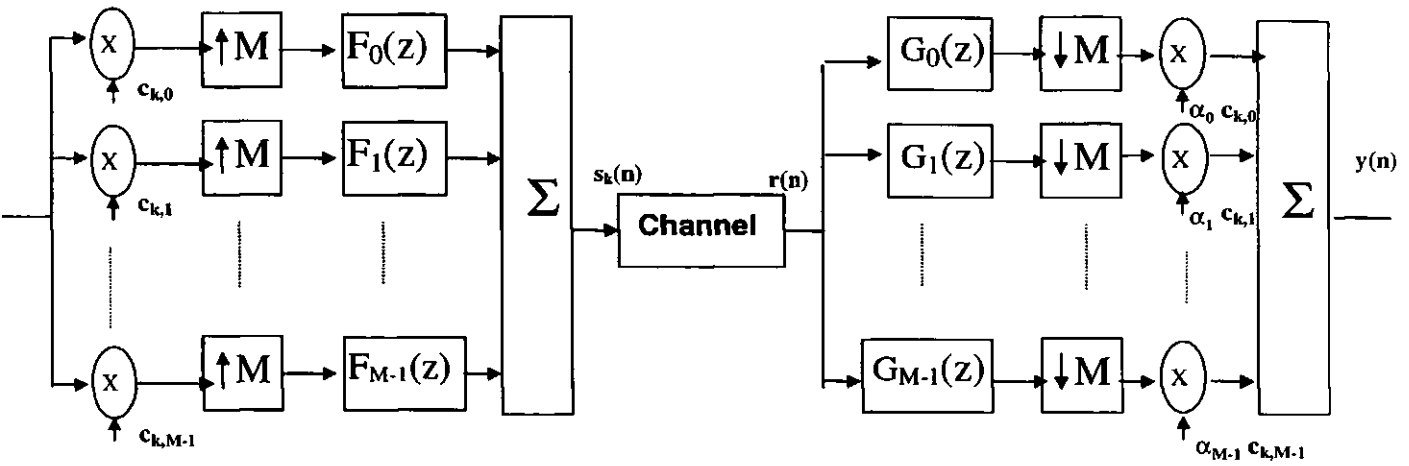

Figure 5.1 Wavelet multicarrier CDMA transmission system

The transmitted signal is generated as follows. A single data symbol is copied into the M branches. In the m^{th} branch, the symbol is multiplied by the m^{th} chip of k^{th} user code, $c_k[m]$, up sampled by M factor and then filtered using synthesis filter $F_m(z)$. The transmitted signal of the k^{th} user, $s_k(z)$, is given by:

$$s_k(z) = \mathbf{F(z)}\,\mathbf{C_k}\,a_k(z^M), \tag{5.1}$$

where $\mathbf{F}(z) = [F_0(z)\ F_1(z)\ \cdots\ F_{M-1}(z)]$ is a row vector representing the transmitter synthesis filters in which $F_m(z)$ is the wavelet generator filter of the m^{th} branch, $\mathbf{C}_k$ is the user's signature code which is the k^{th} column vector of code matrix

$$\mathbf{C} = \begin{bmatrix} c_{0,0} & c_{1,0} & \cdots & c_{K-1,0} \\ c_{0,1} & c_{1,1} & & c_{K-1,1} \\ \vdots & & & \\ c_{0,M-1} & c_{1,M-1} & & c_{K-1,M-1} \end{bmatrix} \tag{5.2}$$

and a_k is the k^{th} user's input symbol. Throughout the paper, a bold letter is used to indicate a vector or a matrix variable.

5.2 Wavelet Demodulation

The basic wavelet receiver, shown in Figure 5.1 consists of M parallel branches; each consists of an analysis filter followed by a down sampler. Each of the analysis filters is a matched counter-part of the corresponding synthesis filter. Furthermore, the two filter banks must be biorthogonal satisfying the following biorthogonality constraint [3]:

$$\sum_{n} g_i(n) f_j(Ml-n) = \delta(l)\delta(i-j), \tag{5.3}$$

where $f_i(n)$ is the discrete-time transmitter filter and $g_i(n)$ is the discrete-time receiver filter, and i = 0,1, ... , M-1. In the z domain, equation (5.3) is written as follows:

$$\mathbf{G}(z)\,\mathbf{F}(z) = \mathbf{I}, \tag{5.4}$$

where $\mathbf{G}(z) = [G_0(z)\, G_1(z) \quad \cdots \quad G_{M-1}(z)]^T$.

Considering the transmission through the AWGN channel, the k^{th} user received signal, $r_k(z)$, is given by:

$$r_k(z) = H_k(z)\, s_k(z) + n(z), \tag{5.5}$$

where $H_k(z)$ is the channel carrying the k^{th} user signal and the term n(z) represents the additive white Gaussian noise (AWGN) with a two-sided power spectral density of No/2.

Consider K active users (K ≤ M) sharing the AWGN channel. The received signal, r(z), is given by:

$$r(z) = \sum_{k=0}^{K-1} H_k(z)\, s_k(z) + n(z). \tag{5.6}$$

Substituting for $s_k(z)$ from equation (5.1) and considering the channel is frequency - nonselective, we have:

$$r(z) = \sum_{k=0}^{K-1} \mathbf{F}(z)\, \mathbf{C}_k . \mathbf{H}_k\, a_k(z^M) + n(z), \tag{5.7}$$

where $\mathbf{H}_k$ is the k[th] column vector of channel matrix $\mathbf{H}$, and each element of the vector represents the channel amplitude scaling for each sub-band in use

$$\mathbf{H} = \begin{bmatrix} h_{0,0} & h_{1,0} & \cdots & h_{K-1,0} \\ h_{0,1} & h_{1,1} & & h_{K-1,1} \\ \vdots & & & \\ h_{0,M-1} & h_{1,M-1} & & h_{K-1,M-1} \end{bmatrix}. \tag{5.8}$$

Equation 5.7 can be simplified to the following equation:

$$r(z) = \sum_{k=0}^{K-1} \mathbf{F}(z)\, \mathbf{E}_k(z)\, a_k(z^M) + n(z), \tag{5.9}$$

where the inner product of the spreading sequence and the channel amplitude scaling

$$\mathbf{E}_k = \mathbf{C}_k . \mathbf{H}_k \tag{5.10}$$

is the k[th] column vector of matrix $\mathbf{E}$ and it also represents the effective spreading sequence of the k[th] user's signal at the output of the channel. For a flat-faded channel, $\mathbf{E}_k$ is constant across each of the sub-bands.

$$\mathbf{E} = \begin{bmatrix} c_{0,0}h_{0,0} & c_{1,0}h_{1,0} & \cdots & c_{K-1,0}h_{K-1,0} \\ c_{0,1}h_{0,1} & c_{1,1}h_{1,1} & & c_{K-1,1}h_{K-1,1} \\ \vdots & & & \\ c_{0,M-1}h_{0,M-1} & c_{1,M-1}h_{1,M-1} & & c_{K-1,M-1}h_{K-1,M-1} \end{bmatrix}. \tag{5.11}$$

The signal at the output of the m[th] branch of the k[th] user receiver is:

$$\boldsymbol{\omega}(z) = \mathbf{G}(z)\, r(z^{\frac{1}{M}}), \tag{5.12}$$

where $\boldsymbol{\omega}(z) = [\omega_0(z)\ \omega_1(z)\ \cdots\ \omega_{M-1}(z)]^T$. Substituting for r(z), we have:

$$\boldsymbol{\omega}(z) = \sum_{k=0}^{K-1} \mathbf{G}(z)\, \mathbf{F}(z)\, \mathbf{E}_k\ a_k(z) + \mathbf{N}(z), \tag{5.13}$$

where the filtered noise $\mathbf{N}(z)$ is given by:

$$\mathbf{N}(z) = \mathbf{G}(z)\, n(z^{\frac{1}{M}}). \tag{5.14}$$

Using the biorthogonality property, equation (5.13) can be simplified to:

$$\omega(z) = \sum_{k=0}^{K-1} \mathbf{E}_k \; a_k(z) + \mathbf{N}(z)$$

$$\boldsymbol{\omega}(z) = \mathbf{E}\,\mathbf{a}(z) + \mathbf{N}(z). \tag{5.15}$$

The decision variable in the k[th] user's receiver is written as follows:

$$\mathbf{y_k}(\mathbf{z}) = \boldsymbol{\beta}_\mathbf{k}\; \boldsymbol{\omega}(\mathbf{z}), \tag{5.16}$$

where $\boldsymbol{\beta}_\mathbf{k}$ is the k[th] row of matrix β,

$$\beta = \begin{bmatrix} \beta_{0,0} & \beta_{0,1} & \beta_{0,M-1} \\ \beta_{1,0} & \cdots & \vdots \\ \vdots & & \\ \beta_{K-1,0} & \cdots & \beta_{K-1,M-1} \end{bmatrix} \tag{5.17}$$

which is KxM matrix of $\beta_{k,m}$, and $\beta_{k,m} = \alpha_{k,m}\, c_{k,m}$ is the sub-band gain factor $\alpha_{k,m}$ (which depends on the combining strategy employed) multiplied by the code chip $c_{k,m}$.

In general for all K users these decision variables are:

$$\mathbf{y(z)} = \boldsymbol{\beta}\,\boldsymbol{\omega}\mathbf{(z)}. \tag{5.18}$$

Substituting $\omega(z)$, the decision variables become:

$$\mathbf{y(z)} = \boldsymbol{\beta}\,\mathbf{E}\,\mathbf{a(z)} + \boldsymbol{\xi}(z), \tag{5.19}$$

where the noise term becomes $\boldsymbol{\xi}(z) = \boldsymbol{\beta}\,\mathbf{G}(z)\, n(z^{\frac{1}{M}})$ (5.20)

and the column vector $\xi(z) = [\xi_0(z)\, \xi_1(z) \;\; \cdots \;\; \xi_{K-1}(z)]^T$,

$\mathbf{a}(z) = [\, a_0(z) \;\; a_1(z) \;\; a_2(z) \;\; .... \;\; a_{K-1}(z)\,]^T$,

and $\mathbf{y}(z) = [\, y_0(z) \;\; y_1(z) \;\; y_2(z) \;\; ..... \;\; y_{K-1}(z)\,]^T$.

The decision variables, $\mathbf{y}(z)$, can be split up into three terms, identified as the desired signal that is given by Diag $\langle \boldsymbol{\beta}\mathbf{E} \rangle$, the multiple access interference (MAI) that is given by $[\boldsymbol{\beta}\,\mathbf{E} - \mathbf{Diag}\langle \boldsymbol{\beta}\,\mathbf{E} \rangle]$, and the channel noise $\underset{\sim}{\xi}$. Consequently, we have:

$$\mathbf{y} = \underbrace{Diag\langle \boldsymbol{\beta}\,\mathbf{E} \rangle\,\mathbf{a}}_{desired\ signal} + \underbrace{[\boldsymbol{\beta}\,\mathbf{E} - Diag\langle \boldsymbol{\beta}\,\mathbf{E} \rangle]\,\mathbf{a}}_{MAI\ signal} + \underbrace{\underset{\sim}{\xi}}_{filtered\ noise} \tag{5.21}$$

It can easily be shown that for a single user channel, the MAI term becomes zero. The matched filter detection scheme described above optimises system's performance in the AWGN channel. As the user roams within the wireless network, their mobility generates multipath transmission that disturbs the channel's orthogonality causing degradation in the system's performance. We propose a two-stage optimisation technique, which is described in this section. The first stage is based on the fact that signal energy is spread in the frequency domain, so a frequency diversity scheme (MMSE combining technique) is used to combat the fading effects of the mobile channel. This diversity comes from the fact that each subband carries the same information signal. The second stage uses a MMSE multi-user detector to eliminate the MAI interference. It is clear that using both techniques at the same time would require optimising a KM x KM matrix (where K is the number of active users and M is the number of sub-bands), which would impose a colossal computation cost. Clearly, the computation required in the proposed scheme is much less than optimising the M x M matrix in the first stage followed by optimising the K x K matrix. We have assumed that the channel effects in the two stages are independent.

5.3 The Principle of MMSE Estimation

The objective of an estimation process (including detection method) is to make the estimation error e(n) as small as possible using certain statistical criterion for optimisation. The estimation error is defined as the difference between the desired response a(n) and the filter output signal y(n)

$$e(n) = a(n) - y(n). \tag{5.22}$$

The procedure to optimise the filter response is to minimise the cost function J(n) based on certain powers of the absolute value of the estimation error, for example

$|e|_{\min}$, $|e|^2_{\min}$ (MMSE), etc.

Now consider the minimum mean squared error (MMSE) method and take the mean squared error as the cost function such that :

$$J(n) = E\left(e(n)\, e^*(n)\right) = E\left(|e(n)|^2\right). \tag{5.23}$$

To attain the minimum point then the partial derivative (usually called as *gradient operator*) must be zero

$$\nabla_k J(n) = 0 \quad k = 0,1,\cdots \tag{5.24}$$

$$\frac{\partial J}{\partial a_k} + j\frac{\partial J}{\partial b_k} = 0 \quad k = 0,1,\cdots, \tag{5.25}$$

where a_k, b_k are the real and the imaginary parts of the filter coefficients respectively

$$w_k = a_k + j\, b_k. \tag{5.26}$$

Using equations (5.22), (5.23) and (5.25) we can solve equation (5.24) and get the following result

$$E\left(x(n-k)\, e^*_{\min}(n)\right) = 0 \quad k = 0,1,\cdots, \tag{5.27}$$

where $x(n)$ is the input signal.

This is the necessary and sufficient condition for the cost function J to attain the minimum point. This is also known as the *orthogonality principle*,"The estimation error is orthogonal to each input signal that enters into the estimation at time n " [198].

The estimation result is the filter output signal when it attains minimum mean square error (MMSE).

$$\hat{a}(n) = y(n)\Big|_{e(n)=e_{\min}}, \tag{5.28}$$

where

$$y(n) = \sum_{k=0}^{\infty} w_k^* \; x(n-k) \tag{5.29}$$

is the output filter signal and w is the filter coefficients.

Now we can write

$$e_{\min} = a(n) - \hat{a}(n). \tag{5.30}$$

Assuming both averages of the random variables a(n) and $\hat{a}$(n) are zero and evaluating the mean square value of both sides of equation (5.30) we get

$$J_{\min} = \sigma_a^2 - \sigma_{\hat{a}}^2. \tag{5.31}$$

Reformulate the orthogonality principle by substituting equations (5.22) and (5.23) into (5.26)

$$E\left(x(n-i)\left(a^*(n) - \sum_{k=0}^{\infty} w_{opt,k} \; x^*(n-k) \right)\right) = 0, \tag{5.32}$$

where $w_{opt,k}$ is the i^{th} coefficient of the optimum filter.

Rearranging the above equation, we get

$$\sum_{k=0}^{\infty} w_{opt,k} \; E\left(x(n-i)\, x^*(n-k)\right) = E\left(x(n-i)\, a^*(n)\right). \tag{5.33}$$

We may rewrite the above equation as follows:

$$\sum_{k=0}^{\infty} w_{opt,k}\ r_{xx}(k-i) = r_{xa}(-i)\,, \tag{5.33}$$

where $r_{xx}(k-i)$ is the autocorrelation of the input signal x(n) for a lag of (k-i) and $r_{xa}(-i)$ is the cross correlation between the input signal x(n) and the desired signal a(n) for a lag of (-i)

The optimum filter coefficients can be defined in terms of autocorrelation of the input signal x(n) and the cross correlation between the input signal x(n) and the desired signal a(n). The equation (5.33) is known as Wiener-Hopf equation [198].

In matrix form this equation can be written as follows

$$\mathbf{R}_{xx}\mathbf{w}_{opt} = \mathbf{R}_{xa}, \tag{5.34}$$

where $\mathbf{R}_{xx}$ is M by M autocorrelation matrix of the input signal $x(n)$, M is the filter length, $\mathbf{x}(n) = [x(n), x(n-1), \cdots x(n-M+1)]^T$ and $\mathbf{R}_{xa}$ is M by 1 cross correlation matrix between the input signal $x(n)$ and the desired signal $a(n)$.

We may rearrange equation 5.34 above to get the filter coefficients

$$\mathbf{w}_{opt} = \mathbf{R}_{xx}^{-1}\mathbf{R}_{xa}, \tag{5.35}$$

where we assume $\mathbf{R}_{xx}$ to be non singular. The optimal filter (called as the Wiener filter as well) is the filter which minimises the mean squared error between the desired signal and the estimated signal by applying the linear filter $\hat{\mathbf{a}} = \mathbf{w}_{opt}^{H}\mathbf{x}$. This filter depends upon the inverse of the covariance matrix of the observation signal $\mathbf{x}$ and the cross-correlation vector of the observation signal $\mathbf{x}$ and the desired signal $\mathbf{a}$.

The corresponding minimum mean square error (MMSE) in matrix form is as follows

$$J_{\min} = \sigma_a^2 - \mathbf{R}_{xa}^{H}\mathbf{w}_{opt}. \tag{5.36}$$

We can write this equation into this

$$J_{\min} = \sigma_a^2 - \mathbf{R}_{\mathbf{xa}}^H \mathbf{R}_{\mathbf{xx}}^{-1} \mathbf{R}_{\mathbf{xa}}. \tag{5.37}$$

5.4 Optimum Combining Strategy

Let the received signal at the output of the down samplers be defined by $\mathbf{x}_k(z)$ vector such that

$$\mathbf{x}_k(z) = \mathbf{C}_k . \omega(z), \tag{5.38}$$

where $\mathbf{x}_k(z) = [x_{k,0} \;\; x_{k,1} \;\; \ldots \;\; x_{k,M-1}]^T$.

Substituting for $\omega(z)$ from equation (5.15), we get:

$$\mathbf{x}_k(z) = \mathbf{C}_k . [\mathbf{E}(z)\,\mathbf{a}(z) + \mathbf{N}(z)]. \tag{5.39}$$

The minimum mean square error (MMSE) criteria chooses the Mx1 vector α which minimises:

$$E([a_k - \alpha_k^H \mathbf{x}_k]^2, \tag{5.40}$$

where the superscript H denotes Hermitian transposition and the estimated data signal is given as:

$$\hat{a}_k = \mathrm{sgn}(\alpha_k^H \mathbf{x}_k). \tag{5.41}$$

Using the Wiener-Hopf equation (5.35), the optimum condition is achieved when the filter coefficients (α_k) satisfy the following equation:

$$\alpha_{opt} = \mathbf{R}_{\mathbf{xx}}^{-1} \mathbf{R}_{\mathbf{xa}}, \tag{5.42}$$

where $\mathbf{R}_{\mathbf{xx}}$ is the auto-correlation of the input signal $\mathbf{x}$ and $\mathbf{R}_{\mathbf{xa}}$ is the cross-correlation between the input signal and the data signal $\mathbf{a}$. Substituting for $\mathbf{x}_k(z)$ in the equation (5.39) we get:

$$\mathbf{R}_{XX} = \mathrm{E}(\mathbf{E}\,\mathbf{a}\,\mathbf{a}^{\mathrm{H}}\,\mathbf{E}^{\mathrm{H}}) + \mathrm{E}(\mathbf{N}\,\mathbf{N}^{\mathrm{H}}). \tag{5.44}$$

The noise signal, $\nu_m(z)$, at the output of the analysis filter $G_m(z)$ in the m^{th} branch is:

$$\nu_m(z) = G_m(z)\, n(z^{\frac{1}{M}}). \tag{5.45}$$

The variance of this noise is:

$$E(\nu_m^2) = E(G_m^2(z)\, n^2(z^{\frac{1}{M}})) = E(G_m^2(\omega)\, n^2(\frac{\omega}{M})) \tag{5.46}$$

Simplifying further this equation and taking the approximation:

$$E(\nu_m^2) = \int_0^1 G_m^2(\omega)\, n^2(\frac{\omega}{M})\, d\omega \approx \frac{\sigma^2}{M}. \tag{5.47}$$

In matrix form, the variance is:

$$\mathrm{E}(\mathbf{N}\,\mathbf{N}^{\mathrm{H}}) = \mathrm{E}(\mathbf{G}^2(z)\,\mathbf{n}^2(z^{\frac{1}{M}})) = (\mathrm{M}\frac{\sigma^2}{\mathrm{M}})\,\mathbf{I} = \sigma^2\,\mathbf{I} \tag{5.48}$$

The auto-correlation matrix of the input signal **x** can be shown to be:

$$\mathbf{R}_{XX} = [\mathrm{E}(\mathbf{H}\,\mathbf{H}^{\mathrm{H}}) + \sigma^2\,\mathbf{I}]. \tag{5.49}$$

Assuming independent and identically distributed (IID) fading at the subbands, and calculating $E(\mathbf{H}\,\mathbf{H}^{H})$ we will get

$$E(\mathbf{H}\,\mathbf{H}^{H}) = \begin{bmatrix} \sum_{i=0}^{K-1} (h_{i,0})^2 & 0 & \cdots & 0 \\ 0 & \sum_{i=0}^{K-1} (h_{i,1})^2 & & 0 \\ \vdots & & & \\ 0 & 0 & & \sum_{i=0}^{K-1} (h_{i,M-1})^2 \end{bmatrix}. \tag{5.50}$$

The cross-correlation $\mathbf{R}_{xa}$ can be written as:

$$\mathbf{R}_{xa} = \mathrm{E}(\mathbf{x}\ \mathbf{a}_k). \tag{5.51}$$

Substituting for **x** in equation (5.51) and simplifying, $\mathbf{R}_{xa}$ is given by:

$$\mathbf{R}_{xa} = \mathbf{H}_k . \tag{5.52}$$

Substituting $\mathbf{R}_{xx}$ and $\mathbf{R}_{xa}$ into equation (5.42), we get:

$$\alpha_{opt} = [E(\mathbf{H}\,\mathbf{H}^H) + \sigma^2 \mathbf{I}]^{-1}\,\mathbf{H}_k . \tag{5.53}$$

Equation (5.53) gives the optimum coefficients α_{opt} that minimises the mean square error between the estimated data signal and the desired data signal. Considering the same assumptions as in [88] (synchronous downlink system and full loading (K=M)), equation (5.53) reduces to:

$$\alpha_m = \frac{h_m}{M h_m^2 + \sigma^2}, \tag{5.54}$$

which is similar to that given by [88].

It can bee seen from the above equation that the optimised coefficients are determined by the background noise signal and the MAI signal specified by the channel distortion $|h_m|$.

5.5 Multiuser Detection

5.5.1. Matched Filter Detector

Here we discuss the case of multiuser matched filter detection in the wavelet- based MC-CDMA system. This detection consists of a bank of K filters as depicted in Figure 5.2. Each filter is matched to each user signature waveform. Actually this matched filter process has been discussed in wavelet demodulation (see section 5.2). In order to detect the data signal correctly, the matched filter detector requires the knowledge of the signature waveform and the timing of the desired user or users.

We can see from equation 5.21 that for single user, under AWGN channel and no fading ($h_m=1$) , the matched filter is the optimum detector. This optimality property is still intact for the case multiuser and synchronous wavelet based MC-CDMA system under AWGN channel as the second term of equation 5.21 becomes zero. But when the wavelet based MC-CDMA signal is transmitted through non uniform channel, matched filter is not the optimum detector anymore.

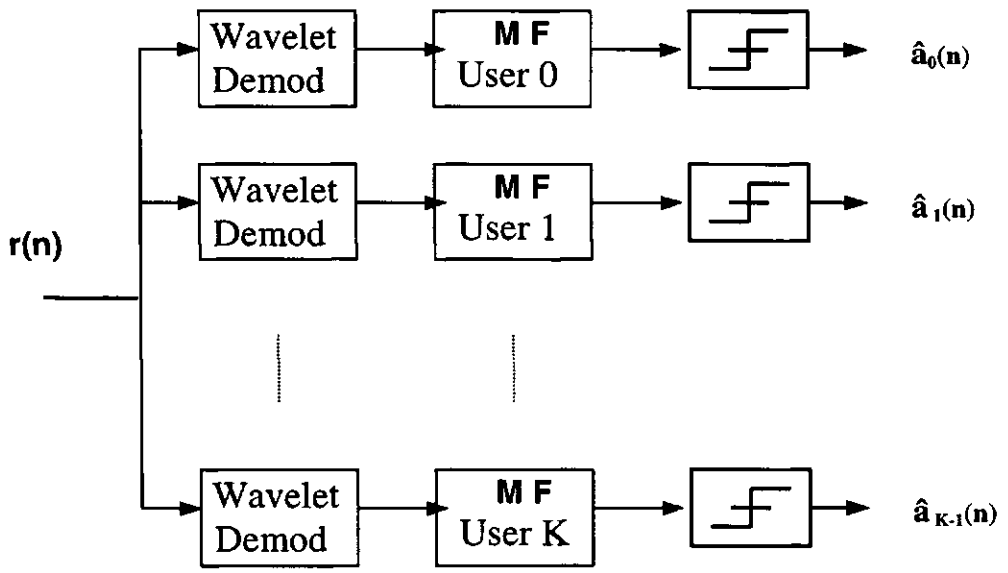

Figure 5.2 Bank of matched filters used for detection

5.5.2 Decorrelating Detector

The output signal vector of the bank of K matched filters is given in equation 5.20 and now let

$$\gamma = \beta \mathbf{E}. \tag{5.55}$$

The equation becomes as follows

$$\mathbf{y} = \gamma\,\mathbf{a} + \xi\,. \tag{5.56}$$

The decorrelating detector cancels all the multiple access interference (MAI) signal by just multiplying by the inverse matrix γ (if exists) so that the output becomes

$$\mathbf{y}' = \gamma^{-1}\,\mathbf{y} = \mathbf{a} + \gamma^{-1}\,\xi\,. \tag{5.57}$$

The matched filter is the optimum detector to combat the background noise when there is no multiple access interference (MAI) signal. The decorrelating detector, on the other hand, is the optimum detector to combat the MAI signal when there is no background noise as can be seen from the equation 5.57. This multiuser detection is depicted in Figure 5.3.

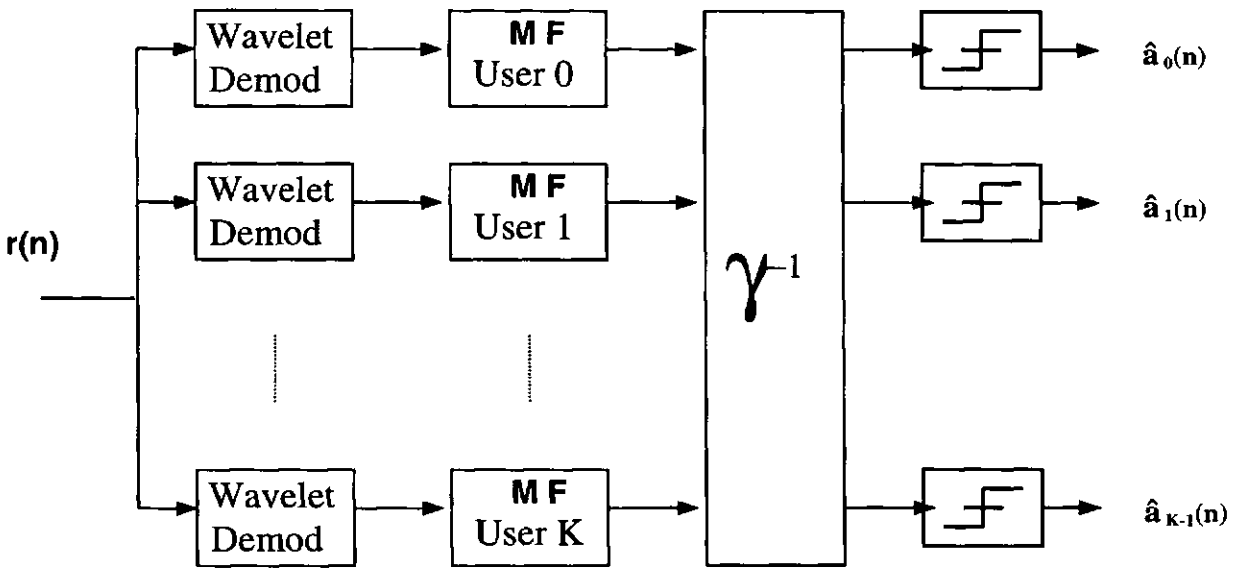

Figure 5.3 Decorrelating multiuser detection

5.5.3 MMSE Multiuser Detector

As both the MAI signal and the background noise signal exist in the real channel, a method to compromise between matched filter and the decorrelating detector is called minimum mean square error (MMSE) detector. This multiuser detection is depicted in Figure 5.4.

The MMSE multiuser detector not only rejects the multiple access interference (MAI) signal, but also reduces the effect of narrowband interference caused by the same frequency operating systems and intersymbol interference caused by multipath channel.

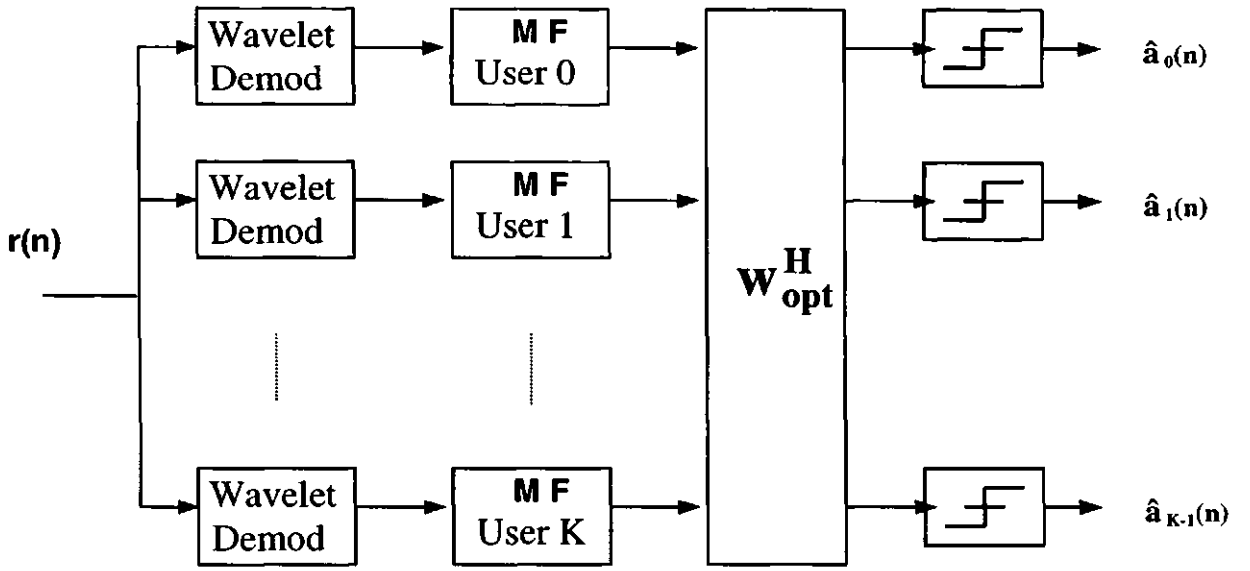

Figure 5.4 MMSE multiuser detection

A common and efficient approach in estimating a random variable **a** based on the observation of **y** is to find the function **a(y)** that minimises the mean square error (MSE):

$$E([\mathbf{a} - \mathbf{a}(\mathbf{y})]^2), \tag{5.58}$$

where **y** is given by equation (5.20) as:

$$\mathbf{y} = \boldsymbol{\beta}\mathbf{E}\mathbf{a} + \xi. \tag{5.59}$$

Applying the MMSE criteria in the wavelet multi-user detection, the problem is then simplified to choosing the K x K matrix **w** that minimises

$$E([\mathbf{a} - \mathbf{w}^H \mathbf{y}]^2), \tag{5.60}$$

and the estimated data is given as:

$$\hat{\mathbf{a}} = \mathrm{sgn}(\mathbf{w}^{H}\mathbf{y}). \tag{5.61}$$

According to the adaptive filter theory (Wiener-Hopf equation (5.35)), the optimum condition is achieved when the filter coefficients satisfy the following equation [135]

$$\mathbf{w}_{opt} = \mathbf{R}_{yy}^{-1}\mathbf{R}_{ya}, \tag{5.62}$$

where

$$\mathbf{R}_{yy} = E(\mathbf{y}\,\mathbf{y}^{T}) \tag{5.63}$$

is the auto-correlation of the input signal y. Substituting y, the above equation becomes

$$\mathbf{R}_{yy} = E(\boldsymbol{\beta}\,\mathbf{E}\,\mathbf{a}\,\mathbf{a}^{T}\mathbf{E}^{T}\,\boldsymbol{\beta}^{T}) + E(\boldsymbol{\xi}\,\boldsymbol{\xi}^{T}), \tag{5.64}$$

where $\xi(z)$ is defined in equation (5.19)

$$\boldsymbol{\xi}(\mathbf{z}) = \boldsymbol{\beta}\,\mathbf{G}(\mathbf{z})\,\mathbf{n}(\mathbf{z}^{\frac{1}{M}}). \tag{5.65}$$

Using equations (5.45), (5.46 and (5.47)), the expected value of the noise signal coming out from the whole filters in matrix form

$$E(\boldsymbol{\xi}\,\boldsymbol{\xi}^{T}) = \boldsymbol{\beta}\left(E(\mathbf{G}^{2}(\mathbf{z})\,\mathbf{n}^{2}(\mathbf{z}^{\frac{1}{M}}))\right)\boldsymbol{\beta}^{T} = \boldsymbol{\beta}\,(M\,\frac{\sigma^{2}}{M})\,\boldsymbol{\beta}^{T} = \sigma^{2}\,\boldsymbol{\beta}^{2}. \tag{5.66}$$

Going back to the auto-correlation equation 5.64

$$\mathbf{R}_{yy} = \boldsymbol{\beta}\,\mathbf{E}\,\mathbf{I}\,\mathbf{E}^{T}\,\boldsymbol{\beta}^{T} + \sigma^{2}\,\boldsymbol{\beta}^{2}. \tag{5.67}$$

Another step of simplification yields

$$\mathbf{R}_{yy} = \boldsymbol{\beta}\,\mathbf{E}^{2}\,\boldsymbol{\beta}^{T} + \sigma^{2}\,\boldsymbol{\beta}^{2}. \tag{5.68}$$

Now the cross-correlation between the input signal y and the desired data signal a is as follows

$$\mathbf{R}_{ya} = E(\mathbf{y}\,\mathbf{a}^{T}). \tag{5.69}$$

Substituting y the above equation becomes

$$\mathbf{R}_{ya} = E(\boldsymbol{\beta}\mathbf{E}\mathbf{a}\mathbf{a}^{T}) = \boldsymbol{\beta}\mathbf{E}. \tag{5.70}$$

Substituting $\mathbf{R}_{yy}$ and $\mathbf{R}_{ay}$ into equation 5.62, we get

$$\mathbf{w}_{opt} = (\beta\mathbf{E}\mathbf{E}^{H}\beta^{H} + \sigma^{2}\beta^{2})^{-1}(\boldsymbol{\beta}\mathbf{E}). \tag{5.71}$$

Now let

$$\boldsymbol{\gamma} = \boldsymbol{\beta}\mathbf{E}. \tag{5.72}$$

Then equation (5.71) can be re-written as:

$$\mathbf{w}_{opt} = \left[\boldsymbol{\gamma}\boldsymbol{\gamma}^{H} + \sigma^{2}\boldsymbol{\beta}^{2}\right]^{-1}\boldsymbol{\gamma}\ . \tag{5.73}$$

Equation (5.73) gives the optimum filter coefficients that minimise the mean square error between the estimated data signal and the desired data signal and consequently optimises the performance of the WB-MC-CDMA system detection. The optimised receiver which is the combination of MMSE combiner and MMSE multiuser detection is shown in Figure 5.5.

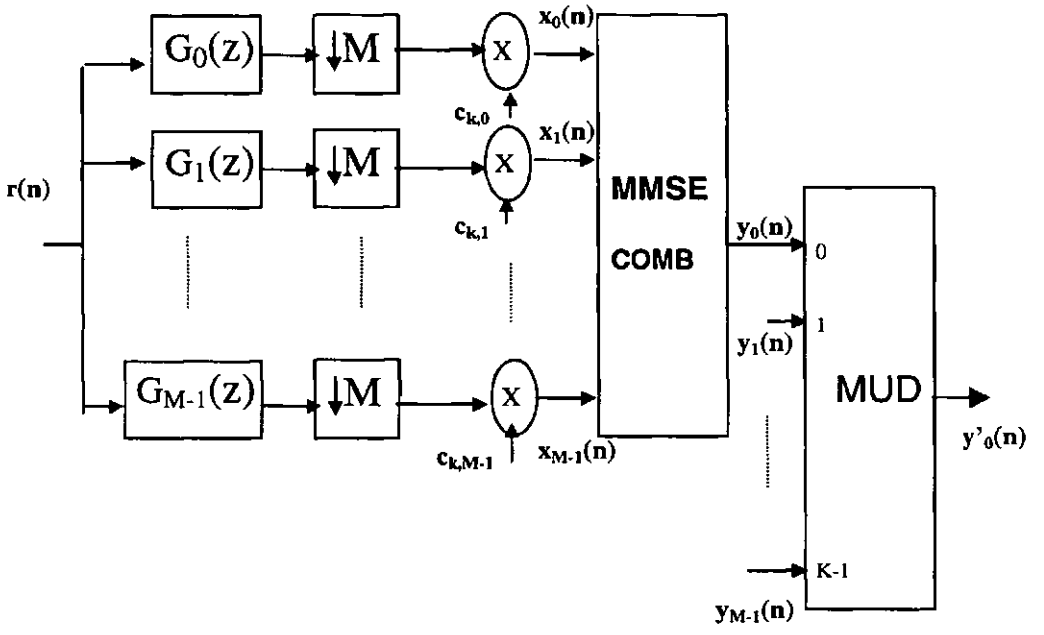

Figure 5.5 Wavelet multicarrier CDMA optimised receiver

5.6 Adaptive Implementation

The preset MMSE multiuser detector alleviates the effect of the MAI signal and the background noise signal but it requires the knowledge of the following parameters :

1. The signature waveform of the desired user
2. The signature waveform of the interfering users
3. The timing (bit epoch and carrier phase) of the desired user
4. The timing (bit epoch and carrier phase) of the interfering users
5. The received amplitudes of the interfering users (relative to that of the desired user).
6. The background noise level

Moreover, these type of MMSE multiuser detectors have significant computation complexity (see section 6.6) and are not suitable for a system with large number of users and high data rate signal. In order to reduce the receiver burden in term of prior required parameters, the computation complexity and more importantly to adapt with the channel variation, an adaptive version of MMSE can be an interesting solution. It only requires the information of the timing of the desired user (item 3) and the training sequence.

Minimum mean square error multiuser detector (MMSE-MUD) can be made adaptive by updating the linear filter coefficients according to the channel conditions. The coefficients are calculated each bit epoch via an adaptation algorithm such as the Linear Mean Square (LMS) or Recursive Least Squares (RLS) algorithms [134,198,199]. Both algorithms converge to the optimal filter; however, the RLS has the advantage of much faster convergence at the price of much greater complexity.

The adaptive MMSE detection has the advantage of not only suppressing the interference from other active users or multiple access interference (MAI), but also reducing the effect of narrowband interference and intersymbol interference caused by multipath channel.

5.6.1 Steepest Descent Method

The optimal solution for filter coefficients that gives the minimum mean square error for an input signal **x** and the desired signal **a** is defined by Wiener-Hopf equation 5.35 with the mean square error as cost function J(n)

$$J(n) = \sigma_a{}^2 - \mathbf{w}^H(n)\,\mathbf{R}_{xa} - \mathbf{R}_{xa}^H\,\mathbf{w}(n) + \mathbf{w}^H(n)\,\mathbf{R}_{xx}\,\mathbf{w}(n) \qquad (5.74)$$

which gives the minimum mean square error as written in equation (5.36)

The above procedure is the analytical solution for finding the optimal estimation and is straightforward but requires a high computation complexity especially for a large number of tap weights and high data rate signal. An alternative procedure is using the adaptive implementation such as the steepest descent method.

The algorithm to find the minimum mean square error is as follows

1. Begin with the initial value w(0) for the tap weight vector as a guess of the point where the error performance surface may be located.
2. Using this initial value, compute the *gradient vector* which is the derivative of the mean square error J(n).
3. Compute the next value of the tap weight vector by changing the present value in opposite direction of the gradient vector. Mathematically it can be written as :

$$\mathbf{w}(n+1) = \mathbf{w}(n) + \frac{\mu}{2}\left(-\nabla J(n)\right), \qquad (5.75)$$

where $\nabla J(n)$ denotes the value of gradient vector at time n, μ is the step size and $\mathbf{w}(n)$ denotes the value of tap weight vector at time n.

4. Go back to step 2 and repeat the procedures.

From the equation (5.74) the gradient vector can be found as follows

$$\nabla J(n) = -2\mathbf{R}_{\mathbf{xa}} + 2\mathbf{R}_{\mathbf{xx}}\,\mathbf{w}(n). \tag{5.76}$$

Substitute equation (5.36) into (5.74), the updated tap weight vector can be written as

$$\mathbf{w}(n+1) = \mathbf{w}(n) + \mu\,\left[\mathbf{R}_{\mathbf{xa}} - \mathbf{R}_{\mathbf{xx}}\mathbf{w}(n)\right]. \tag{5.77}$$

Applying this steepest descent method for combining method (subband axis) in WB-MC-CDMA systems, we will get the following recursive equation :

$$\boldsymbol{\alpha}(n+1) = \boldsymbol{\alpha}(n) + \mu_S\left[\mathbf{R}_{\mathbf{xa}} - \mathbf{R}_{\mathbf{xx}}\boldsymbol{\alpha}(n)\right]. \tag{5.78}$$

Applying this steepest descent method for multiuser detection (user axis) in WB-MC-CDMA systems, we will get the following recursive equation :

$$\mathbf{w}(n+1) = \mathbf{w}(n) + \mu_u\left(\mathbf{R}_{\mathbf{ya}} - \mathbf{R}_{\mathbf{yy}}\mathbf{w}(n)\right). \tag{5.79}$$

5.6.2 LMS Method

Basically the least mean square (LMS) algorithm is the same as the steepest descent (SD) algorithm except that SD uses deterministic gradient whereas LMS uses stochastic gradient [198]. Therefore LMS algorithm is more applicable than SD algorithm.

Here the autocorrelation matrix $\mathbf{R}_{\mathbf{xx}}$ and the cross correlation vector $\mathbf{R}_{\mathbf{xa}}$ are estimated using the present value of $\mathbf{x}(n)$ and $a(n)$,

$$\mathbf{R}_{\mathbf{xx}} = \mathbf{x}(n)\,\mathbf{x}^{H}(n), \tag{5.80}$$

$$\mathbf{R}_{\mathbf{xa}} = \mathbf{x}(n)\, a(n)\,. \tag{5.81}$$

Accordingly, the instantaneous estimate of the gradient vector is

$$\hat{\nabla} J(n) = -2\mathbf{x}(n)\, a^{*}(n) + 2\mathbf{x}(n)\, \mathbf{x}^{H}(n)\, \hat{\mathbf{w}}(n)\,. \tag{5.82}$$

Hence we get the LMS recursive updated filter coefficients as follows

$$\hat{\mathbf{w}}(n+1) = \hat{\mathbf{w}}(n) + \mu\ \mathbf{x}(n)\left(a^{*}(n) - \mathbf{x}^{H}(n)\, \hat{\mathbf{w}}(n) \right). \tag{5.83}$$

The LMS algorithm to find the minimum mean square error is as follows

1. Begin with the initial value $\mathbf{w}(0)$ for the tap weight vector as guess of the point where the error performance surface may be located.
2. Using this initial value, compute the *gradient vector* which is the derivative of the mean square error J(n) using equation (5.82).
3. Compute the next value of the tap weight vector by changing the present value in opposite direction of the gradient vector using equation (5.83).
4. Go back to step 2 and repeat the procedures.

Now applying this LMS algorithm into combining method (subband axis) in WB-MC-CDMA systems, we will get the following recursive equation:

$$\boldsymbol{\alpha}(n+1) = \boldsymbol{\alpha}(n) + \mu_{S}\ \mathbf{x}(n)\left(a(n) - \mathbf{x}^{\mathbf{T}}(n)\, \boldsymbol{\alpha}(n) \right). \tag{5.84}$$

The implementation of this LMS algorithm into combining method along subband axis is depicted in Figure 5.6.

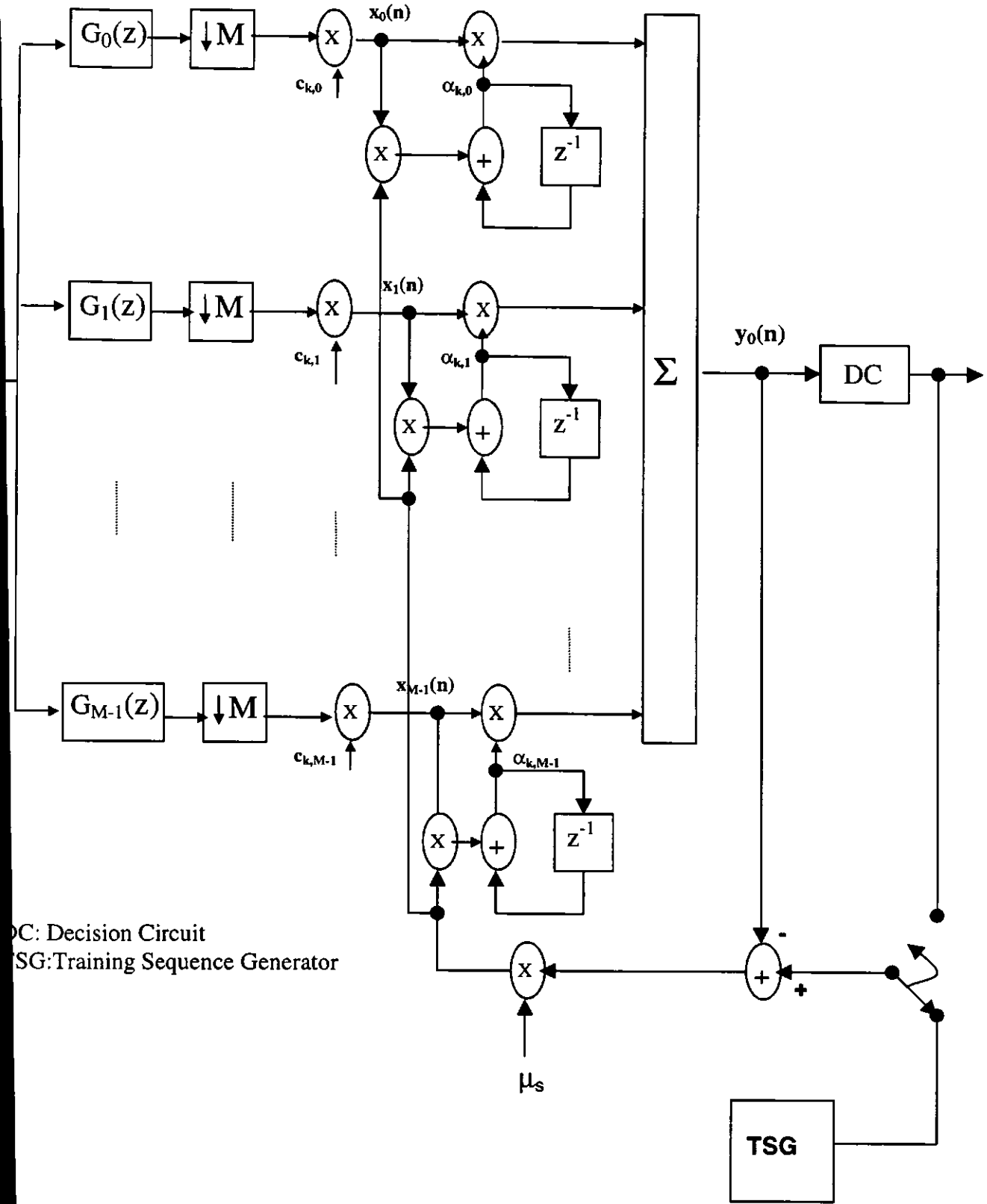

Figure 5.6 Wavelet multicarrier CDMA adaptive LMS combining receiver

Applying the LMS algorithm into multiuser detection method (user axis) in WB-MC-CDMA systems, we will get the following recursive equation:

$$\mathbf{w}(n+1) = \mathbf{w}(n) + \mu_u \, \mathbf{y}(n)\left(\mathbf{a}^{\mathrm{T}}(n) - \mathbf{y}^{\mathrm{T}}(n)\,\mathbf{w}(n)\right). \qquad (5.85)$$

The implementation of this LMS algorithm into multiuser detection method (user axis) is depicted in Figure 5.7.

The value of the step size μ restrains the rate of convergence (ROC) of the LMS algorithm and modifies the MMSE. Incorrect step size causes the system to lose convergence. The optimum value of μ is chosen to compromise between ROC and MMSE.

5.6.3 RLS Method

Recursive least squares (RLS) algorithm is the adaptive form of least squares algorithm so that we can compute the updated estimate of filter coefficients at iteration n given the least square estimate of this vector at time *(n-1)* [198]. In least square algorithm, the filter coefficients are chosen to minimise the sum of error squares.

The algorithm can be written as follows :

Initialisation, usually as follows

$$\mathbf{p}(0) = \delta^{-1}\mathbf{I},$$

$$\mathbf{w}(\mathrm{n}) = \mathbf{0}.$$

For each time (iteration) n=0,1, ... compute

vector gain : $$\mathbf{k}(n) = \frac{\lambda^{-1}\,\mathbf{p}(n-1)\,\mathbf{x}(n)}{1+\lambda^{-1}\,\mathbf{x}^{H}(n)\,\mathbf{p}(n-1)\,\mathbf{x}(n)}$$

apriori estimation error: $$\xi(n) = a(n) - \hat{\mathbf{w}}^{H}(\mathrm{n}-1)\,\mathbf{x}(n)$$

coefficients update: $$\hat{\mathbf{w}}(n) = \hat{\mathbf{w}}(n-1) + \mathbf{k}(n)\,\xi(n)$$

inverse correlation matrix update: $\mathbf{p}(n) = \lambda^{-1}\mathbf{p}(n-1) - \lambda^{-1}\,\mathbf{k}(n)\,\mathbf{x}^{H}(n)\,\mathbf{p}(n-1)$

Applying this RLS algorithm to combining method (subband axis) in WB-MC-CDMA system we will update the coefficients by the following recursive equation:

$$\boldsymbol{\alpha}(n) = \boldsymbol{\alpha}(n-1) + \mathbf{k}_{s}(n)\left(a(n) - \mathbf{x}^{\mathrm{T}}(n)\,\boldsymbol{\alpha}(n-1)\right), \tag{5.86}$$

where $$\mathbf{k}_{s}(n) = \frac{\lambda^{-1}\,\mathbf{p}(n-1)\,\mathbf{x}(n)}{1+\lambda^{-1}\,\mathbf{x}^{\mathrm{T}}(n)\,\mathbf{p}(n-1)\,\mathbf{x}(n)}, \tag{5.87}$$

λ is forgetting factor and $\mathbf{p(n)}$ is correlation matrix.

Applying this RLS algorithm to multiuser detection (user axis) in WB-MC-CDMA system we will update the coefficients by the following recursive equation:

$$\mathbf{w}(n) = \mathbf{w}(n-1) + \mathbf{k}_{u}(n)\left(\mathbf{a}^{\mathrm{T}}(n) - \mathbf{y}^{\mathrm{T}}(n)\,\mathbf{w}(n-1)\right), \tag{5.88}$$

where $$\mathbf{k}_{u}(n) = \frac{\lambda^{-1}\,\mathbf{p}(n-1)\,\mathbf{y}(n)}{1+\lambda^{-1}\,\mathbf{y}^{\mathrm{T}}(n)\,\mathbf{p}(n-1)\,\mathbf{y}(n)}, \tag{5.89}$$

λ is forgetting factor and $\mathbf{p(n)}$ is correlation matrix.

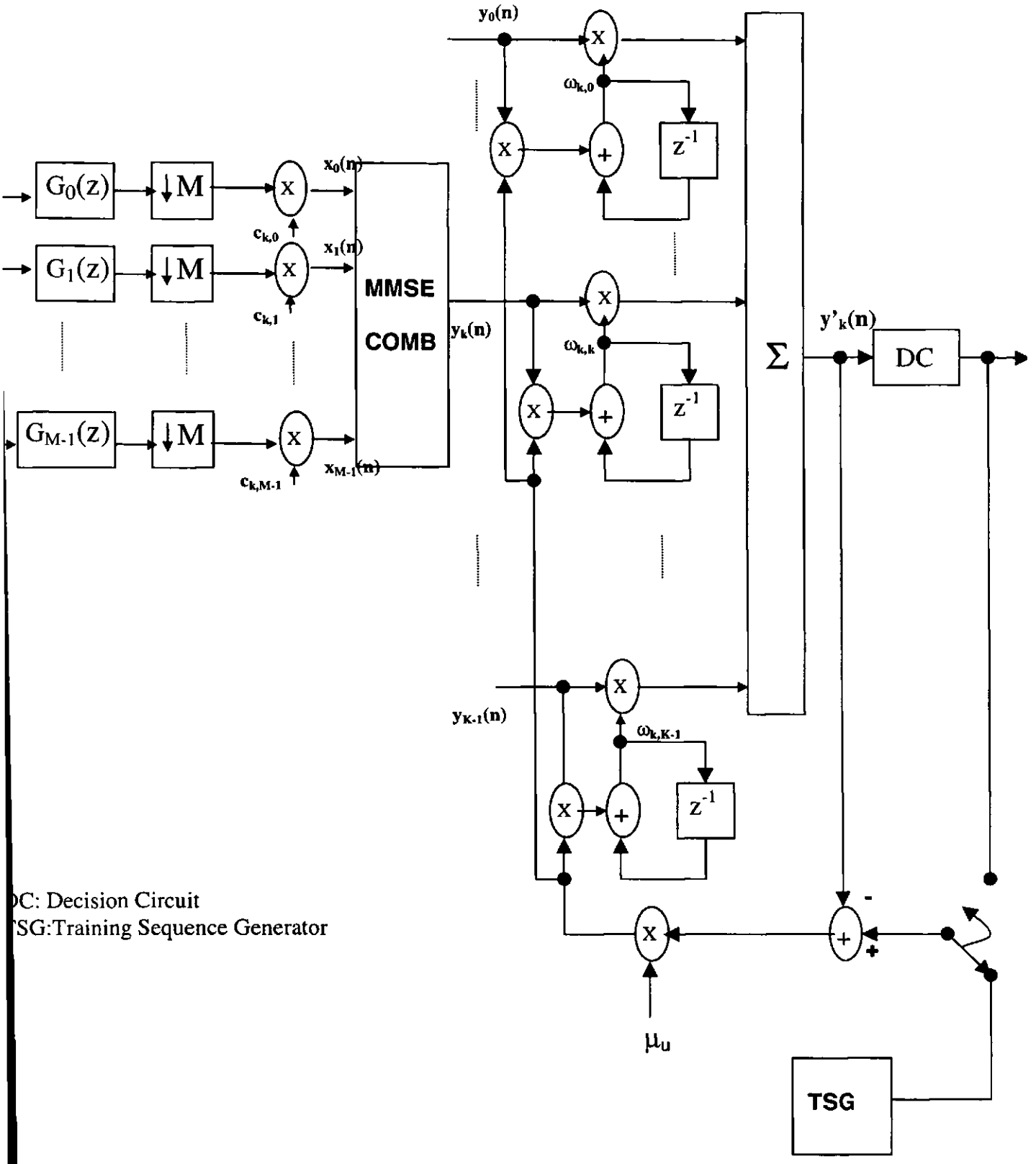

DC: Decision Circuit
TSG:Training Sequence Generator

Figure 5.7 Wavelet multicarrier CDMA adaptive LMS multiuser detector

5.7 Numerical Results

A 32-band WB-MC-CDMA transmission system is considered and the BER at the output of the MMSE and decorrelator (Decorr) detectors are simulated. The MMSE detector is optimised along the band axis only (MMSE-Comb), and along the user axis only (MMSE-MUD), and it is optimised along both the band and the user axis simultaneously (MMSE-Comb-MUD) and finally made adaptive on the user axis (LMS-MUD). The BER performance of those multiuser detectors in the multipath fading channel and with varying number of users is shown in Figure 5.8 and with varying $\frac{E_b}{N_0}$ is shown in Figure 5.9. In both cases, the variances of the Rayleigh random sources are [1, 0.8, 0.5, and 0.2].

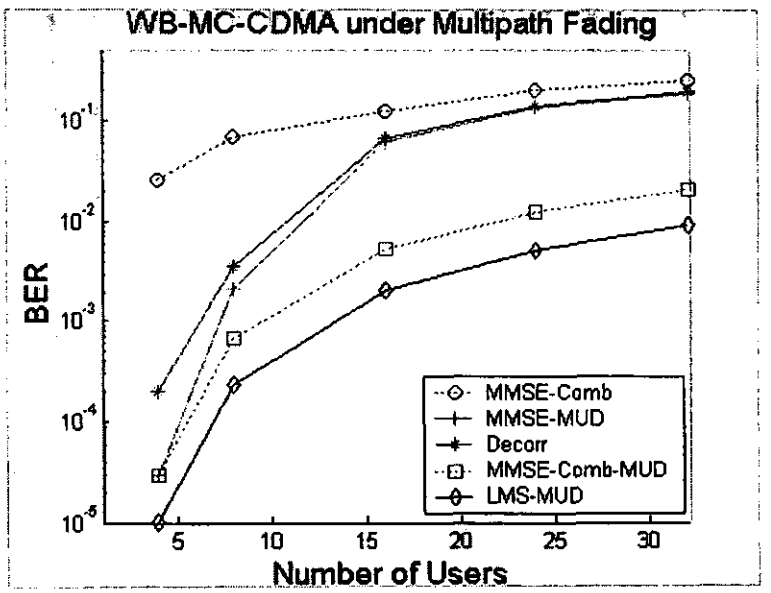

Figure 5.8 BER of WB-MC-CDMA system with MUD under multipath channel for different number of users

The joined MMSE combining and MMSE multiuser detection (MMSE-Comb-MUD) shows better BER performance under multipath channel compared with decorrelator, MMSEC alone and MMSE-MUD alone. The proposed MUD gets BER improvement at the

cost of higher computation complexity but still retains the near-far resistance. The adaptive MMSE multiuser detection (LMS-MUD) has shown further improvement of BER performance and lower computation complexity but requires a training sequence.

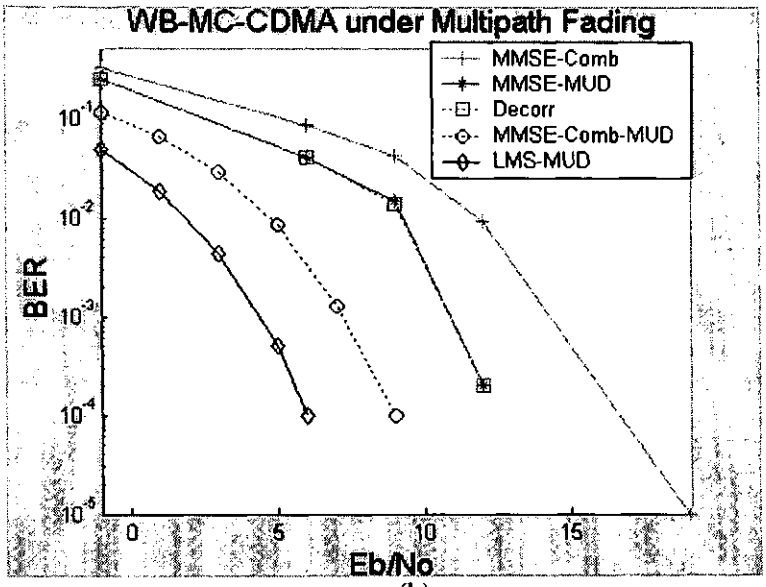

(b)

Figure 5.9 BER of WB-MC-CDMA system with MUD under multipath channel for various $\frac{E_b}{N_0}$

CHAPTER VI

SYSTEM PERFORMANCE EVALUATION

The system performance is evaluated in terms of the achievable bit error rate (BER), near-far resistance and computation complexity. We present the theoretical analysis of BER performance of our WB-MC-CDMA system and then compare the analytical results with the simulation results when transmission is carried out through AWGN and Rayleigh fading channels. The analysis of the near-far resistance of the system assumed unequal users' powers. The computation complexity of the system is discussed at the end of this chapter.

6.1 BER Performance

The bit error rate (BER) performance of a multi-user communication system is dependent upon the quality of the received signal which contains the desired signal, the multi-user interference signal and the noise signal. The quality of the received signal is measured in term of the signal to noise power ratio which depends on the channel model (AWGN and Rayleigh fading channels) as well as the link direction in use (uplink and downlink). Furthermore the BER performance of the system is determined by the type of multi-user detector in use.

In AWGN channel, the subband amplitude scaling $h_{k,m}$ is constant over time. Thus, using the equation of the received signal representation (equation 3.45), the mean power at m^{th} subband of the k^{th} user is

$$P_{k,m} = E(r_m(t)) = E(h_{k,m}^2) = h_{k,m}^2 . \qquad (6.1)$$

Each user has total mean power

$$P_k = \sum_{m=0}^{M-1} P_{k,m} = \sum_{m=0}^{M-1} h_{k,m}^2 . \tag{6.2}$$

In Rayleigh fading channel this subband amplitude scaling $h_{k,m}$ has the following distribution:

$$f(h_{k,m}) = \frac{h_{k,m}}{\sigma_{k,m}^2} e^{-\frac{h_{k,m}^2}{2\sigma_{k,m}^2}} . \tag{6.3}$$

This Rayleigh distribution has the time average and variance as follows

$$\text{mean}\ (h_{k,m}) = \sigma_{k,m}\sqrt{\frac{\pi}{2}} , \tag{6.4}$$

$$\text{var}(h_{k,m}) = \sigma_{k,m}^2 (2 - \frac{\pi}{2}) . \tag{6.5}$$

Using equation 3.45, the mean power at m^{th} subband of the k^{th} user is

$$P_{k,m} = E(r_m(t)) = E(h_{k,m}^2) = 2\,\sigma_{k,m}^2 . \tag{6.6}$$

Each user has total mean power

$$P_k = \sum_{m=0}^{M-1} P_{k,m} = 2 \sum_{m=0}^{M-1} \sigma_{k,m}^2 . \tag{6.7}$$

In uplink (reverse) transmission, the base station receives the signals from active mobile terminals through channels with different transmission characteristic. Therefore there is a set of M random amplitudes $\{h_{k,m}\}$ $m = 0,1 \cdots M-1$ and a set of M random phases $\{\theta_{k,m}\}$ $m = 0,1 \cdots M-1$ associated with each user k=0,1…K-1. Assuming these random variables are independent between users, the correction of amplitude and phase of the desired user does not simultaneously perform the correction of amplitude and phase of the interfering users.

In downlink (forward) transmission, the mobile terminal receives the desired signal from the base station to user m=0 and the signals from the base station destined to other users

(m=1,2, ... M-1) through the same channel. Therefore there is only one set of M random amplitudes $h_{k,m} = h_{0,m} \quad \forall k$ and one set of M random phases $\theta_{k,m} = \theta_{0,m} \quad \forall k$ for all users. In this case, the correction of amplitude and phase of the desired user simultaneously perform the correction of amplitude and phase of the interfering users as well.

6.1.1 Matched Filter Detection

Using matched filter detection in multi-user channel, the receiver consists of a matched-filter bank each of which is matched to the corresponding user's signature waveform as discussed in section 5.1.1.

Now let us define

$$\boldsymbol{\gamma} = \boldsymbol{\beta}\,\mathbf{E}, \tag{6.8}$$

so that we can write equation 5.20 as

$$\mathbf{y(z)} = \boldsymbol{\beta}\,\mathbf{E}\,\mathbf{a(z)} + \boldsymbol{\xi}\mathbf{(z)} \tag{6.9}$$

We then can expand γ into the following equation

$$\gamma = \begin{bmatrix} \beta_{0,0} & \beta_{0,1} & \beta_{0,M-1} \\ \beta_{1,0} & \cdots & \vdots \\ \vdots & & \\ \beta_{K-1,0} & \cdots & \beta_{K-1,M-1} \end{bmatrix} \begin{bmatrix} c_{0,0}h_{0,0} & c_{1,0}h_{1,0} & \cdots & c_{K-1,0}h_{K-1,0} \\ c_{0,1}h_{0,1} & c_{1,1}h_{1,1} & & c_{K-1,1}h_{K-1,1} \\ \vdots & & & \\ c_{0,M-1}h_{0,M-1} & c_{1,M-1}h_{1,M-1} & & c_{K-1,M-1}h_{K-1,M-1} \end{bmatrix} \tag{6.10}$$

where

$$\beta_{k,m} = \alpha_{k,m}\, c_{k,m} \tag{6.11}$$

Defining each element γ as the following:

$$\gamma = \begin{bmatrix} \gamma_{0,0} & \gamma_{0,1} & \gamma_{0,K-1} \\ \gamma_{1,0} & \gamma_{1,1} & \vdots \\ \vdots & & \\ \gamma_{K-1,0} & \cdots & \gamma_{K-1,K-1} \end{bmatrix}, \tag{6.12}$$

we can then calculate these elements from equation 6.10

$$\gamma_{0,0} = \alpha_{0,0}c_{0,0}\ c_{0,0}h_{0,0} + \alpha_{0,1}c_{0,1}\ c_{0,1}h_{0,1} + \quad \cdots \quad + \alpha_{0,M-1}c_{0,M-1}\ c_{0,M-1}h_{0,M-1}, \tag{6.13}$$

$$\gamma_{0,1} = \alpha_{0,0}c_{0,0}\ c_{1,0}h_{1,0} + \alpha_{0,1}c_{0,1}\ c_{1,1}h_{1,1} + \quad \cdots \quad + \alpha_{0,M-1}c_{0,M-1}\ c_{1,M-1}h_{1,M-1}, \tag{6.14}$$

$$\gamma_{1,0} = \alpha_{1,0}c_{1,0}\ c_{0,0}h_{0,0} + \alpha_{1,1}c_{1,1}\ c_{0,1}h_{0,1} + \quad \cdots \quad + \alpha_{1,M-1}c_{1,M-1}\ c_{0,M-1}h_{0,M-1}, \tag{6.15}$$

$$\gamma_{1,1} = \alpha_{1,0}c_{1,0}\ c_{1,0}h_{1,0} + \alpha_{1,1}c_{1,1}\ c_{1,1}h_{1,1} + \quad \cdots \quad + \alpha_{1,M-1}c_{1,M-1}\ c_{1,M-1}h_{1,M-1}, \tag{6.16}$$

$$\cdots$$

$$\gamma_{0,K-1} = \alpha_{0,0}c_{0,0}\ c_{K-1,0}h_{K-1,0} + \alpha_{0,1}c_{0,1}\ c_{K-1,1}h_{K-1,1} + \quad \cdots \quad + \alpha_{0,M-1}c_{0,M-1}\ c_{K-1,M-1}h_{K-1,M-1}$$

$$\cdots \tag{6.17}$$

$$\gamma_{K-1,0} = \alpha_{K-1,0}c_{K-1,0}\ c_{0,0}h_{0,0} + \alpha_{K-1,1}c_{K-1,1}\ c_{0,1}h_{0,1} + \quad \cdots \quad + \alpha_{K-1,M-1}c_{K-1,M-1}\ c_{0,M-1}h_{0,M-1}$$

$$\cdots \tag{6.18}$$

$$\gamma_{K-1,K-1} = \alpha_{K-1,0}c_{K-1,0}\ c_{K-1,0}h_{K-1,0} + \alpha_{K-1,1}c_{K-1,1}\ c_{K-1,1}h_{K-1,1} + \quad \cdots \quad + \alpha_{K-1,M-1}c_{K-1,M-1}\ c_{K-1,M-1}h_{K-1,M}$$

(6.19)

In order to see the desired component, MUI signal and noise term respectively one can split the signal into these three terms as follows

$$\mathbf{y(z)} = \underbrace{Diag\langle \boldsymbol{\beta}\,\mathbf{E}\rangle\,\mathbf{a(z)}}_{desired\ signal} + \underbrace{\left[\boldsymbol{\beta}\,\mathbf{E} - Diag\langle \boldsymbol{\beta}\,\mathbf{E}\rangle\right]\mathbf{a(z)}}_{MAI\ signal} + \underbrace{\boldsymbol{\xi}(\mathbf{z})}_{filtered\ noise}. \tag{6.20}$$

Now take o^{th} user signal

$$\mathbf{y}_0(\mathbf{n}) = \underbrace{\gamma_{0,0}\ \mathbf{a}_0(\mathbf{n})}_{desired\ signal} + \underbrace{\gamma_{0,1}\ \mathbf{a}_1(\mathbf{n}) + \quad \cdots \quad + \gamma_{0,K-1}\ \mathbf{a}_{K-1}(\mathbf{n})}_{MAI\ signal} + \underbrace{\xi_0(\mathbf{n})}_{noise}, \tag{6.21}$$

where

$$\gamma_{0,k} = \sum_{m=0}^{M-1} \alpha_{0,m}c_{0,m}\ c_{k,m}h_{k,m} \quad k = 0,1\cdots K-1. \tag{6.22}$$

Therefore the decision variable signal can also be written into those three terms

$$\mathbf{y}_0(\mathbf{n}) = \mathbf{y}_{01}(\mathbf{n}) + \mathbf{y}_{02}(\mathbf{n}) + \mathbf{y}_{03}(\mathbf{n}), \tag{6.23}$$

where $\mathbf{y}_{01}$, $\mathbf{y}_{02}$, $\mathbf{y}_{03}$ are the desired signal, MAI signal and noise signal respectively.

The average probability of error can be written as

$$P_e = \frac{1}{2}\left(P(y_0 > 0 | a_0 = -1) + P(y_0 < 0 | a_0 = +1)\right). \tag{6.24}$$

Assuming the transmitted bits are equiprobable, equation 6.24 can be simplified as:

$$P_e = P(y_0 < 0 | a_0 = +1). \tag{6.25}$$

Then the probability of error is

$$P_e = Q\sqrt{\frac{(mean(y_0))^2}{\text{var}(y_0)}}, \tag{6.26}$$

where

$$Q(x) = \frac{1}{\sqrt{2\pi}} \int_x^{\infty} e^{-\frac{t^2}{2}} dt \quad [134]. \tag{6.27}$$

The mean value of y_0 is given by

$$E(\mathbf{y}_0) = E(\mathbf{y}_{01} | a_0 = +1) + E(\mathbf{y}_{02}) + E(\mathbf{y}_{03}). \tag{6.28}$$

Under perfect conditions (synchronous system, perfect channel estimation etc.), the mean value of the desired signal is the bit energy multiplied by a constant factor,

$$E(\mathbf{y}_{01} | a_0 = +1) = \gamma_{0,0}\sqrt{E_b} = \left(\sum_{m=0}^{M-1} \alpha_{0,m} c_{0,m}\, c_{0,m} h_{0,m}\right)\sqrt{E_b}, \tag{6.29}$$

$$E(\mathbf{y}_{01} | a_0 = +1) = \sqrt{E_b} \sum_{m=0}^{M-1} \alpha_{0,m} h_{0,m}. \tag{6.30}$$

The mean value of the MAI signal is zero

$$E(\mathbf{y}_{02}) = 0. \tag{6.31}$$

The mean value of the noise signal is also zero

$$E(\mathbf{y}_{03}) = 0. \tag{6.32}$$

The variance of y_0 is given by

$$\text{var}(\mathbf{y}_0) = \text{var}(\mathbf{y}_{01}) + \text{var}(\mathbf{y}_{02}) + \text{var}(\mathbf{y}_{03}). \tag{6.33}$$

The variance of the desired signal is zero

$$\text{var}(\mathbf{y}_{01}) = 0. \tag{6.34}$$

The variance of the MAI signal is given by

$$\text{var}(\mathbf{y}_{02}) = E(\mathbf{y}_{02}{}^2) = \sum_{k=1}^{K-1} \gamma_{0,k}{}^2 \, E(a_k{}^2), \tag{6.35}$$

$$\text{var}(\mathbf{y}_{02}) = \sum_{k=1}^{K-1} \left(\sum_{m=0}^{M-1} \alpha_{0,m} c_{0,m} \, c_{k,m} h_{k,m} \right)^2 E_b. \tag{6.36}$$

It can be seen when there is no fading $(h_{k,m} = 1)$ and for synchronous system operation, the variance given by equation 6.36 becomes zero, otherwise it generates MAI signal. Let this MAI signal be denoted as $\mathbf{I_0}$.

The variance of the noise signal is half of the one-sided noise spectral density multiplied by a constant factor due to the subband equalisation

$$\text{var}(\mathbf{y}_{03}) = \frac{N_0}{2} \sum_{m=0}^{M-1} (\beta_{0,m})^2 = \frac{N_0}{2} \sum_{m=0}^{M-1} (\alpha_{0,m} c_{0,m})^2, \tag{6.37}$$

$$\text{var}(\mathbf{y}_{03}) = \frac{N_0}{2} \sum_{m=0}^{M-1} (\alpha_{0,m})^2. \tag{6.38}$$

Therefore, the probability of error for 0^{th} user is

$$P_e = Q \sqrt{\frac{(mean(y_{01}))^2}{I_0 + N}}, \tag{6.39}$$

$$P_e = Q \sqrt{\frac{(\gamma_{0,0})^2 E_b}{\sum_{k=1}^{K-1} \gamma_{0,k}{}^2 \, E_b + \frac{N_0}{2} \sum_{m=0}^{M-1} (\alpha_{0,m})^2}}. \tag{6.40}$$

Here we consider matched filter multi-user detection with equal gain combining (EGC)

$$\alpha_{k,m} = \sqrt{\frac{1}{M}}. \tag{6.41}$$

Equations (6.13) to (6.19) lead the following general equation

$$\gamma_{k1,k2} = \sum_{m=0}^{M-1} \alpha_{k1,m} c_{k1,m} c_{k2,m} h_{k2,m} , \tag{6.42}$$

so that $\gamma_{0,0} = \sum_{m=0}^{M-1} \frac{1}{M} c_{0,m} c_{0,m} h_{0,m}$, (6.43)

$$\gamma_{0,0} = \frac{1}{M} \sum_{m=0}^{M-1} h_{k,m} = \bar{h}_0 , \tag{6.44}$$

where $\bar{h}_0$ is the subband (m) average of the time average of the amplitude scaling for 0^{th} user and $\gamma_{0,k} = \sum_{m=0}^{M-1} \frac{1}{M} c_{0,m} c_{k,m} h_{k,m}$, (6.45)

$$\text{var}(\gamma_{0,k}) = \sigma_k^2 = \frac{f_{0,k}}{M} \sum_{m=0}^{M-1} (h_{k,m})^2 = f_{0,k} \, (\bar{h}_k)^2 . \tag{6.46}$$

where $f_{0,k}$ is MAI factor which is from 0 to 1.

In uplink transmission and AWGN channel, the probability of error for 0^{th} user is

$$P_e = Q \sqrt{\frac{(\bar{h}_0)^2 E_b}{\sum_{k=1}^{K-1} f_{0,k} \, (\bar{h}_k)^2 \, E_b + \frac{N_0}{2}}} . \tag{6.47}$$

In downlink transmission and AWGN channel, the probability of error for 0^{th} user is

$$P_e = Q \sqrt{\frac{\bar{h}^2 E_b}{f_0 (K-1) \bar{h}^2 \, E_b + \frac{N_0}{2}}} , \tag{6.48}$$

where $\bar{h}$ is the subband (m) average of the time average of the amplitude scaling for all users $\bar{h} = \frac{1}{M} \sum_{m=0}^{M-1} h_m$ and f_0 is MAI factor.

For uplink transmission through Rayleigh channel, equation (6.4) and (6.5) can be used to find the mean and variance of the MAI signal as:

$$\text{mean}\,(\gamma_{0,0}) = (\bar{h}_0)^2 = \sigma_0^2 \frac{\pi}{2}, \tag{6.49}$$

$$\text{and}\ \ \text{var}(\gamma_{0,k}) = \text{var}(h_k) = \sigma_k^2 (2 - \frac{\pi}{2}). \tag{6.50}$$

The probability of error for 0^{th} user is

$$P_e = Q\sqrt{\frac{\sigma_0^2 \frac{\pi}{2} E_b}{\sum_{k=1}^{K-1} f_{0,k}\ \sigma_k^2\ (2-\frac{\pi}{2})\ E_b + \frac{N_0}{2}}}, \tag{6.51}$$

where σ_k is the standard deviation parameter in Rayleigh distribution for k^{th} user.

For downlink transmission through Rayleigh channel, these parameters are the same for all users so that the probability of error for 0^{th} user is

$$P_e = Q\sqrt{\frac{\sigma^2 \frac{\pi}{2} E_b}{f_0\ (K-1)\,\sigma^2\ (2-\frac{\pi}{2})\ E_b + \frac{N_0}{2}}}. \tag{6.52}$$

6.1.2 MMSE Multiuser Detection

The MMSE multi-user detector minimises the squared error on a convex function which then can be found using gradient projection method as discussed in section 5.3. Now apply the same method to MMSE detector using the optimum filter coefficients obtained from equation (5.64). The output signal of this detector is

$$\mathbf{y'(n)} = \mathbf{w}_{\mathbf{opt}}^{H}\ \mathbf{y(n)} \tag{6.53}$$

Substituting for w_{opt} and y, we get

$$\mathbf{y'(n)} = \left[\boldsymbol{\gamma}\,\boldsymbol{\gamma}^{\mathbf{T}} + \boldsymbol{\sigma}^2\,\boldsymbol{\beta}^2\right]^{-1} \boldsymbol{\gamma}^{\mathbf{T}}\,[\boldsymbol{\gamma}\,\mathbf{a(n)} + \boldsymbol{\xi}\mathbf{(n)}] \tag{6.54}$$

Although it is difficult to simplify this equation we can still feel and see that MMSE detector optimises the output when received signal is corrupted by MAI signal and additive

Gaussian noise signal. When the Gaussian noise is zero $\sigma \to 0$, this detector behaves like decorrelator which cancels MAI signals. As $\sigma \to \infty$, this detector behaves like the conventional matched filter detector.

Apart from that, the desired component, MUI signal and noise term are still held like equation (6.13)

$$\mathbf{y}'(\mathbf{n}) = \underbrace{Diag\left\langle \mathbf{w}_{\text{opt}}^{H}\ \boldsymbol{\beta}\,\mathbf{E}\right\rangle \mathbf{a}(\mathbf{n})}_{\textit{desired signal}} + \underbrace{\left[\mathbf{w}_{\text{opt}}^{H}\ \boldsymbol{\beta}\,\mathbf{E} - Diag\left\langle \mathbf{w}_{\text{opt}}^{H}\ \boldsymbol{\beta}\,\mathbf{E}\right\rangle\right]\mathbf{a}(\mathbf{n})}_{\textit{MAI signal}} + \underbrace{\mathbf{w}_{\text{opt}}^{H}\ \xi(\mathbf{z})}_{\textit{filtered noise}} . \qquad (6.55)$$

The o^{th} user output signal is

$$\mathbf{y}'_{0}(\mathbf{n}) = \underbrace{\gamma'_{0,0}\,\mathbf{a}_{0}(\mathbf{n})}_{\textit{desired signal}} + \underbrace{\left[\gamma'_{0,1}\,\mathbf{a}_{1}(\mathbf{n}) + \cdots + \gamma'_{0,K-1}\,\mathbf{a}_{K-1}(\mathbf{n})\right]}_{\textit{MAI signal}} + \underbrace{(\mathbf{w}_{\text{opt}})_{0}\,\xi(n)}_{\textit{filtered noise}} , \qquad (6.56)$$

where

$$\gamma' = \begin{bmatrix} \gamma'_{0,0} & \gamma'_{0,1} & \gamma'_{0,K-1} \\ \gamma'_{1,0} & \gamma'_{1,1} & \vdots \\ \vdots & & \\ \gamma'_{K-1,0} & \cdots & \gamma'_{K-1,K-1} \end{bmatrix} \qquad (6.57)$$

is multiplication result between the Hermitian (complex conjugate transpose) optimised coefficients and the original γ

$$\gamma' = \begin{bmatrix} w_{0,0} & w_{1,0} & w_{K-1,0} \\ w_{0,1} & w_{1,1} & \vdots \\ \vdots & & \\ w_{0,K-1} & \cdots & w_{K-1,K-1} \end{bmatrix} \begin{bmatrix} \gamma_{0,0} & \gamma_{0,1} & \gamma_{0,K-1} \\ \gamma_{1,0} & \gamma_{1,1} & \vdots \\ \vdots & & \\ \gamma_{K-1,0} & \cdots & \gamma_{K-1,K-1} \end{bmatrix} . \qquad (6.58)$$

Completing this multiplication will give the following results.

$$\gamma'_{0,0} = w_{0,0}\gamma_{0,0} + w_{1,0}\gamma_{1,0} + \cdots + w_{K-1,0}\gamma_{K-1,0} = \sum_{k=0}^{K-1} w_{k,0}\gamma_{k,0} , \qquad (6.59)$$

$$\gamma'_{0,1} = w_{0,0}\gamma_{0,1} + w_{1,0}\gamma_{1,1} + \cdots + w_{K-1,0}\gamma_{K-1,1} = \sum_{k=0}^{K-1} w_{k,0}\gamma_{k,1} , \qquad (6.60)$$

$$\gamma'_{1,0} = w_{0,1}\gamma_{0,0} + w_{1,1}\gamma_{1,0} + \cdots + w_{K-1,1}\gamma_{K-1,0} = \sum_{k=0}^{K-1} w_{k,1}\gamma_{k,0} , \qquad (6.61)$$

$$\gamma'_{1,1} = w_{0,1}\gamma_{0,1} + w_{1,1}\gamma_{1,1} + \cdots + w_{K-1,1}\gamma_{K-1,1} = \sum_{k=0}^{K-1} w_{k,1}\gamma_{k,1}\,, \tag{6.62}$$

$$\gamma'_{0,K-1} = w_{0,0}\gamma_{0,K-1} + w_{1,0}\gamma_{1,K-1} + \cdots + w_{K-1,0}\gamma_{K-1,K-1} = \sum_{k=0}^{K-1} w_{k,0}\gamma_{k,K-1}\,, \tag{6.63}$$

$$\gamma'_{K-1,0} = w_{0,K-1}\gamma_{0,0} + w_{1,K-1}\gamma_{1,0} + \cdots + w_{K-1,K-1}\gamma_{K-1,0} = \sum_{k=0}^{K-1} w_{k,K-1}\gamma_{k,0}\,, \tag{6.64}$$

$$\gamma'_{K-1,K-1} = w_{0,K-1}\gamma_{0,K-1} + w_{1,K-1}\gamma_{1,K-1} + \cdots + w_{K-1,K-1}\gamma_{K-1,K-1} = \sum_{k=0}^{K-1} w_{k,K-1,}\gamma_{k,K-1}\,. \tag{6.65}$$

Again the new decision variable signal can also be written into those three terms

$$\mathbf{y}'_0(\mathbf{n}) = \mathbf{y}'_{01}(\mathbf{n}) + \mathbf{y}'_{02}(\mathbf{n}) + \mathbf{y}'_{03}(\mathbf{n})\,, \tag{6.66}$$

where $\mathbf{y}'_{01}$, $\mathbf{y}'_{02}$, $\mathbf{y}'_{03}$ are the desired signal, MAI signal and noise signal respectively.

The mean value of the desired user signal is the bit energy multiplied by a constant factor

$$E(\mathbf{y}'_{01}|a_0 = +1) = \gamma'_{0,0}\sqrt{E_b}\,. \tag{6.67}$$

The mean value of the MAI signal is zero

$$E(\mathbf{y}'_{02}) = 0\,. \tag{6.68}$$

The mean value of the noise signal is also zero

$$E(\mathbf{y}'_{03}) = 0\,. \tag{6.69}$$

The variance of the desired user signal is zero

$$\mathrm{var}(\mathbf{y}'_{01}) = 0\,. \tag{6.70}$$

The variance of the MAI signal is given by

$$\mathrm{var}(\mathbf{y}'_{02}) = E(\mathbf{y}'^{2}_{02}) = \sum_{k=1}^{K-1} (\gamma'_{0,k})^2\, E_b\,. \tag{6.71}$$

Let this MAI signal be $\mathbf{I}'_0$.

As $$\boldsymbol{\beta}' = \mathbf{w}^H_{\mathbf{opt}}\, \boldsymbol{\beta}\,, \tag{6.72}$$

hence $$\boldsymbol{\alpha}' = \mathbf{w}^H_{\mathbf{opt}}\, \boldsymbol{\alpha}\,. \tag{6.73}$$

And it can be shown that

$$\alpha'_{0,m} = \sum_{k=1}^{K-1} w_{k,0}\, \alpha_{k,m}\,, \tag{6.74}$$

then the variance of the noise signal has the same form as equation (6.35)

$$\mathrm{var}(\mathbf{y}_{03}) = \frac{N_0}{2} \sum_{m=0}^{M-1} (\alpha'_{0,m})^2\,. \tag{6.75}$$

The probability of error is also the same form as equation (6.38)

$$P_e = Q\sqrt{\frac{(\gamma'_{0,0})^2 E_b}{\sum_{k=1}^{K-1} \gamma'_{0,k}{}^2 E_b + \frac{N_0}{2}\sum_{m=0}^{M-1}(\alpha'_{0,m})^2}}\,. \tag{6.76}$$

Equation (6.76) requires the following definition

$$\boldsymbol{\gamma}' = \mathbf{w}_{\mathrm{opt}}^{H}\, \boldsymbol{\gamma}\,. \tag{6.77}$$

In other way, the equations (6.59) to (6.65) lead to the following general equation

$$\gamma'_{k1,k2} = \sum_{k=0}^{K-1} w_{k,k1}\gamma_{k,k2}\,. \tag{6.78}$$

So the desired signal is $\gamma'_{0,0} = \sum_{k=0}^{K-1} w_{k,0}\gamma_{k,0}\,.$ (6.79)

This signal average does not change much

$$\mathrm{mean}(\gamma'_{0,0}) \approx \mathrm{mean}(\gamma_{0,0}) = \bar{h}_0\,. \tag{6.80}$$

On the other hand, the multiple access interference signals are reduced considerably due to the $\mathbf{w}_{\mathrm{opt}}^{H}$ factor. The filtered noise signal increases a bit due to the same factor.

6.1.3 Numerical Results

The BER performances of the system using AWGN channel (Figure 6.1) and Rayleigh

fading channel (Figure 6.2) are presented in this section. A 32-channel Wavelet-based MC-CDMA system is simulated using Rayleigh fading with variance of one. The Rayleigh channel used for the simulation is generated using Rayleigh random sources.

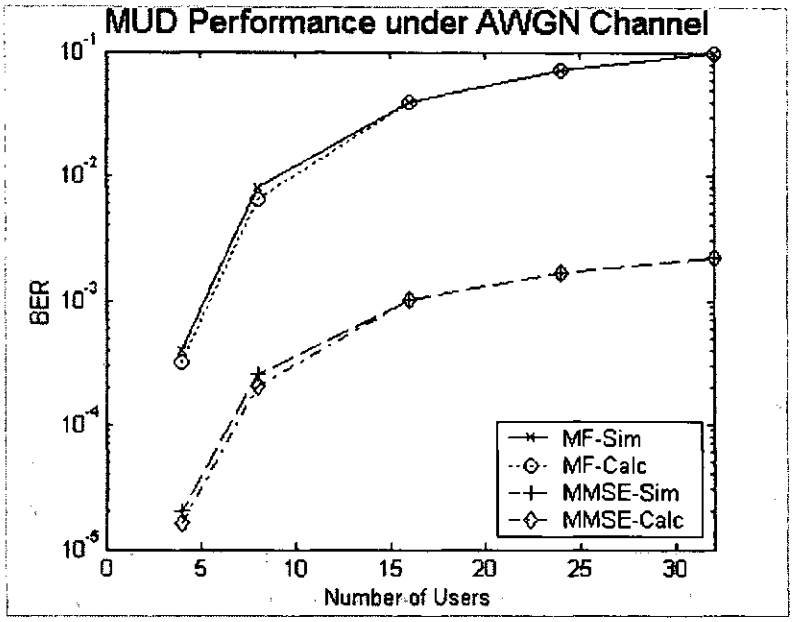

Figure 6.1 BER performance under AWGN channel versus number of users
Eb/No=10 dB, calculation using equation 6.47 for MF and equation 6.76 for MMSE

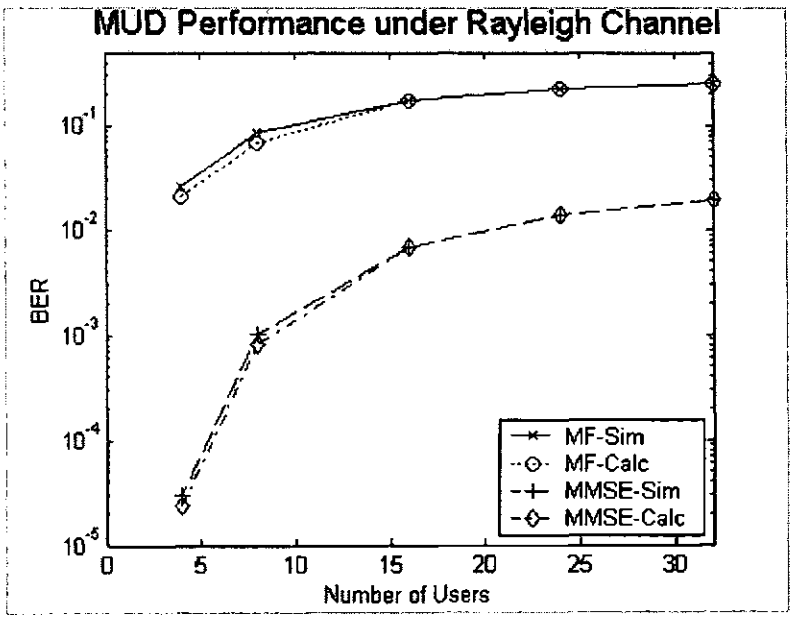

Figure 6.2 BER performance under Rayleigh fading channel versus number of users
Eb/No=10 dB, calculation using equation 6.51 for MF and equation 6.76 for MMSE

The BER performance was evaluated using conventional matched filter detectors and MMSE multi-user detector. The theoretical BER results for matched filter detection are computed using equation (6.47) for AWGN channel and equation (6.51) for Rayleigh fading channel. The MMSE multiuser detection uses equation (6.76) instead.

The theoretical and the simulated results are compared in graphs Figure 6.1 for AWGN channel and Figure 6.2 for Rayleigh fading channel.

As expected the MMSE detector performs better than the matched filter detector in term of BER performance because this type of multiuser detector is optimised along both the subband and the user axis simultaneously (MMSE-Comb-MUD).

6.2 Near-Far Resistance

The conventional matched filter detection of the desired signal in multi-user channel contains spurious components from all interfering users (see equation 5.20). When the multi-user interference grows, the bit error rate increases until the conventional detector is unable to recover the data signal transmitted by the weak users. This phenomenon is usually called near-far problem. Verdu defined multi-user efficiency as the ratio between the effective energy e_k and the actual energy E_k. [90,200] to achieve certain bit error rate. The effective energy e_k is the energy required to achieve the same bit error rate in AWGN channel without interference

$$\eta_k = \frac{e_k}{E_k}. \tag{6.81}$$

Near-far resistance is equal to the asymptotic multi-user efficiency which can be expressed as [90,200]

$$\eta_k = \lim_{\sigma \to 0} \frac{e_k}{E_k}. \tag{6.82}$$

When $\sigma \to 0$ MMSE detector converges to decorrelator and therefore we start from decorrelator-MUD to analyse the near-far resistance. The near-far resistance is equal to the asymptotic multi-user efficiency which is the multi-user efficiency for $\sigma \to 0$.

Let us write the output signal of the combiner (equation 5.20) in the time domain :

$$\mathbf{y(n)} = \gamma\, \mathbf{a(n)} + \xi\mathbf{(n)}. \tag{6.83}$$

Applying decorrelator detector on the combiner output signal we get the following signal

$$\mathbf{y'(n)} = \gamma^{-1}\, \mathbf{y(n)} = \mathbf{a(n)} + \gamma^{-1}\, \xi\mathbf{(n)}. \tag{6.84}$$

This equation can be written as

$$\mathbf{y'(n)} = \mathbf{a(n)} + \xi'\mathbf{(n)}, \tag{6.85}$$

where

$$\xi'\mathbf{(n)} = \gamma^{-1}\, \xi\mathbf{(n)}. \tag{6.86}$$

The mean value of this noise term is

$$E(\xi'\xi'^{\mathbf{T}}) = E(\gamma^{-1})\, E(\xi\xi^{\mathbf{T}})\, E((\gamma^{-1})^{\mathbf{T}}) \tag{6.87}$$

As can be seen in equation (6.42), γ factor is the multiplication of the channel attenuation and the equalisation factor, therefore the average value is one for each subband in each user

$$E(\gamma) \approx \mathbf{I}, \tag{6.88}$$

which leads the first factor of equation

$$E(\gamma^{-1}) \approx \mathbf{I}, \tag{6.89}$$

and also the third factor

$$E((\gamma^{-1})^{\mathbf{T}}) \approx \mathbf{I}. \tag{6.90}$$

From the definition of ξ in equation (5.19), the second factor becomes

$$E(\xi\xi^{\mathbf{T}}) \approx \sigma^2\, E(\beta^2) \approx \sigma^2\, \alpha^2. \tag{6.91}$$

And therefore going back to equation (6.87) we get the final result

$$E(\xi'\xi'^{\mathrm{T}}) \approx \mathbf{I}\,\sigma^2\,\boldsymbol{\alpha}^2\,\mathbf{I} \approx \sigma^2\,\boldsymbol{\alpha}^2 \tag{6.92}$$

The bit error rate for k^{th} user is as follows

$$P_e = Q\left(\sqrt{\frac{A^2}{\sigma^2\,(\alpha^2)_{k,k}}}\right) = Q\left(\frac{A}{\sigma\,\alpha_{k,k}}\right). \tag{6.93}$$

From equation 6.81 we get the multi-user efficiency for k^{th} user

$$\eta_k = \frac{1}{(\alpha_{k,k})^2}. \tag{6.94}$$

Thus the near-far resistance for decorrelator detector is

$$\eta_k = \frac{1}{(\alpha_{k,k})^2}\ . \tag{6.95}$$

When $\sigma \to 0$ MMSE detector converges to decorrelator and therefore the asymptotic multi-user efficiency (or the near-far resistance) is identical to that of decorrelator

$$\eta_k = \frac{1}{(\alpha_{k,k})^2}. \tag{6.96}$$

As can be seen the MMSE detector is near-far resistant because it does not depend on the other users' powers. The near-far resistance can also be seen from the MMSE detector output signal

$$\mathbf{y}'(\mathbf{n}) = \mathbf{w}_{\mathrm{opt}}^{H}\ \mathbf{y}(\mathbf{n}). \tag{6.97}$$

Substituting w_{opt} and y, we get

$$\mathbf{y}'(\mathbf{n}) = \left[\boldsymbol{\gamma}\,\boldsymbol{\gamma}^{\mathrm{T}} + \boldsymbol{\sigma}^2\,\boldsymbol{\beta}^2\right]^{-1}\boldsymbol{\gamma}^{\mathrm{T}}\left[\boldsymbol{\gamma}\,\mathbf{a}(\mathbf{n}) + \boldsymbol{\xi}(\mathbf{n})\right]. \tag{6.98}$$

When $\sigma \to 0$ the above equation becomes

$$\mathbf{y}'(\mathbf{n}) = (\boldsymbol{\gamma})^{-1}\,(\boldsymbol{\gamma}^{\mathrm{T}})^{-1}\,\boldsymbol{\gamma}^{\mathrm{T}}\,\boldsymbol{\gamma}\,\mathbf{a}(\mathbf{n}), \tag{6.99}$$

$$\mathbf{y}'(\mathbf{n}) = \mathbf{a}(\mathbf{n}). \tag{6.100}$$

The output signal of one user does not depend on the other user power (MAI) and therefore it is near-far resistant.

6.3 Computation Complexity

The computation complexity is defined as the number of multiplications and the number of additions required to perform certain task, operation or block, such as multicarrier modulation using Fourier system or wavelet system, multicarrier demodulation at the receiver side, multi-user detection block using decorrelator, MMSE-MUD, or other method. Detail analysis of the computation requirement for the proposed system is presented in the next section.

6.3.1 Computation Cost in the MCM Modulation-Demodulation System

6.3.1.1 FFT-based MCM

N point FFT will need $N/2 \log_2 N$ complex multiplications and $N \log_2 N$ complex additions [201]. Hence M-channel Fourier-based multicarrier modulation requires $M/2 \log_2 M$ complex multiplications and $M \log_2 M$ complex additions (using standard IFFT for implementing multicarrier modulation). The same computation complexity is required in multicarrier demodulation process in the receiver side.

6.3.1.2 Wavelet-based MCM

A cosine modulated filter bank (M-band) with lattice structure can be implemented using 2M polyphase filters, 2M complex modulators and 2M-point DFT [1]. Using normal structure without lattice structure we will need M polyphase filters, M complex modulators and M-point DFT. Therefore wavelet based multicarrier modulation can be implemented using M polyphase filters of m-length which is the *overlap factor (m=N/M)*, M

modulators and M-point FFT. The number of complex multiplications in each process is then as follows:

M polyphase filters : m M,

M modulators: M,

M-point FFT : M/2 $\log_2$ M.

The total number of complex multiplications is

$$M\,(m+1+0.5\log_2 M). \tag{6.101}$$

The number of complex additions in each process is

M polyphase filters : (m-1) M,

M modulators: M-1,

M-point FFT : M $\log_2$ M.

The total number of additions is

$$M\,(m+\log_2 M)-1. \tag{6.102}$$

Hence compared with the Fourier based system, the wavelet based system needs M(m+1) extra complex multiplications and (Mm-1) extra complex additions. But as the speed of digital electronic components becomes faster nowadays this extra computation burden becomes less expensive. In the receiver side, wavelet based multicarrier demodulation will have the same number of complex multiplications which is M (m+1+ 0.5 $\log_2$ M) and the same number of complex additions which is M (m+ $\log_2$ M)-1.

6.3.2. Computation Cost in the Detection System

The multi-user detection is independent from the multicarrier demodulation process. As can be seen the figure 5.2, wavelet-based multicarrier CDMA receiver employs a bank of analysis filters each of which is matched with the correspondent synthesis filters in the

transmitter side. In the user's domain, the matching with the user signature waveform is done in despreading process using desired user's code.

6.3.2.1 MMSE Combiner

After the despreading process, the next task of the receiver is to combine the signal energy that is scattered in all subbands. There are a number of methods that can be used, for example: Equal Gain Combining (EGC), Maximum Ratio Combining (MRC) and Minimum Mean Square Error (MMSE). As all these channel equalisers are linear transformation (see also the equation in table 6.2), the number of complex multiplications is in fact equal to the number of subbands, which is M. The number of complex additions is (M-1). This calculation is a function of data symbol rate . The equalisation coefficients in fact should be calculated as well. Although it is not a function of data signal rate , these coefficients must be updated when the channel changes- and hence this computation should be taken into account as well. Rewrite these optimised coefficients in equation (5.53)

$$\alpha_{opt} = \left[M\,(\mathbf{H}\,\mathbf{H}^{\mathbf{T}}) + \sigma^2\,\mathbf{I} \right]^{-1} \mathbf{H_k}.$$

Let us take an example of direct multiplication of 2x3 matrix **A** and 3x2 matrix **B**.

$$\begin{pmatrix} a_{11} & a_{12} & a_{13} \\ a_{21} & a_{22} & a_{23} \end{pmatrix} \begin{pmatrix} b_{11} & b_{12} \\ b_{21} & b_{22} \\ b_{31} & b_{32} \end{pmatrix} = \begin{pmatrix} c_{11} & c_{12} \\ c_{21} & c_{22} \end{pmatrix},$$

$$\begin{aligned} c_{11} &= a_{11}b_{11} + a_{12}b_{21} + a_{13}b_{31} \\ c_{12} &= a_{11}b_{12} + a_{12}b_{22} + a_{13}b_{32} \\ c_{21} &= a_{21}b_{11} + a_{22}b_{21} + a_{23}b_{31} \\ c_{22} &= a_{21}b_{12} + a_{22}b_{22} + a_{23}b_{32} \end{aligned}$$

Using standard calculation, to get an inner product of 2 matrix A_{2x3} B_{3x2} it needs 3x2x2=12 multiplications and 2x2x2=8 addditions. In general form, 2 matrix multiplication $A_{n1x\,n2}$ $B_{n2x\,n3}$ requires ***n1 n2 n3*** multiplications and ***n1 (n2-1) n3*** addditions.

Consequently, to obtain the optimal coefficients of MMSE combiner, the computation needs the number of complex multiplication and complex addition as follows:

The matrix multiplication of $\mathbf{H}\,\mathbf{H}^{T}$ requires the number of complex multiplications (Nm) and the number of complex additions (Na) as follows

Nm= $\mathbf{M^2 K}$,

Na= $\mathbf{M^2 (K-1)}$.

The scalar M multiplications :

Nm= $\mathbf{M^2}$,

Na= **0.**

The matrix additions

Nm= **0,**

Na= $\mathbf{M^2}$.

The matrix inversion

Nm= $\mathbf{M^3}$,

Na= $\mathbf{M^2 (M-1)}$.

The matrix multiplications with $\mathbf{H_k}$

Nm= $\mathbf{M^2}$,

Na= $\mathbf{M (M-1)}$.

Finally the total of complex multiplications and complex additions to determine the coefficients are as follows

$$\text{Nm}= \mathbf{M^2 K+ M^2 +M^3 +M^2 = M^2 (2+K+ M)}, \tag{6.103}$$

$$\text{Na}= \mathbf{M^2 (K-1)+ M^2+M^2 (M-1)+M (M-1)= M^3+M^2 K-M}. \tag{6.104}$$

6.3.2.2 Decorrelator

As the output signal of the combiner still contains multiple access interference (MAI) signal, then it is multi-user detector job to deal with these signals. Decorrelator multi-user detector mitigates or cancels multiple access interference (MAI) by decorrelating the other user's components from the desired user's signal. This is a linear transformation (see also the equation on table 2). The number of complex multiplications is equal to the number of active users (K). And the number of complex additions is (K-1). These calculations are a function of data symbol rate. The computation of the filter coefficients should be calculated as well. Although it is not a function of data signal rate these coefficients must be updated when the user structure in the serving network changes or the channel characteristics change and hence this computation should be taken into account as well. Rewriting equation (5.20) in other form

$$\mathbf{y(n)} = \gamma\, \mathbf{a(n)} + \xi\mathbf{(n)}. \tag{6.105}$$

The output signal of the decorrelator can be written

$$\mathbf{y'(n)} = \gamma^{-1}\, \mathbf{y(n)}. \tag{6.106}$$

Direct matrix inversion (if it exists) has computation complexity : $O(K^3)$ [202,203]. If γ is symmetric or Hermitian, and has positive diagonal elements, then a Cholesky factorisation is used to solve the equation, but it still has the degree of computation complexity of $O(K^3)$ [204] which means that the number of multiplication is $Nm = \mathbf{K^3}$. Matrix inversion using Strassen method has lower computation complexity : $O(K^{2.8})$ [205].

The matrix γ contents changes when there is another user coming into the network or leaving the network. It also changes when the channel changes. Therefore when the users' structure in network changes or the channel changes the matrix γ must be updated. Then to obtain the optimal coefficient of the decorrelator, the number of complex multiplication and complex addition are as follows:

The calculation of matrix γ which is $\gamma = \beta\, \mathbf{E} = (\alpha \cdot \mathbf{C}^{\mathbf{T}})(\mathbf{C} \cdot \mathbf{H})$ requires the number of complex multiplications (Nm) and the number of complex additions (Na) as follows

Nm= $(\mathbf{M\,K} + \mathbf{M\,K}) + \mathbf{M^2\,K} = \mathbf{M^2\,K} + 2\,\mathbf{MK}$,

Na= $0 + \mathbf{K^2\,(M-1)} = \mathbf{(M-1)\,K^2}$.

The matrix inversion needs

Nm= $\mathbf{K^3}$,

Na= $\mathbf{K^2\,(K-1)}$.

And hence the total complex multiplications and complex additions are

Nm= $\mathbf{K^3} + \mathbf{M^2\,K} + 2\,\mathbf{MK}$, (6.107)

Na= $\mathbf{K^2(M+K-2)}$. (6.108)

6.3.2.3 MMSE-MUD

This multi-user detector mitigates the effect of both MAI signal and the Gaussian noise signal. This is also a linear transformation (see also the equation on table 6.2). The number of complex multiplications is equal to the number of active users, which is K. And the number of complex additions is (K-1). These calculations are a function of data symbol rate. The same as in decorrelator MUD, the filter coefficients of minimum mean squared error multiuser detector (MMSE-MUD) must be calculated and updated when the users' structure in network changes or the channel changes and hence this computation should be taken into account as well. We write the equation (5.73) here to identify the computation complexity

$$\mathbf{w}_{opt} = \left[\gamma^{\mathbf{T}}\,\gamma + \sigma^2\,\beta^2\right]^{-1}\gamma^{\mathbf{T}}.$$

Calculating these optimal coefficients requires the number of complex multiplications and complex additions as follows:

The matrix multiplication of $\gamma^T \gamma$ requires the number of complex multiplications (Nm) and the number of complex additions (Na) as follows

Nm= $\mathbf{K^3}$,

Na= $\mathbf{K^2 (K-1)}$.

The scalar σ^2 multiplications :

Nm= $\mathbf{K^2}$,

Na= **0.**

The matrix additions

Nm= **0,**

Na= $\mathbf{K^2}$.

The matrix inversion

Nm= $\mathbf{K^3}$,

Na= $\mathbf{K^2 (K-1)}$.

The matrix multiplications with γ^T

Nm= $\mathbf{K^3}$,

Na= $\mathbf{K^2 (K-1)}$.

Finally the total number of complex multiplications to determine the coefficients is

Nm= $\mathbf{2MK^2 + 2MK + 3K^3 + K^2}$, (6.109)

and the correspondent number of complex additions required is

Na= $\mathbf{2MK^2 + 3K^3 - 5K^2}$. (6.110)

6.3.2.4 MMSE Comb-MUD

Here we refer to the MMSE Comb-MUD which combines the optimisation along the subband axis using MMSE method and also along the user axis to minimise the multiple

access interference (MAI) using MMSE method as well. Therefore the number of complex multiplications to calculate the detector output signal is (M+K) and the number of complex additions is (M+K-2).

The number of complex multiplications to determine the coefficients is simply the total number of that combination which is as follows

$$Nm = M^2(2+K+M) + 2MK^2 + 2MK + 3K^3 + K^2,$$

$$Nm = M^3 + M^2K + 2M^2 + 2MK^2 + 2MK + 3K^3 + K^2. \quad (6.111)$$

And the corresponding number of complex additions is

$$Na = M^3 + M^2K - M + 2MK^2 + 3K^3 - 5K^2. \quad (6.112)$$

From the operation displayed in Figure 5.1 for WB-MC-CDMA transceiver we can write the equation to perform such operation for each block as written briefly in Table 6.1. These equations have also been discussed in the chapter 5.

Block	Equation
Spreading	$b_{k,m}(n) = c_{k,m}\, a_k(n)$
MCM Modulation	$v_{k,m}(z) = F_m(z)\, b_{k,m}(z) \qquad s_k(z) = \sum_{m=0}^{M-1} v_{k,m}(z)$
Channel	$\mathbf{r(z)} = \sum_{k=0}^{K-1} \mathbf{F(z)\, E_k\, a_k(z^m)} + \mathbf{n(z)}$
MCM Demodulation	$\mathbf{w(z)} = \sum_{k=0}^{K-1} \mathbf{E_k\, a_k(z)} + \boldsymbol{\eta}\mathbf{(z)}$ where $\boldsymbol{\eta}\mathbf{(z)} = \mathbf{G(z)\, n(z^{\frac{1}{M}})}$
Despreading	$\mathbf{x_k(n) = C_k \cdot w(n)}$
MUD	
MMSE Combiner	$\mathbf{y_k(n) = \alpha_k^T\, x_k(n)} \qquad \alpha_{opt} = \left[M\,(\mathbf{H\,H^T}) + \sigma^2\,\mathbf{I}\right]^{-1}\mathbf{H_k}$
Decorrelator	$\mathbf{y(n) = \gamma\, a(n) + \xi(n)} \qquad \mathbf{y'(n) = \gamma^{-1}\, y(n)}$
MMSE MUD	$\mathbf{y'(n) = w_{opt}^H\, y(n)} \qquad \mathbf{w}_{opt} = \left[\boldsymbol{\gamma}\,\boldsymbol{\gamma}^{\mathbf{T}} + \sigma^2\,\boldsymbol{\beta}^2\right]^{-1}\boldsymbol{\gamma}$
Optimised MUD	MMSE Comb+MMSE-MUD

Table 6.1 The brief equations to perform the designed function in WB-MC-CDMA system

	Wavelet-Based		Fourier-Based	
	Nm	**Na**	**Nm**	**Na**
Spreading	M	-	M	-
MCM Modulation	$M(m+1+0.5\log_2 M)$	$M(m+\log_2 M)-1$	$0.5M\log_2 M$	$M\log_2 M$
MCM Demod	$M(m+1+0.5\log_2 M)$	$M(m+\log_2 M)-1$	$0.5M\log_2 M$	$M\log_2 M$
Despreading	M	-	M	-
MUD :				
MMSE Combiner	M	M-1	M	M-1
Decorrelator	K	K-1	K	K-1
MMSE MUD	K	K-1	K	K-1
Optimised MUD	(M+K)	M+K-2	(M+K)	M+K-2

Table 6.2 The number of complex multiplications and complex additions to calculate the output signal for each functional block per symbol

From the block diagram (Figures 5.1) and the brief equation (Table 6.1) we then can determine the numbers of complex multiplications and complex additions required to perform a functional block. These numbers which represent the computation cost are written in Table 6.2. Determining the coefficients in multi-user detection requires the numbers of complex multiplications and complex additions as displayed in Table 6.3.

	Nm	**Na**
MMSE Combiner	$\mathbf{M^2(2+K+M)}$	$\mathbf{M^3+M^2K-M}$
Decorrelator	$\mathbf{K^3+M^2K+2MK}$	$\mathbf{K^2(M+K-2)}$
MMSE MUD	$\mathbf{2MK^2+2MK+3K^3+K^2}$	$\mathbf{2MK^2+3K^3-5K^2}$
MMSE Comb-MUD	$\mathbf{M^3+M^2K+2M^2+2MK^2+2MK+3K^3+K^2}$	$\mathbf{M^3+M^2K-M+2MK^2+3K^3-5K^2}$

Table 6.3 The number of complex multiplications and complex additions to calculate the detector coefficients

The cost of the modulation-demodulation in the wavelet-based system is analysed and found to be higher by an additional M(m+1) operations per symbol (where m=N/M is the overlap factor) than if the processing is achieved by the conventional Fourier-based system. The cost of computing the coefficients of various detectors considered in this paper is shown in Figure 6.3. Clearly the complexity of the proposed MMSE detector is more than that of the decorrelator. However the BER performance of MMSE detector is superior to that of the decorrelator when data is transmitted through an AWGN or Rayleigh channel (see section 6.1).

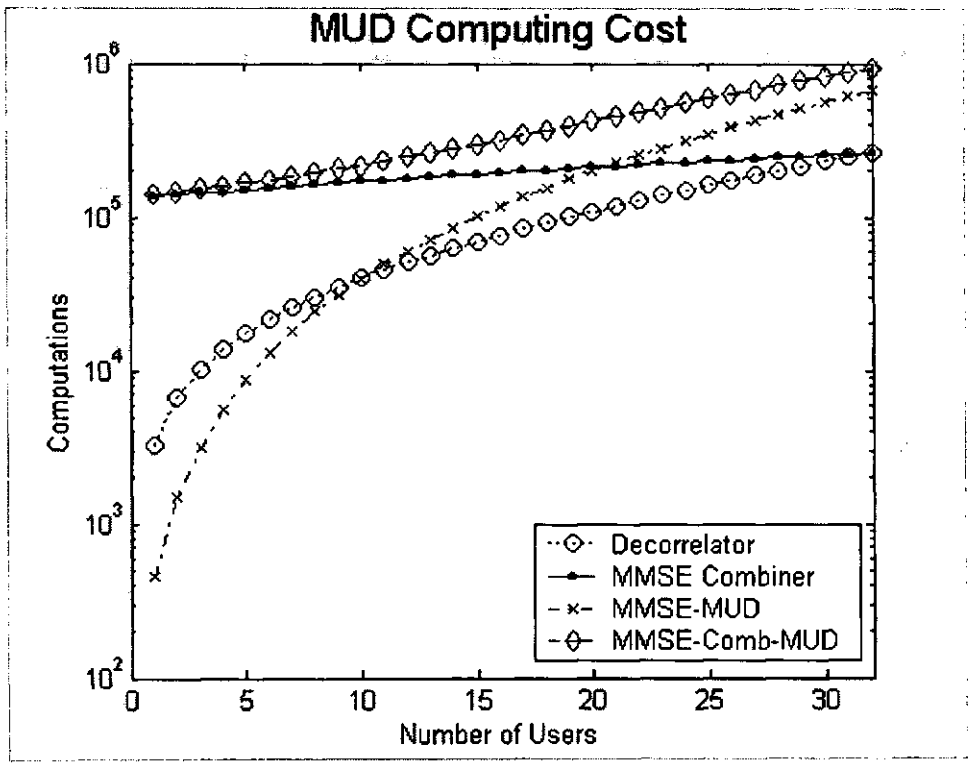

Figure 6.3 Cost of computing the detector coefficients

CHAPTER VII

CONCLUSIONS

7.1 Contributions and Innovations

The author's contributions to knowledge are summarised below.

Chapter II

- The description of M-band wavelet system and its power spectral density
- The description of a general model for multi-user and/or multi-carrier digital communication systems.

Chapter III

- The description of all types of wavelet systems to implement a multi-carrier system.
- The description and implementation of M-band wavelet basis (instead of the conventional DFT basis) to provide orthogonality between subbands in multicarrier CDMA (MC-CDMA) systems.
- The description and analysis of wavelet-based MC-CDMA (WB-MC-CDMA) transmitter system.
- The description and analysis of WB-MC-CDMA receiver system.
- The evaluation of WB-MC-CDMA system and the simulation results.
- The comparison of the evaluation results between Fourier-based MC-CDMA (FB-MC-CDMA) and WB-MC-CDMA simulation system.

Chapter IV

- The description and analysis of the time synchronisation scheme using M-band wavelet correlation properties in WB-MC-CDMA systems.
- The description and analysis of the timing acquisition in WB-MC-CDMA systems.
- The description and analysis of the timing tracking in WB-MC-CDMA systems.
- The results and evaluation of the timing acquisition in WB-MC-CDMA systems.
- The results and evaluation of the timing tracking in WB-MC-CDMA systems.
- The description and analysis of the frequency offset estimation in WB-MC-CDMA systems.
- The results and evaluation of the frequency offset estimation simulation.
- The description and analysis of the phase offset estimation in WB-MC-CDMA systems
- The results and evaluation of the phase offset estimation simulation

Chapter V

- The description and analysis of the wavelet modulation-demodulation system
- The description and analysis of the matched filter detection for WB-MC-CDMA systems
- The description and analysis of the MMSE combining method for WB-MC-CDMA systems
- The description and analysis of the MMSE multiuser detection for WB-MC-CDMA systems
- The description and analysis of the adaptive implementation of MMSE multiuser detection for WB-MC-CDMA systems
- The evaluation and simulation of multiuser detection for WB-MC-CDMA systems

Chapter VI

- The description and analysis of BER performance of WB-MC-CDMA system under AWGN channel
- The description and analysis of BER performance of WB-MC-CDMA system under Rayleigh channel
- The results and evaluation of BER performance of WB-MC-CDMA system
- The description and analysis of near-far resistance of the MMSE-MUD for WB-MC-CDMA systems
- The description and analysis of computation complexity of the wavelet modulation-demodulation and multiuser detection for WB-MC-CDMA systems
- The comparison of computation complexity for FB-MC-CDMA and WB-MC-CDMA systems

7.2 Conclusions

Multi-carrier communication is commonly employed to combat channel distortion and improves the spectral efficiency. The basic idea of the scheme entails the division of the available spectrum into subbands of relatively narrow bandwidth such that the subchannels are nearly distortionless. The combination of multi-carrier modulation and CDMA into multi-carrier (MC) CDMA appears to be very attractive in mobile communications because it meets the challenges for next generation systems which are high data rate (wideband) system, robust against multipath fading and multiple access interference, higher spectral efficiency and network capacity. Traditionally the multi-carrier modulation is implemented

using discrete Fourier transform (DFT) basis.

The aims for the work in this thesis were to investigate the implementation of M-band wavelet basis instead of DFT basis for multicarrier modulation in MC-CDMA systems to further enhance the performance in term of the above challenges. The theoretical analysis and the simulation have been done and shown that the proposed system (WB-MC-CDMA system) has superior performance in term of bit error rate (BER), spectral efficiency and robustness against multipath fading and narrow band interference. These superiorities are achieved at the price of the higher computation complexity and a bit higher peak-to-average power ratio (PAPR).

In order to maintain the signal orthogonality, the receiver must achieve synchronisation in time and frequency. We exploit the wavelet correlation properties to perform time synchronisation. We propose a maximum likelihood system for coarse timing synchronisation (ML acquisition) followed by early late sample tracking (ELS tracking) for fine time synchronisation. The performance of ML acquisition and ELS tracking under AWGN channel are obtained analytically and through simulation and compared with the Cramer-Rao Bound. The designed acquisition circuit performs close to the Cramer-Rao Bound. The characteristic of the tracking circuit has also been discussed and the locking of the tracking circuit is achieved without ambiguity.

In this research we consider a frequency offset estimator which takes advantage of the fact that the frequency offset is the phase rotation rate of the signal. Therefore the frequency offset is simply the derivative of the signal argument. We also considered a phase offset estimator which averages the signal argument over number of samples. The performance of the frequency offset estimator has been obtained and shown that the error variance becomes

smaller for higher Eb/No. The performance of the phase offset estimator has also been obtained and shown that the error variance is inversely proportional to Eb/No value.

There are two levels of orthogonality, i.e. along subband axis and user axis. The problems of the detection to retrieve the data symbol are: first, how to combine the signal scattered in all subbands to exploit the frequency diversity. Second, how to mitigate the multiple access interference signal. Therefore we propose an approach where the detection is performed on both axis using minimum mean squared error algorithm in subband axis and user axis. The first one is called MMSE combiner to exploit the frequency diversity available in MC-CDMA signal. The second is called MMSE multiuser detection. The adaptive implementation of MMSE multiuser detection has also been discussed in this thesis.

The joined MMSE combining (MMSEC) and MMSE multiuser detection (MMSE-MUD) shows the best BER performance under Rayleigh channel compared with matched filter, decorrelator, MMSEC alone and MMSE-MUD alone. The adaptive MMSE multiuser detection has shown further improvement of BER performance. The BER improvement of MMSE-MUD is achieved at the cost of higher computation complexity. This MMSE-MUD also retains the near-far resistance as the decorrelator.

7.3 Future Works

The concepts of wavelet systems to implement a multicarrier modulation applied for wireline and wireless communications have been studied and developed in some literatures [45-77,160-165,206-208]. There are though still some interesting issues worth of investigations.

As the wavelet system here is used to provide the orthogonality between subbands, it would be ideal if the design of this wavelet together with the biorthogonality includes system parameters such as bandwidth efficiency, PAPR, etc. This in turn will further enhance the superiority of the wavelet basis over the DFT basis in multiuser multicarrier communication systems. It would also be beneficial to research design schemes to reduce the computation complexity by implementing it in a more efficient structure.

Usually we need extra bandwidth for forward error correction (FEC) coding such as block coding, convolutional coding, turbo coding etc. Using wavelet basis for multicarrier modulation, it is possible to perform the detection with Viterbi algorithm because wavelet filtering can be regarded as a convolutional coding. This wavelet coding might provide error correction without sending additional parity bits at the transmitter. Further investigations about this potential breakthrough are required.

We use Walsh-Hadamard code to provide orthogonality between users in this project. It would be useful to compare this code in WB-MC-CDMA systems with other codes such as Kasami code, PN code or wavelet code etc.

We use uniform rate for each user and each subband in this research. As users can demand different bandwidth we can implement a multirate WB-MC-CDMA system which provides different rate for users by allocating them with certain number of codes or wavelets.

We implement adaptive MMSE multiuser detection using least mean square (LMS) method in WB-MC-CDMA system. We need to investigate the possibility to use RLS method or even blind adaptive MMSE where the system requires only the knowledge of timing and signature waveform of the desired users as in matched filter detection. It is possible as well

to mitigate the multiple access interference (MAI) signal by interference cancellation (IC) method such as: serial interference cancellation (SIC), parallel interference cancellation (PIC), partial PIC (PPIC) etc.

It would be remarkable if we can get the superiorities of WB-MC-CDMA system and implement it in software defined radio for cellular systems. The tranceiver then can be reconfigured and reprogrammed easily just by software.

There is a possibility to combine Walsh-Hadamard transform (for spreading) and M-band wavelet transform (for multicarrier modulation) in one block so that it reduces the complexity in implementation.

So far we investigate and discuss the system in the time-frequency domain. In order to improve the signal quality, it is possible to work on the space domain as well by using multiple antennas. Currently the time-space algorithm is being investigated in some research institutions [209-212]. Using time-space coding for WB-MC-CDMA system, the signal quality will be improved even under severe multipath fading channel.

REFERENCES

1. V.K. Garg, G. Vijay, J. Wilkes. *Wireless And Personal Communications Systems (PCS): Fundamentals and Applications.* Prentice Hall PTR, 1995.

2. K. Tachikawa. W-CDMA Mobile Communication Systems. John Wiley & Sons, 2002.

3. 3GPP, "The 3rd Generation Partnership Project Agreement". http://www.3gpp.org/

4. WCY. Lee,. *Mobile Cellular Telecommunications, Analog And Digital Systems.* New York, Mc Graw-Hill, 1995.

5. VK. Garg, K. Smolik and J.E. Wilkes. *Applications of CDMA in Wireless/Personal Communications.* Prentice Hall, 1996.

6. ES Sousa, *Spread Spectrum for PCS. IEEE GTC London 1996.*

7. AJ. Viterbi. *CDMA Cellular Systems.* New York, McGraw Hill, 1995.

8. AJ. Viterbi, *CDMA: Principles of Spread Spectrum Communication.* Addison-Wesley, Reading, Massachusetts, USA, 1995.

9. RA. Scholtz, "The origins of spread-spectrum communications. *IEEE Transactions on Communications 30(5),* 1982, pp. 822-854.

10. K. Karkkainen, "Code Families and Their Performance Measures for CDMA and Military Spread-Spectrum Systems". Acta Universitatis Ouluensis C89, 1996,University of Oulu Press, Oulu, Finland.

11. RC. Dixon. *Spread Spectrum Systems with Commercial Applications.* John Wiley and Sons, New York City, New York, USA, 1994.

12. RL. Peterson, RE. Ziemer and DE Borth. *Introduction to Spread Spectrum Systems.* Prentice-Hall, Englewood Cli_s, New Jersey, USA, 1995.

13. J. Wang, and M Moeneclaey and LB Milstein,"DS-CDMA with predetection diversity for indoor radio communications", *IEEE Transactions on Communications,* Vol. 42. No.2/3/4. Febr./March/April 1994. pp.1929-1938.

14. M.K. Simon, J.K. Omura, R.A. Scholtz and B.K. Levitt. *Spread Spectrum Communications Handbook.* McGraw-Hill, New York City, New York, USA, 1994.

15. R. Prasad. *CDMA for Wireless Personal Communications.* Artech House, 1996.

16. A. Fukasawa, T. Sato, Y. Takizawa, T. Kato, M. Kawabe, and R. Fisher, "Wideband CDMA System For Personal Radio Communications", *IEEE Communications Magazine,* October 1996, pp. 116-123.

17. R. van Nee and R. Prasad, *OFDM for Wireless Multimedia Communications.* Artech House, 2000.

18. SB. Weinstein and PM. Ebert, "Data Transmission by Frequency Division Multiplexing Using the Discrete Fourier Transform", *IEEE Transaction on Communication Tech*, vol. Com-19, Oct. 1971, pp. 628- 634.

19. J.P Linnartz and S. Hara, *Special Issue on Multi-Carrier Modulation, Wireless Personal Communication.* Dordrecht (Netherland), Kluwer Academic Publishers, 1996.

20. L. Hanzo, W. Webb and T. Keller. *Single and Multicarrier Modulation: Principles and Applications for Personal Communications, WLANs and Broadcasting* . John Wiley and Sons Ltd, 2000.

21. L. Hanzo, M. Muenster, B.J. Choi and T. Keller. *OFDM and MC-CDMA for Broadband Multi-User Communications, WLANs and Broadcasting.* John Wiley and Sons Ltd, 2003.

22. N. Yee, J.P. Linnartz and G. Fettweis, *"Multicarrier CDMA In Indoor Wirelesss Radio Networks". Proc.Of IEEE PIMRC '93* . Yokohama, Japan, Sept. 1993, pp. 109-113.

23. S. Hara and R. Prasad, *"An Overview of Multi-Carrier CDMA", IEEE Communications Magazine, Dec 1997,* pp. 126-133.

24. N. Yee, JPMG. Linnartz G. Fettweis, *"Multi-Carrier-CDMA in indoor wireless networks", IEICE Transaction on Communications*, Japan, Vol. E77-B, No. 7, July 1994, pp. 900- 904.

25. N. Yee and JPMG. Linnartz, "Multi-Carrier Code Division Multiple Access (MC-CDMA): a new spreading technique for communication over multipath channels", Final Report 93-101 (also 92-092), Microelectronics Innovation and Computer Research Opportunities, University of California, Oakland,USA

26. K. Fazel, S. Kaiser and M. Schnell, "A flexible and high-performance cellular mobile communications system based on orthogonal multicarrier SSMA", *Wireless Personal Communications*, vol. 2, no. 1, 1995, pp. 121-144.

27. K. Fazel and G.P. Fetweiss (ed.) . *Multi-Carrier Spread Spectrum.* Dordrecht (Netherland), Kluwer Academic Publishers, 1997.

28. K. Fazel and S. Kaiser (Eds.). *Multi-Carrier Spread Spectrum and Related Techniques*. Kluwer Academic Publisher, 1999.

29. S. Kaiser, "Trade-Off Between Channel Coding And Spreading In Multi-Carrier CDMA Systems", *Proceeding Of IEEE ISSSTA*, Sept 1996, pp. 1366-1370.

30. GJ. Saulnier, Z. Ye and MJ. Medley, "Performance of a spread spectrum OFDM system in a dispersive fading channel with interference", *MILCOM 1998 - IEEE Military Communications Conference*, no. 1, October 1998 pp. 679-683.

31. S. Kaiser and L. Papke,"Optimal detection when combining OFDM-CDMA with convolutional and Turbo channel coding", *Proc. IEEE Intern. Conf. on Commun. (ICC'96)*, Dallas, USA, June 1996, pp. 343-348.

32. S. Kaiser and K. Fazel, *"A flexible spread-spectrum multi-carrier multiple-access system for multi-media applications", Proc. IEEE Intern. Symp. on Personal, Indoor and Mobile Radio Commun. (PIMRC'97)*, Helsinki, Finland, pp. 100-104, Sept. 1997.

33. Y. Bar-Ness and M. Visser, ``*Adaptive Reduced Complexity Multicarrier CDMA (MC-CDMA) structure for Downlink PCS," European Transaction on Telecommunication*, vol. 10, No. 4, pp. 437-444. July/August 99.

34. JPMG. Linnartz, "Synchronous MC-CDMA in dispersive, mobile Rayleigh channels", *IEEE Benelux Signal Processing Symposium*, SPS200, Hilvarenbeek, March 23-24, 2000, pp.97-105.

35. Prasad R, Hara S, "An overview of multi-carrier CDMA", *Proc. IEEE International Symposium on Spread Spectrum Techniques and Applications (ISSSTA)*, Mainz, Germany, 1996, pp. 107-114.

36. S. Kaiser, OFDM code-division multiplexing in fading channels, *IEEE Transactions on Communications*, Vol. 50, No. 8, Aug 2002, pp. 1266-1273.

37. S. Kondo and L.B. Milstein, "Performance of Multicarrier DS CDMA System",*IEEE Transaction on Communication, Vol 44 No.2 February 1996*, pp. 238-246.

38. L. Vandendorpe, "Multitone spread spectrum multiple access communication systems in a multipath Rician fading channel", *IEEE Trans. on Vehicular Technology*, Vol. 44, n° 2, May 1995, pp. 327-337.

39. E.A. Sourour and M. Nakagawa , *"Performance of Orthogonal Multicarrier CDMA in a Multipath Fading Channe'" . IEEE Transaction on Communication, Vol 44 No.3 March 1996*, pp. 356-367.

40. S. Kaiser, *"OFDM-CDMA versus DS-CDMA: Performance evaluation for fading channels", Proc. IEEE Intern. Conf. on Commun. (ICC'95)*, Seattle, USA, pp. 1722-1726, June 1995.

39. S. Kaiser, *"On the performance of different detection techniques for OFDM-CDMA in fading channels", Proc. IEEE Global Telecommun. Conf. (GLOBECOM'95),* Singapore, pp. 2059-2063, Nov. 1995.

42. D.N Kalofonos, M. Stojanovic and J.G. Proakis. *"Performance of a MC-CDMA System in a Rayleigh Fading Channel, in the Presence of Channel Estimation Error". Proceedings of the 6th International Conference on Advances in Communications and Control (COMCON 6),* pp. 729-737, June 1997.

43. CW. You and DS. Hong, "Multicarrier CDMA systems using time-domain and frequency-domain spreading codes", *IEEE Transactions on Communications,* Vol. 51, No. 1, Jan 2003, pp. 17- 21.

44. I. Daubechies, *"Ten Lectures on Wavelets," CBMS-NSF Lecture Notes No. 61, SIAM,* Philadelphia,1992, ISBN 0-89871-274-2.

45. A.N. Akansu, M.V. Tazebay, M.J. Medley and P.K. Das, ``Wavelet and Subband Transforms: Fundamentals and Communication Applications," *IEEE Communications Magazine,* Dec. 1997, pp. 104-115.

46. A.N. Akansu and R.A. Haddad. *Multiresolution Signal Decomposition: Transforms, Subbands, & Wavelets,* Academic Press, October 1992.

47. P.P. Vaidyanathan. *Multirate Systems and Filter Banks.* Prentice Hall, September 1992.

48. I. Daubechies, *"Orthonormal Bases of Compactly Supported Wavelets", Comm. Pure & Appl. Math. 41,* pp. 909--996, 1988.

49. G.W. Wornell, *"Emerging Applications of Multirate Signal Processing and Wavelets in Digital Communications", Proceedings of the IEEE, Vol. 84, No. 4,* April 1996, pp. 586-603.

50. C.K. Chui . *An Introduction to Wavelets (Wavelet Analysis and Its Applications, Vol.1).* Academic Press, January 1992.

51. C.K. Chui. *Wavelets : A Tutorial in Theory and Applications (Wavelet Analysis and Its Applications, Vol 2).* Academic Press, Incorporated, January 1992.

52. G.W. Wornell. *Signal Processing With Fractals : A Wavelet-Based Approach.* Prentice Hall, 1995.

53. A.N. Akansu and M.J.T. Smith, Eds. *Subband and Wavelet Transforms : Design and Applications.* Kluwer Academic Publishers, October 1995.

54. G.W. Wornell,*"Wavelet-Based Representations for the 1/f Family of Fractal Processes", Proceedings of the IEEE, Vol. 81, No. 10,* October 1993.

55. G.W. Wornell and A.V. Oppenheim,*"Estimation of Fractal Signals from Noisy Measurements Using Wavelets", IEEE Transactions on Signal Processing, Vol. 40, No. 3,* March 1992.

56. G.W. Wornell and A.V Oppenheim,*"Wavelet-Based Representations for a Class of Self-Similar Signals with Application to Fractal Modulation", IEEE Transactions on Information Theory, Vol. 38, No. 2,* March 1992, pp. 785-800.

57. RKC. Tan and AHJ. Lin . "A Time-Scale Modification Algorithm Based on the Subband Time-Domain Technique for Broad-Band Signal Applications" *Journal of the AES.* VOL 48 No.5, May 2000, pp. 436-448.

58. A. Scaglione, G. B. Giannakis, and S. Barbarossa. " Minimum Redundancy Filterbank Precoders for Blind Channel Identification Irrespective of Channel Nulls," *Proc. of IEEE Wireless Comm. and Networking Conferenc e (WCNC'99),* New Orleans, LA, September 21-24, 1999, Vol.2 pp.787-791.

59. F. Dovis, M.Mondin, F. Daneshgaran. *"The Modified Gaussian: a Novel Wavelet with Low Sidelobes with Applications to Digital Communications", IEEE Communications Letters,* August 1998, pp. 208-210.

60. F. Daneshgaran, M. Mondin, F. Dovis. *"Symbol Synchronization for Multicarrier Modulation", Proc. Conf on Inform. Sciences and Syst. CISS 98,* Princeton University, Princeton NJ, 18-20 March 1998, pp. 572–577.

61. F. Daneshgaran, M.Mondin, F. Dovis. *"Performance of Wavelet-Based Shaping Pulses on Linear and Non-Linear Channels", Proc. Conf. on Inform. Sciences and Syst. CISS '99,* The Johns Hopkins Univ., Baltimore MA, March 1999. pp. 131–135.

62. M.J. Medley, G.J. Saulnier and P. Das, *"Applications of the Wavelet Transform in Spread Spectrum Communications Systems", Proceedings of SPIE, vol. 2242,* 1994, pp. 54-68.

63. A. R. Lindsey, " Improved spread-spectrum communication with a wavelet packet based transceiver," *Proc. of International Symp. on Time-Frequency and Time-Scale Analysis'96,* pp. 417-420, 1996.

64. A.N. Akansu, P. Duhamel, X. Lin, M de Courville. *"Orthogonal Transmultiplexers in Communication: A Review," IEEE Transactions on Signal Processing,* April 1998, pp.979-995.

65. K.J Hetling, G.J. Saulnier and P. Das ,*"Optimized Filter Design for PR-QMF Based Spread Spectrum Communications", 1995 IEEE International Conference on Communications Conference Record,* June 1995, pp 1350 - 1354.

66. K.J. Hetling, G.J. Saulnier and P. Das, "PR-QMF Based Codes for Multipath/ Multiuser Communications", *1995 IEEE Globecom Conference Record, Communication Theory Mini-Conference*, November 1995, pp. 105-109.

67. K.J. Hetling, M.J. Medley, G.J. Saulnier and P. Das, *"A Wavelet Coding Based Spread Spectrum Communications System", 1994 IEEE MILCOM Conference Record,* October 3-5, 1994, pp. 760-764.

68. M.K. Tsatsanis and G.B. Giannakis, "Multi-rate Filter Banks for Code Division Multiple Access Systems". Proceeding IEEE ICASSP, Vol. II, pp 1484-1487, May 1995.

69. G.W. Wornell,*"Spread-Response Precoding for Communication over Fading Channels", IEEE Transactions on Information Theory, Vol. 42, No. 2,* March 1996,pp. 488-501.

70. G.W. Wornell,*"Spread-Signature CDMA: Efficient Multiuser Communication in the Presence of Fading", IEEE Trans. Inform. Theory, Vol. 41, No. 5,* September 1995,pp. pp1418-1438.

71. K. J. Hetling, G. J. Saulnier and P. Das,"Performance of Filter Bank-Based Spreading Codes for Multipath/Multiuser Interference," *Proceedings of the SPIE, Wavelet Applications III,* Harold H Szu; Ed., Vol. 2762, March 1996, pp. 501-512.

72. Q. Shi and S. Cheng,*"Optimal spreading sequence design based on PR-QMF theory". Electronic Letters,* 18th March 1999, Vol.35, No.6, pp. 447-448.

73. S.D Sandberg and M.A Tzannes, *"Overlapped Discrete Multitone Modulation for High Speed Copper Wire Communications", IEEE Journal on Selected Areas in Communications,* Vol.13 No.9, Dec 1995, pp. 1571-1585.

74. M.A. Tzannes, M.C. Tzannes and H.L. Resnikoff,*"The DWMT: A Multicarrier transceiver for ADSL using M-band wavelet transforms." ANSI T1E1.4 Committee Contribution No. 93-067.* Miami, FL, March 1993.

75. M.A Tzannes, M.C. Tzannes, J. Proakis, P.N. Heller,*"DMT Systems, DWMT Systems, and Digital Filter Banks," Proc. IEEE ICC.* New Orleans, Louisiana, 1994, pp. 311-315.

76. R. Gross, M.Tzannes, S. Sandberg, H. Padir and X. Zhang, "Discrete Wavelet Multitone (DWMT) System for Digital Transmission over HFC Links", *SPIE Proceedings*, Volume 2609,1995, pp. 168-175.

77. K. Chang, X. Lin and M. Kyeong, " Performance analysis of wavelet-based MC-CDMA for FPLMTS/IMT-2000," Proc. of *ISSSTA*, Sept. 1996, pp. 1443-1446.

78. T.M. Schmidl and D.C. Cox , *"Robus Frequency And Timing Synchronization", IEEE Transaction On Communication,* Vol.45 No.12. December 1997,pp. 1613-1621.

79. JJ van de Beek, M. Sandell and PO. Börjesson. " ML Estimation of Time and Frequecy Offset in OFDM Systems". *IEEE Trans. on Signal Processing*, vol. 45, no. 7, pp. 1800-1805, July 1997.

80. M. Sandell, JJ van de Beek and PO. Börjesson. "Timing and Frequency Synchronization in OFDM Systems Using the Cyclic Prefix", *Proceedings of International Symposium on Synchronization*, pp. 16-19, Essen, Germany, December 1995.

81. JJ van de Beek, M. Sandell, M. Isaksson and PO. Börjesson. "Low-Complex Frame Synchronization in OFDM Systems", *Proceedings of IEEE International Conference on Universal Personal Communication (ICUPC'95)*, pp. 982-986, Tokyo, Japan, November 1995.

82. JJ van de Beek, O. Edfors, M. Sandell, SK. Wilson and PO. Börjesson. *"On Channel Estimation in OFDM Systems", Proceedings of IEEE Vehicular Technology Conference (VTC)* 1995, vol. 2, pp. 815-819.

83. B. Muquet, W. Zhengdao,GB. Giannakis, M. de Courville and P. Duhamel,"Cyclic prefixing or zero padding for wireless multicarrier transmissions?", *IEEE Transactions on Communications,* Vol. 50, No.12, Dec 2002, pp. 2136-2148.

84. M.Visser and Y. Bar-Ness, "OFDM Frequency Offset Correction Using an Adaptive Decorrelator", *Proceedings of the 32nd Annual Conference on Information Science and Systems*, Princeton Univ., NJ, pp. 483-488, March 18-20, 1998.

85. AC. McCormick, PM. Grant and GJR. Povey " A differential phase-shift keying multicarrier code division multiple access system with an equal gain combining receiver" *IEEE Transactions on Vehicular Technology*, Vol. 49(5), September 2000, pp.1907-1917.

86. M. Schnell and S. Kaiser, *"Diversity considerations for MC-CDMA systems in mobile Communications", Proc. IEEE Fourth Intern. Symp. on Spread Spectrum Techniques & Applications (ISSSTA'96)*, Mainz, Germany, pp. 131-135, Sept.1996.

87. N. Yee and JPMG. Linnartz, "Controlled equalization for Multi-Carrier CDMA" VTC 1994, Stockholm, June 1994, pp.1665-1669.

88. N. Yee and JPMG. Linnartz, *"Wiener filtering for Multi-Carrier CDMA", IEEE / ICCC conference on Personal Indoor Mobile Radio Communications (PIMRC) and Wireless Computer Networks (WCN),* The Hague, September 19-23, 1994, Vol. 4, pp. 1344-1347.

89. G. Xue, J. Weng, T. Le-Ngoc and S. Tahar,"Multiuser Detection Techniques: An Overview", *Research Report*, Dept. of Electrical & Computer Eng., Concordia University, Oct. 1998.

90. S. Verdu, *Multiuser Detection*, Cambridge: Cambridge Univ. Press, 1998.

91. S. Verdu. "Multiuser detection. *Advances in Statistical Signal Processing*. JAI Press, Greenwich, Connecticut, USA, 2, 1993, pp. 369-409.

92. S. Verdu, *Optimum multiuser signal detection, Ph.D. thesis*, Department of Electrical and Computer Engineering, University of Illinois at Urbana-Champaign, Urbana, Illinois, USA, 1984.

93. S. Verdu. "Minimum probability of error for asynchronous Gaussian multiple access channels". *IEEE Transactions on Information Theory* 32(1), 1986, pp 85-96.

94. A. Duel-Hallen , J. Holtzman ,Z. Zvonar. "Multiuser detection for CDMA systems", *IEEE/ACM Personal Communications 2*, 1995, pp. 46-58.

95. S. Moshavi. "Multi-user detection for DS-CDMA communications", *IEEE Communications Magazine 34(10)*, 1996,pp. 124-137.

96. P. Jung, PD. Alexander. "A unified approach to multiuser detectors for CDMA and their geometrical interpretations", *IEEE Journal on Selected Areas in Communications* 14(8), 1996: pp. 1595-1601.

97. M. Juntti. *Multiuser Demodulation For DS-CDMA Systems In Fading Channels*. PhD Thesis. University of Oulu,1998.

98. AC. McCormick, PM. Grant and JS. Thompson " A Comparison of Multi-User Detectors for Uplink Multi-Carrier CDMA " in *Proceedings COST 262 Workshop: Multiuser Detection in Spread Spectrum Communications*, 17th-18th Jan 2001, Schloss Reisenburg near Ulm, Germany, pp103-107.

99. U. Madow,"Blind Adaptive Interference Suppression for DS-CDMA", *Proceedings of the IEEE*, Vol.86 No.10, Oct. 1998, pp.2049-2069.

100. L. Durak and O. Arikan, "Short-time Fourier transform: two fundamental properties and an optimal implementation, *IEEE Transactions on Signal Processing*, Vol. 51, No.5, May 2003, pp. 1231- 1242.

101. C.S. Burrus, R.A. Gopinath and H. Guo. *Introduction to Wavelets and Wavelet Transforms : A Primer*. Prentice Hall, August 1997.

102. JC. Goswami and AK. Chan , *Fundamentals of Wavelets : Theory, Algorithms, and Applications*, Wiley-Interscience, Feb 1999.

103. G. Kaiser, *A Friendly Guide to Wavelets*, Springer Verlag, June 1994.

104. A.L. Graps, *"An Introduction to Wavelets", IEEE Computational Sciences and Engineering*, Vol. 2, No. 2, Summer 1995, pp 50-61.

105. R. Kuc, *Introduction to Digital Signal Processing*, McGraw Hill, February 1988.

106. D.E Newland. *An Introduction to Random Vibrations, Spectral and Wavelet Analysis*. Essex, Longman Scientific & Technical, 1993.

107. R.K. Young. *Wavelet Theory and Its Applications*. Kluwer Academic Publishers, 1992.

108. R.M. Rao. *Wavelet Transforms : Introduction to Theory and Applications*. Addison Wesley Longman, May 1998.

109. C. Taswell. *Handbook of Wavelet Transform Algorithms*. Birkhauser Boston, May 1997.

110. G. Strang G and T. Nguyen . *Wavelets & Filter Banks*. Wellesley Cambridge Press, 1997.

111. L.R. Soares, H.M. de Oliveira, R.J.S. Cintra and R.M. Campello de Souza, "Fourier Eigenfunctions, Uncertainty Gabor Principle And Isoresolution Wavelets", *XX Simposio Brasileiro de telecomunicacoes-SBT'03*, Rio de Janeiro, 5-8 October 2003, pp. 384-389.

112. P. Steffen, P. Heller, R. A. Gopinath, and C. S. Burrus," Theory of regular *M*-band wavelet bases", *IEEE Trans. Signal Processing*, 41(12), December 1993, pp.3497-3511.

113. O. Shentov, S. K. Mitra, A. Hossen and U. Heute, " Subband DFT - Part I: Definition, Interpretation and Extensions ", *Signal Processing*, vol. 42, No. 3, Feb 1995, pp. 261-278.

114. A. Hossen, U. Heute, O. Shentov, and S. K. Mitra, " Subband DFT - Part II: Accuracy, Complexity and Applications ", *Signal Processing*, vol. 42, No. 3, Feb 1995, pp. 279-294.

115. R. A. Gopinath and C. S. Burrus, "Unitary FIR filter banks and symmetry. *IEEE Trans. on CAS II*, 41(10), October 1994, pp. 695-700.

116. A.N. Akansu, M.V. Tazebay, R.A. Haddad, *"A New Look at Digital Orthogonal Transmultiplexers for CDMA Communications", IEEE Transactions on Signal Processing*, Jan. 1997, pp. 263-267.

117. F. Daneshgaran."Coherent Frequency-Hopped CDMA and Orthogonal Frequency Division Multiplexing With Wavelets," Electronics Letters, Vol.31, No.6. March 1995, pp.428-429.

118. F. Daneshgaran, M. Mondin and F. Dovis. *" Permutation Spreading in Wavelet OFDM Systems", SPIE International Symposium '99*, 18-23 July 1999, Denver CO (USA) Vol. 3813, Paper No. 96.

.119. H Steendam and M. Moeneclaey. *Optimization of OFDM on Frequency-Selective Time-Selective Fading Channels.* Proc. ISSSE'98. Pisa, Italy. Sept.29-Oct.2 1998. pp. 398-403.

120. AC. McCormick, PM. Grant and JS. Thompson " A Comparison of Convolutional and Walsh Coding in OFDM Wireless LAN Systems", presented at 11th International Symposium on Personal, Indoor and Mobile Radio Communications, 18-21 September 2000, London, England, U.K. pp.166-169.

121. K. Fazel and S. Kaiser, *"Analysis of non-linear distortions on MC-CDMA," Proc. IEEE Int'l Conference on Communications (ICC'98),* Atlanta, USA,pp. 1028-1034, June 1998.

122. K.-W. Cheong and J. M. Cioffi, " Discrete wavelet transforms in multi-carrier modulation," *Proc. of GLOBECOM'98*, vol. 5, 1998, pp. 2794-2799.

123. A. R. Lindsey, " Wavelet packet modulation for orthogonally multiplexed communication," *IEEE Trans. Signal Processing*, vol. 45, no. 5, May 1997, pp.1336-1339.

124. A. R. Lindsey, " Improved spread-spectrum communication with a wavelet packet based transceiver," *Proc. of International Symp. on Time-Frequency and Time-Scale Analysis'96*, 1996, pp. 417-420.

125. A. N. Akansu and X. Lin, " A comparative performance evaluation of DMT (OFDM) and DWMT (DSBMT) based DSL communications systems for single and multitone interference," *Proc. of ICASSP'98*, pp. 3269-3272, 1998.

126. J.E. Odegard, R.A. Gopinath, C.S. Burrus,*"Design of Linear Phase Cosine Modulated Filter Banks for Subband Image Compression"*, *Rice University CML Technical Report CML TR94-06*, 1994.

127. R. A. Gopinath and C. S. Burrus, "On cosine-modulated wavelet orthonormal bases", *IEEE Trans. on Image Processing*, 4(2), February 1995, pp. 162-176.

128. TQ. Nguyen, "Digital Filter Banks Design - Quadratic-Constrained Formulation," *IEEE Transaction on Signal Processing*, September 95, pp. 2103-2108.

129. TQ. Nguyen, PP. Vaidyanathan, "Structures for M-Channel Perfect-Reconstruction FIR QMF Banks Which Yield Linear-Phase Analysis Filters", *IEEE Trans. on Acoustics, Speech and Signal Processing*, March 1990, pp. 433-446.

130. C. D. Creusere and S. K. Mitra, "A Simple Method for Designing High-Quality Prototype Filters for M-band Pseudo QMF Banks ", *IEEE Trans. on Signal Processing,* vol. 43, pp. 1005-1007, April 1995.

131. CM. Liu and WC. Lee. "A Unified Fast Algorithm for Cosine Modulated Filter Banks in Current Audio Coding Standards ". *Journal of the AES.* 1999 December, Vol 47 Number 12, pp. 1061-1075.

132. H. Malvar, "Modulated QMF filter banks with perfect reconstruction," Electronics Letters, vol. 26, June 21 1990, pp. 906-907.

133. HD. Tuan, LH. Nam, H. Tuy and TQ. Nguyen, "Multicriterion Optimized QMF Bank Design", *IEEE Transactions on Signal Processing*, Vol. 51, No.10, Oct. 2003, pp. 2582- 2591.

134. J.G. Proakis. *Digital Communications.* New York, Mc Graw Hill, 1995.

135. B. Sklar. *Digital Communications: Fundamentals and Applications (2nd Ed),* Prentice Hall , January 2001.

136. R. Steele and L. Hanzo (Editor). *Mobile Radio Communications.* 2nd edition , John Wiley & Sons, October 1999.

137. B. Sklar, "Rayleigh fading channels in mobile digital communication systems," *IEEE Communications Magazine,* vol. 35, no. 7, Juy 1997, pp. 90-109.

138. W.D. Rummler, "A New Selective Fading Model: Application to Propagation Data", *Bell System Technical Journal*, Vol. 58, pp. 1037-1071, 1979.

139. E. Kunnari, "Modeling and simulation of Rice fading with temporal, spatial and spectral correlation - Part I: Characterization of fading", *Proc. Finnish Wireless Communications Workshop*, Oulu, Finland, Oct. 2003, pp. 101-105.

140. H. Iwai, 'A Wideband Multipath Fading Model', *ICICE Japan Trans. on Communications*, Feb. 1993,pp.304-310.

141. M. Jeruchim, P. Balaban and K.S. Shanmugan. *Simulation of Communication Systems (Applications of Communications Theory).* Plenum Publishing Corporation, December 1992.

142. H. Meyr, M. Moeneclaey and SA. Fechtel. *Digital Communication Receivers : Synchronization, Channel Estimation, and Signal Processing.* John Wiley & Sons, October 1997.

143. H. Meyr and G. Ascheid. *Synchronization in Digital Communications : Phase-, Frequency-Locked Loops, and Amplitude Control.* John Wiley & Sons, March 1990.

144. VM. Baronkin, YV. Zakharov and TC. Tozer," Frequency estimation in slowly fading multipath channels, *IEEE Transactions on Communications,* Vol. 50, No. 11, Nov 2002, pp. 1848- 1859..

145. JJ van de Beek, *"Estimation of Synchronization Parameters", Licentiate Thesis TULEA* 1996:14L, Division of Signal Processing, Luleå University of Technology, Sweden, May 1996

146. P. Stoica and O. Besson, " Training sequence design for frequency offset and frequency-selective channel estimation", *IEEE Transactions on Communications*, Vol. 51, Issue 11, Nov. 2003, pp. 1910- 1917.

147. Y. Wang ,E. Serpedin and P. Ciblat, "Optimal blind nonlinear least-squares carrier phase and frequency offset estimation for general QAM modulations", *IEEE Transactions on Wireless Communications*, Vol. 2, Issue 5, Sept. 2003, pp. 1040- 1054.

148. M. Karan , R. C. Williamson & B. D. O. Anderson, "Performance of the Maximum Likelihood Constant Frequency Estimator for Frequency Tracking", *IEEE Transactions on Signal Processing*, vol. 42(10), 1994,pp. 2749-2757.

149. B. C. Lovell and R. C. Williamson, "The Statistical Performance of Some Instantaneous Frequency Estimators", *IEEE Transactions on Signal Processing,* vol. 40(7), pp. 1708-1723, 1992.

150. B. C. Lovell , P. J. Kootsookos & R. C. Williamson, "Efficient Frequency Estimation and Time-Frequency Representations", *the International Symposium of Signal Processing and its Applications*, pp. 170-173, 1990.

151. H. Liu and U. Tureli, "A high-efficiency carrier estimator for OFDM communication, *IEEE Communication Letters.*, 2(4), pp. 104-106, 1998.

152. U. Tureli, H. Liu, M.D. Zoltowski, "OFDM blind carrier offset estimation: ESPRIT," *IEEE Trans. Commun.*, 48(9), pp. 1459-1461, 2000.

153. M. Ghogho, A. Swami and G. Giannakis, "Optimized null-subcarrier selection for CFO estimation in OFDM over frequency-selective fading channels," *Proc.Globecom-2001*, San Antonio, USA, Nov. 2001, pp. 202-206.

154. M. Ghogho and A. Swami, "Blind frequency offset estimator for OFDM systems transmitting constant modulus symbols" *IEEE Communication Letters*, vol. 6, no.8, Aug. 2002, pp.343-345.

155. M. Luise and R. Reggiannini, "*Carrier Frequency Acquisition And Tracking For OFDM Systems*", *IEEE Transaction On Communication*, Vol.44 No.11. November 1996, pp. 1590-1598.

156. H. Steendam, M. Moeneclaey and H. Sari, *"The effect of carrier phase jitter on the performance of orthogonal frequency-division multiple access systems", IEEE Trans. on Comm.*, Vol. 46, No. 4, Apr 98, pp. 456-459

157. H. Steendam and M. Moeneclaey, *"The Effect of Carrier Phase Jitter on MC-CDMA Performance", IEEE Trans. on Comm.*, Vol. 47, No. 2, Feb 99, pp. 195-198

158. H. Steendam and M. Moeneclaey, *"The Sensitivity of MC-CDMA to Synchronisation Errors", European Transactions on Telecommunications, ETT special issue on MC-SS*, Jul-Aug 99, Vol 10, no 4, pp. 429-436

159. T. Pollet, M.V. Bladel, and M. Moeneclaey, BER sensitivity of OFDM systems to carrier frequency offset and Wiener phase noise," *IEEE Trans. on Communications*, 43(2/3/4), pp. 191-193, 1995.

160. J. Louveaux, L. Cuvelier, L. Vandendorpe and T. Pollet, "Baud rate timing recovery scheme for filter bank-based multicarrier transmission", *IEEE Transactions on Communications*, Vol. 51, No. 4, April 2003, pp. 652- 663.

161. S. Ohno and GB. Giannakis, "Optimal training and redundant precoding for block transmissions with application to wireless OFDM", *IEEE Transactions on Communications*, Vol. 50, Issue 12, Dec 2002, pp. 2113- 2123.

162. A. Scaglione, GB. Giannakis and S. Barbarossa, "Redundant filterbank precoders and equalizers. I. Unification and optimal designs", *IEEE Transactions on Signal Processing*, Vol. 47, Issue 7, Jul 1999, pp. 1988-2006.

163. A. Scaglione, GB. Giannakis and S. Barbarossa, "Redundant filterbank precoders and equalizers. II. Blind channel estimation, synchronization, and direct equalization", *IEEE Transactions on Signal Processing*, Vol. 47, Issue 7, Jul 1999, pp. 2007-2022.

164. F. Daneshgaran and M. Mondin," Clock synchronisation without self-noise using wavelets, *Electronics Letters* , Vol: 31 Issue: 10 , 11 May 1995, pp. 775 –776.

165. F. Daneshgaran and M. Mondin, "Wavelet-based design for reduced jitter timing recovery," *IEEE Trans. Communications*, vol. 45, pp. 1523-1526, Dec. 1997.

166. F. Daneshgaran, M.Mondin, F. Dovis. *"Symbol Synchronization for Multichannel Frequency Diversity Transmission Over Fading Channels", Proc. of Vehicular Technology Conference (VTC'99)*, May '99, Houston TX, USA, vol.1, pp. 103 –107.

167. U. Mengali and A.N. D'Andrea. *Synchronization Techniques for Digital Receivers (Applications of Communications Theory)*. Plenum Publishing Corporation, November 1997.

168. SM. Kay. *Fundamentals of Statistical Signal Processing : Estimation Theory.* Prentice Hall, April 1993.

169. S.Glisic and B.Vucetic. *Spread Spectrum for Wireless Communications.* Artech, 1997.

170. R. Pichna, Q. Wang. "Power Control", *Gibson JD (ed) The Mobile Communications Handbook*, CRC Press, chap 23, 1996, pp. 370-380.

171. A. Bury, J. Egle and J. Lindner, "Diversity comparison of spreading transforms for multicarrier spread spectrum transmission", *IEEE Transactions on Communications*, Vol. 51, No. 5, May 2003, pp. 774- 781.

172. Q. Xiaoyuan, MS. Alouini and K.Young-Chai,"Closed-form analysis of dual-diversity equal-gain combining over rayleigh fading channels", *IEEE Transactions on Wireless Communications*, Vol. 2, Issue 6, Nov. 2003, pp. 1120- 1125.

173. N. Benvenuto, S. Tomasin and L. Tomba, " Equalization methods in OFDM and FMT systems for broadband wireless communications, *IEEE Transactions on Communications*, Vol. 50, No. 9, Sept 2002, pp. 1413- 1418.

174. B. Farhang-Boroujeny and L. Lekun,"Analysis of post-combiner equalizers in cosine-modulated filterbank-based transmultiplexer systems", *IEEE Transactions on Signal Processing*, Vol. 51, Issue 12, Dec. 2003, pp. 3249-3262.

175. Z. Li and M. Latva-aho, "Multicarrier CDMA System with Parallel Interference Cancellation in Fading Channel", *Proc. of MC-SS 2001 Third Int'l Workshop on Multi-Carrier Spread-Spectrum*, Oberpfaffenhofen, Germany, Sept. 26-28, 2001, pp. 273-280.

176. S. Kaiser and J. Hagenauer, *"Multi-carrier CDMA with iterative decoding and soft-interference cancellation", Proc. IEEE Global Telecom. Conf. (GLOBECOM'97),* Phoenix, USA, pp. 6-10, Nov. 1997.

177. S. Beheshti and G.W. Wornell, *"Iterative Interference Cancellation and Decoding for Spread-Signature CDMA Systems", Proc. Vehicular Tech. Conference,* Phoenix, Arizona May 1997, vol.1, pp. 26 -30.

178. S. Beheshti, S.H. Isabelle and G.W. Wornell,*"Joint Intersymbol and Multiple-Access Interference Suppression Algorithms for CDMA Systems", European Transactions on Telecommunications, Special Issue on Code-Division Multiple-Access Techniques for Wireless Communication Systems, Vol. 9, No. 5*, pp. 403-418, Sept./Oct. 1998.

179. AC. McCormick, PM. Grant and JS. Thompson "A Hybrid Uplink Multi-Carrier CDMA Interference Cancellation Receiver " *IEE Proceedings - Communications*, Vol 148(2), April 2001, pp119-124.

180. AC. McCormick, PM. Grant and JS. Thompson " A Novel Interference Cancellation Receiver for Uplink Multi-Carrier CDMA", presented at 2000 *IEEE Sixth International Symposium on Spread Spectrum Techniques and Applications*, 6-8 September 2000, Parsippany, New Jersey, USA, pp 155-158.

181. TK Kashihara, "Adaptive cancellation of mutual interference in spread spectrum multiple access ", *Proc. IEEE International Conference on Communications(ICC),* 1980, pp. 44.4.1-44.4.5.

182. R. Kohno, H. Imai, M. Hatori , "Cancellation technique of co-channel interference in asynchronous spread-spectrum multiple-access systems". *IEICE Transactions on Communications 65-A*, 1983, pp. 416-423.

183. GE. Bottomley, "CDMA downlink interference suppression using I/Q projection", *IEEE Transactions on Wireless Communications*, Vol. 2, Issue 5, Sept. 2003, pp. 890-900.

184. KS . Schneider, "Optimum detection of code division multiplexed signals", *IEEE Transactions on Aerospace and Electronic Systems* 15(1),1979: pp. 181-185.

185. E. Weinstein, M. Feder and A.V. Oppenheim, *"Multi-Channel Signal Separation by Decorrelation," IEEE Transactions on Speech and Audio Processing, Vol. 1, No. 4,* October 1993, pp. 405 -413.

186. A. Kapur, MK. Varanasi and D. Das, "Noncoherent MMSE multiuser receivers and their blind adaptive implementations, *IEEE Transactions on Communications,* Vol. 50, No. 3, Mar 2002, pp. 503-513.

187. A. Host-Madsen and X. Wang,"Performance bounds for linear MMSE receivers in CDMA systems with partial channel knowledge", *IEEE Transactions on Signal Processing*, Vol. 51, Issue 10, Oct. 2003, pp. 2495-2510.

188. D.N Kalofonos, M. Stojanovic and J.G. Proakis,"Performance of Adaptive MC-CDMA Detectors in Rapidly Fading Rayleigh Channels". *2002 issues of IEEE Transactions on Wireless Communications, Vol.2 Issue.2,* March 2003, pp. 229 –239.

189. D.N Kalofonos, M. Stojanovic and J.G. Proakis, *"On the Performance of Adaptive MMSE Detectors for a MC-CDMA System in Fast Fading Rayleigh Channels". Proceedings of the IEEE Personal, Indoor, and Mobile Radio Communications Symposium (PIMRC '98),* Vol.3, pp. 1309-1313, September 1998.

190. AN. Barbosa and SL. Miller. *Adaptive detection of DS/CDMA signals in fading channels. IEEE Trans. Comm.*, 46(5):115-124, January 1998.

191. U. Madow,"Blind Adaptive Interference Suppression for DS-CDMA", *Proceedings of the IEEE*, Vol.86 No.10, Oct. 1998, pp.2049-2069.

192. WM. Younis, AH. Sayed and N. Al-Dhahir, "Efficient adaptive receivers for joint equalization and interference cancellation in multiuser space-time block-coded systems, *IEEE Transactions on Signal Processing*, Vol. 51, No.11, Nov. 2003,pp. 2849- 2862.

193. G. Woodward, R. Ratasuk, ML. Honig and PB. Rapajic, "Minimum mean-squared error multiuser decision-feedback detectors for DS-CDMA", *IEEE Transactions on Communications*, Vol. 50, Issue 12, Dec 2002, pp. 2104- 2112.

194. J. Tellado, LMC. Hoo and JM. Cioffi, "Maximum-likelihood detection of nonlinearly distorted multicarrier symbols by iterative decoding", *IEEE Transactions on Communications,* Vol. 51, No. 2, Feb 2003, pp. 218- 228.

195. S. Buzzi, A. De Maio and M.Lops, "Code-aided blind adaptive new user detection in DS/CDMA systems with fading time-dispersive channels, *IEEE Transactions on Signal Processing*, Vol. 51, No.10, Oct. 2003, pp. 2637- 2649.

196. R. Merched, "Extended RLS lattice adaptive filters", *IEEE Transactions on Signal Processing*, Vol. 51, No.9, Sept. 2003, pp. 2294- 2309.

197. J. Choi and SR. Kim ,"Adaptive MMSE receiver for multirate CDMA systems, *IEEE Transactions on Signal Processing*, Vol. 50, No.12, Dec 2002, pp. 3098- 3106.

198. S. Haykin. *Adaptive Filter Theory.* Prentice Hall, NJ-USA, 1996.

199. B. Widrow , SD Stearns . *Adaptive Signal Processing.* Prentice-Hall, Englewood Cli_s, New Jersey, USA, 1985.

200. S. Verdu,"Optimum multiuser asymptotic efficiency", *IEEE Transactions on Communications 34(9)*, 1986, pp. 890-897.

201. EC. Ifeachor and BW. Jervis. *Digital Signal Processing, A Practical Approach.* Prentice Hall, 1993.

202. GH Golub & CF Van Loan . *Matrix Computations. 2nd Ed,* The John Hopkins University Press, Baltimore, Maryland, 1989.

203. WH. Press et. al. *Numerical Recipes in C*, Cambridge University Press. 1992.

204. WF. McColl, *Foundations of Time Critical Scalable Computing,* Programming Research Group, Oxford. (http://users.comlab.ox.ac.uk/bill.mccoll/hifip/hifip.html).

205. V. Strassen,"Gaussian Elimination is Not Optimal", *Numerische Mathematik,* vol. 13, 1969, pp.354-356.

206. A. Muayyadi and MNA Abu-Rgheff, "Wavelet-based MC-CDMA cellular systems", *IEEE Sixth International Symposium on Spread Spectrum Techniques & Applications*, Sept 2000, New Jersey, USA. pp.145-149.

207. A. Muayyadi and MNA Abu-Rgheff,"A wavelet-based multicarrier CDMA system and its corresponding multiuser detection", *Proceeding IEE – Communications* (accepted to appear on Vol. 150, Issue 07, Dec 2003).

208. A. Muayyadi and MNA Abu-Rgheff,"Wavelet-based Synchronisation in MC-CDMA systems", *proceeding of PREP 2003 Conference*, Exeter, April 2003, pp. 1-2.

209. J. Yueand JD. Gibson," Performance of OFDM systems with space-time coding *Proc. of Wireless Communications and Networking Conference, WCNC2002*, 17-21 March 2002, Vol: 1, pp. 280 –284.

210. L. Hanzo and CH. Wong. *Adaptive Wireless Transceivers: Turbo-Coded, Turbo-Equalised and Space-Time Coded TDMA, CDMA, MC-CDMA and OFDM Systems.* John Wiley & Sons, Inc, March 2002.

211. B. Lu and X. Wang," Iterative receivers for multiuser space-time coding systems", *IEEE Journal on Selected Areas in Communications*, Vol:18 Issue: 11 , Nov. 2000.pp.2322–2335.

212. EG. Larsson, P. Stoica and G. Ganesan. *Space-Time Block Coding for Wireless Communications.* Cambridge University Press, May 2003.

APPENDICES

A. Some Simulation Softwares

1. Sample Main Programme
2. Synthesis Filters
3. Analysis Filters
4. Code Spreading
5. Code Despreading
6. FB-MC-CDMA Transmitter
7. FB-MC-CDMA Receiver
8. WB-MC-CDMA Transmitter
9. WB-MC-CDMA Receiver
10. BER Calculation
11. Frequency Error Estimator
12. Phase Offset Estimator
13. M-band Wavelet Display

B. Papers

1. A. Muayyadi and MNA Abu-Rgheff, 'Wavelet-based MC-CDMA cellular systems', *IEEE Sixth International Symposium on Spread Spectrum Techniques & Applications,* Sept 2000, New Jersey, USA. pp.145-149.

2. A. Muayyadi and MNA Abu-Rgheff, 'Wavelet-based multicarrier CDMA systems and its corresponding multiuser detection', *Proceeding IEE – Communications* (accepted to appear on Vol. 150, Issue 07, Dec 2003).

3. A. Muayyadi and MNA Abu-Rgheff, 'Wavelet-based Synchronisation in MC-CDMA systems', *Proc. of PREP 2003 Conference*, Exeter, April 2003, pp. 1-2.

4. A. Muayyadi and MNA Abu-Rgheff, 'Wavelet-based multicarrier CDMA systems and its time synchronisation', *Int'l journal on Wireless Communications and Mobile Computing* (submitted).

```
% SAMPLE MAIN PROGRAMME
%
% Performance Testing under AWGN Channel
load proto
% Analysis Filters Generation
[g,fhm] = cosmod(p,M,N);
% Synthesis Filters Generation
[f,ff,ch] = mirro(g,M,N);
cd=hadamard(M);  % M-Length Walsh-Hadamard Code
cuser=cd(4,:); % User's Spreading Code
% Random Data Generation
x=randint(1,10000);
% Bipolar Conversion
xdat=2*(x-0.5);
% Spreading
[xsig]=Spreading(M,xdat,cuser);
% FB-MC-CDMA System
% Transmitted Signal
[uv1]= FB_MCCdmaTx(xsig,M);
[uvf]=awgn(uv1,0,'measured'); % Add Noise  SNR=0 dB
[wf]= FB_MCCdmaRx(uvf,M);
[xrf]=DeSpreading(M,wf,cuser);
xf=sign(real(xrf));  % Detection
xf2=round((xf+1)/2);
[ber_fb,fb_err]= BER(x,xf2,0); % Calculate BER
%
% WB-MC-CDMA System
% Transmitted Signal
[uv2]= WB_MCCdmaTx(xsig,f,M);
[uvw]=awgn(uv2,0,'measured'); % Add Noise  SNR=0 dB
[xo]= WB_MCCdmaRx(uvw,g,M);
[xrw]=DeSpreading(M,xo,cuser);
xw=sign(real(xrw));  % Detection
xw2=round((xw+1)/2);
[ber_wb,wb_err]= BER(x,xw2,N/M-1); % Calculate BER
```

```
function [g,fhm] = cosmod(p,M,N);
%
% Function to create a cosinus modulated filter bank
% Analysis Filters
% p is the LPF prototype filter
% M is number of subbands
% N is filter length
%
% Normalisation
ak2=2*sqrt(M);
hmax=0;
for k=1:M
   for n=1:N
   g(k,n) = ak2*p(n)*cos((pi/(2*M))*(n-0.5-N/2)*(2*(k-1)+1)+(-1)^(k-
1)*pi/4);
   end
end
ht=g.';
fht=fft(ht);
fh=fht.';
i(1:N/2)=(0:1/N:(N/2-1)/N);
i(N/2+1:N)=(1/2:1/N:(N-1)/N)-1;
 for k=1:M
fhm(k,:)=20*log10(abs(fh(k,:)));
%   maximum PSD
```

```
 end
for k=1:M
    for n=1:N
   if fhm(k,n) > hmax
         hmax=fhm(k,n);
      end
    end
end
hmax, pause
clf
hold
grid
axis([0 0.5 -80 0]),  ylabel('Normalised Power (dB)','FontSize',14),
xlabel('Normalised Frequency ','FontSize',14)
title(['Frequency Structure Of WB-MCCDMA Systems, M =
',int2str(k)],'FontSize',14)
for k=1:M
plot(i(1:N/2),(fhm(k,1:N/2)-hmax))
plot(i(N/2+1:N),(fhm(k,N/2+1:N)-hmax))
pause
end
pause



function [f,ff,ch] = mirro(g,M,N);
%
% Function to create a cosinus modulated filter bank
%
% Output : f = Synthesis Filters
%          ff = PSD
%       ch = orthogonality checking
% Input
% g is Analysis Filters
% M is number of subbands
% N is filter length
%
% Normalisation
ak2=2*sqrt(M);
for k=1:M
   for n=1:N
   f(k,n)=g(k,N+1-n);   % mirror of analysis filters
   end
   ff(k,:)=fft(f(k,:));
end
for k=1:M
   for j=1:M
         ch(k,j)=0;
      for n=1:N
      ch(k,j)=ch(k,j)+ g(k,n)*f(j,n);
      end
   end
end



function [xsig]=Spreading(M,xdat,cuser);
%
% Function to spread the input signal (in subband domain)
% Output : xsig
% Input :
% xdat : bipolar data signal
```

```
% M : number of subbands
% cuser : user's spreading code
%
sz=size(xdat);
% Multiplication of user's code cuser and data signal xdat
for k=1:M
   for n=1:sz(2)
   xsig(k,n)=cuser(k)*xdat(n);
   end
end


function [xrec]=DeSpreading(M,xo,cuser);
%
% Function to despread the input signal (in subband domain)
% Output : xrec
% Input :
% xo : input signal
% M : number of subbands
% cuser : user's spreading code
%
sz=size(xo);
% Multiplication of user's code cuser and input signal xo
for k=1:M
 for n=1:sz(2)
   xs(k,n)=cuser(k)*xo(k,n);
 end
end
% Equal Gain Combining
xrec=sum(xs)/M;



function [uv]= FB_MCCdmaTx(xsig,M);
%
% Function to build a Fourier-based Multi-Carrier CDMA Transmitter
% Output : uv
% Input :
% xsig is Code-Spread Signal
% M is number of subbands
%
sz=size(xsig);
% FB-MCM
v=ifft(xsig)*sqrt(M);
% MUX
for k=1:M
   for n=1:sz(2)
     uv(k+(n-1)*M)=v(k,n);
  end
end



function [wf]= FB_MCCdmaRx(uv,M);
%
% Function of Fourier-based Multi-Carrier CDMA Demodulation
% Output : wf
% Input :
% uv is FB-MC-CDMA Signal
% M is number of subbands
```

```
%
sz=size(uv);
%DEMUX
for k=1:M
   for n=1:sz(2)/M
   ww(k,n)=uv(k+(n-1)*M);
end
end
% FB-MC Demod
wf=fft(ww)/sqrt(M)



function [uv]= WB_MCCdmaTx(xsig,f,M);
%
% Function to build a Wavelet-based Multi-Carrier CDMA Transmitter
% Output : uv
% Input :
% xsig : code-spread signal
% f : synthesis filters
% M : number of subbands
%
sz=size(xsig);
% Initialisation
for k=1:M
     u(k,1:sz(2)*M)=0;
end
% Up-Sampling
for k=1:M
   for n=1:sz(2)
    u(k,1+(n-1)*M)=xsig(k,n);
   end
end
for k=1:M
   v(k,:)=conv(f(k,:),u(k,:));
end
% Summing-Up Signal
uv=sum



function [xo]= WB_MCCdmaRx(uv,g,M);
%
% Function of Wavelet-based Multi-Carrier CDMA Demodulation
% Output : xo
% Input :
% uv : WB-MC-CDMA Signal
% g : analysis filters
% M : number of subbands
%
% WB-MC Demod
for k=1:M
w(k,:)=conv(g(k,:),uv);
end
% Down-sampling
sz=size(w);
for k=1:M
  for n=1:sz(2)/M
     xo(k,n)=w(k,n*M);
  end
end
```

```
function [outber,no_err]= BER(x,xdatrec,delay);
%
% Function to compute Bit Error Rate
% Output :
%   outber : bit error rate
%   no_err : number of error bits
% Input :
%   x : original/transmitted data signal
%   xdatrec : recovered/detected data signal
%   delay : delay to synchronise both signals
%
no_err=0;
double outber;
sz=size(x);
   errk= xor(x,xdatrec(delay+1:sz(2)+delay));
   no_err = sum(errk);
outber=no_err/sz(2);


function [yc,yd,yd2,foe,foer]=FreqErrorEst(f,g,M,N,fo,snr);
%
% Simulation of Frequency Error Estimation in WB-MC-CDMA System
% Output :
%       yc : phase without CFE
%       yd : phase with CFE
%       yd2 : : phase with CFE (unwrap)
%       foe :
%       foer:
%       foer: Estimated Freq Error in rad
%       foe: Estimated Freq Error in % of Fs
% Input :
%       f : synthesis filters
%       g : Analysis filters
%       M : number of subbands
%       N : filter length
%       fo: CFE (Carrier Fequency Error)
%       fo=0.1  means  freq shift of 10% Fs
%       snr: signal to noise ratio [dB]
cd=hadamard(M);  % Walsh-Hadamard Code
cuser=cd(1,:);
x(1:N)=1;   % Training Sequence of 16 symbols
% Bipolar Conversion
xdat=2*(x-0.5);
% Spreading
[xsig]=Spreading(M,xdat,cuser);
[uv2]= WB_MCCdmaTx(xsig,f,M);
[uvw]=awgn(uv2,snr,'measured');
% CFE
sz=size(uvw);
fs=1;
dfs=fs*fo;  % Frequency Shift of fo
ws=2*pi*dfs;
for i=1:sz(2)
 uve(i)=uvw(i)*(exp(j*ws*i));
end

% Without Freq Error
[xo]= WB_MCCdmaRx(uvw,g,M);
[xc]=DeSpreading(M,xo,cuser);
sz=size(xc);
for i=1:sz(2)
yc(i)=angle(xc(i)); % in rad
end
```

```
% With Freq Error
[xo]= WB_MCCdmaRx(uve,g,M);
[xd]=DeSpreading(M,xo,cuser);
for i=1:sz(2)
yd(i)=angle(xd(i));
end
xw=sign(real(xd));  % Detection
xw2=round((xw+1)/2);
[ber_wb,wb_err]= BER(x,xw2,N/M-1);

% Freq Error Estimation
yd2=unwrap(yd);
sl=diff((yd2(M:sz(2)-M))); % Finding The Slope
foer=mean(sl); % Estimated Freq Error in rad
fvar=var(sl);
foe=foer/(2*pi*M); % Estimated Freq Error in % of Fs



function [yc,yd,pdeg,pvar]=PhaseOffsetEst(f,g,M,N,po,snr);
%
% Simulation of Phase Offset Estimation in WB-MC-CDMA System
% Output :
%       yc : phase without CFE
%       yd : phase with CFE
%       pdeg: Estimated Phase Offset in degree
%       pvar: Variance of Phase Offset Estimation
% Input :
%       f : synthesis filters
%       g : Analysis filters
%       M : number of subbands
%       N : filter length
%       po: phase offset in degree
%       snr: signal to noise ratio [dB]
%
por=po*pi/180; % phase Shift in rad
cd=hadamard(M);  % Walsh-Hadamard Code
cuser=cd(1,:);
x(1:N)=1;   % Training Sequence of 16 symbols
% Bipolar Conversion
xdat=2*(x-0.5);
% Spreading
[xsig]=Spreading(M,xdat,cuser);
[uv2]= WB_MCCdmaTx(xsig,f,M);
[uvw]=awgn(uv2,snr,'measured');

uve=uvw*exp(j*por);  % Phase Shift

% Without Phase Offset
[xo]= WB_MCCdmaRx(uvw,g,M);
[xc]=DeSpreading(M,xo,cuser);
sz=size(xc);
for i=1:sz(2)
yc(i)=angle(xc(i)); % in rad
end

% With Freq Error
[xo]= WB_MCCdmaRx(uve,g,M);
[xd]=DeSpreading(M,xo,cuser);
for i=1:sz(2)
yd(i)=angle(xd(i));
end
```

```
xw=sign(real(xd));  % Detection
xw2=round((xw+1)/2);
[ber_wb,wb_err]= BER(x,xw2,N/M-1);

poe=mean(yd(N/M:sz(2)-N/M)); % Estimated Phase Offset in rad
pvar=var(yd(N/M:sz(2)-N/M)); % Variance of Phase Offset Estimation
pdeg=poe*180/pi; % Estimated Phase Offset in degree
```

```
function [psi]=SW_ItM(h,M,N,Nbr,kali,panj);
%
% Function to display M-band Wavelets
% from filter coefficients
% Output :
%       psi : wavelets
% Input :
%       h : filter coefficients
%       M : number of subbands
%       N : filter length
%       Nbr : number of iterations
%       kali : number of resolutions
%       panj : diplayed time window
%
t=1:panj*N*kali;
konst=sqrt(M);
% Box Function
psi(1:M,1:N*kali)=1;
psi(1:M,N*kali+1:panj*N*kali)=0;
for i=1:Nbr
for t=1:panj*N*kali
temp(1:M,t)=0;
   for n=1:N
      if ((M*t-(n-1)*N*kali)>0 & (M*t-(n-1)*N*kali)< panj*N*kali)
      for k=1:M
         temp(k,t)=temp(k,t)+h(k,n)*psi(1,M*t-(n-1)*N*kali);
      end
      end
   end
end
   for t=1:panj*N*kali
      for  k=1:M
      psi(k,t)=konst*temp(k,t);
      end
   end
end
```